Automatic Fire Detection Using Computer Vision Techniques for UAV-based Forest Fire Surveillance

Chi Yuan

A Thesis

in

The Department

of

Mechanical, Industrial and Aerospace Engineering

Presented in Partial Fulfillment of the Requirements

for the Degree of

Doctor of Philosophy (Mechanical Engineering) at

Concordia University

Montréal, Québec, Canada

May 2017

CONCORDIA UNIVERSITY

SCHOOL OF GRADUATE STUDIES

This is to certify that the thesis prepared

By: **Chi Yuan**

Entitled: **Automatic Fire Detection Using Computer Vision Techniques for**

              UAV-based Forest Fire Surveillance

and submitted in partial fulfillment of the requirements for the degree of

DOCTOR OF PHILOSOPHY (Mechanical Engineering)

complies with the regulations of this University and meets the accepted standards with respect to

originality and quality.

Signed by the Final Examining Committee:

_____ Chair
Dr. Lata Narayanan

_____ External Examiner
Dr. Xavier Maldague

_____ External to Program
Dr. Wei-Ping Zhu

_____ Examiner
Dr. Wen-Fang Xie

_____ Examiner
Dr. Henry Hong

_____ Thesis Supervisor
Dr. Youmin Zhang

Approved by: _____
                      Dr. Ali Dolatabadi, Graduate & PhD Program Director, Department of Mechanical, Industrial and Aerospace Engineering

May 9, 2017

                      _____
                      Dr. Amir Asif, Dean, Faculty of Engineering and Computer Science

Abstract

Automatic Fire Detection Using Computer Vision Techniques for UAV-based Forest Fire Surveillance

Chi Yuan, Ph.D.

Concordia University, 2017

Due to their rapid response capability and maneuverability, extended operational range, and improved personnel safety, unmanned aerial vehicles (UAVs) with vision-based systems have great potentials for forest fire surveillance and detection. Over the last decade, it has shown an increasingly strong demand for UAV-based forest fire detection systems, as they can avoid many drawbacks of other forest fire detection systems based on satellites, manned aerial vehicles, and ground equipments. Despite this, the existing UAV-based forest fire detection systems still possess numerous practical issues for their use in operational conditions. In particular, the successful forest fire detection remains difficult, given highly complicated and non-structured environments of forest, smoke blocking the fire, motion of cameras mounted on UAVs, and analogues of flame characteristics. These adverse effects can seriously cause either false alarms or alarm failures.

In order to successfully execute missions and meet their corresponding performance criteria and overcome these ever-increasing challenges, investigations on how to reduce false alarm rates, increase the probability of successful detection, and enhance adaptive capabilities to various circumstances are strongly demanded to improve the reliability and accuracy of forest fire detection system. According to the above-mentioned requirements, this thesis concentrates on the development of reliable and accurate forest fire detection algorithms which are applicable to UAVs. These algorithms provide a number of contributions, which include: (1) a two-layered forest fire detection method is designed considering both color and motion features of fire; it is expected to greatly

improve the forest fire detection performance, while significantly reduce the motion of background caused by the movement of UAV; (2) a forest fire detection scheme is devised combining both visual and infrared images for increasing the accuracy and reliability of forest fire alarms; and (3) a learning-based fire detection approach is developed for distinguishing smoke (which is widely considered as an early signal of fire) from other analogues and achieving early stage fire detection.

Acknowledgments

This thesis is submitted in partial fulfillment of the requirements for the degree of philosophy doctor (Ph.D.) at Concordia University (CU). Under the supervision of Prof. Youmin Zhang, the presented thesis work is carried out in the Networked Autonomous Vehicles (NAV) lab at the Department of Mechanical, Industrial & Aerospace Engineering (MIAE), Concordia University.

Fortunately, I have been given such great opportunities to collaborate with and be significantly benefited by many outstanding people during my whole Ph.D. study. In particular, my deepest gratitude should go to my supervisor, Prof. Youmin Zhang who has provided me with these valuable chances and resources allowing me to pursue my Ph.D. degree, and to successfully handle various challenges and difficulties in different critical phases of my research. Without his consistent support, encouragement, valuable and insightful guidance, I cannot achieve such significant and satisfactory research progress. His great passion and diligence to research works, positive attitude to both work and life, organizational skills, and keen insight on solving challenging issues have been my relentless source of motivation and inspiration. It is really my great privilege being able to work under his insightful guidance.

In addition, it is my great honor to have Prof. Henry Hong, Prof. Wen-Fang Xie, and Prof. Wei-Ping Zhu joining my examining committee and providing useful feedback and brilliant comments during my comprehensive exam and research proposal. I really appreciate their strong support and inspired advice. I am also very grateful to our current and graduated group members who have provided great help to my research, from the discussion of challenges in research and paper writing, through experimental platform development and algorithm validation, to the problems that

I met in my daily life. It is my great pleasure to conduct research works with them, share opinions with them, and learn from them.

Finally, I would like to thank my family, my parents, my husband, and my lovely daughter, who have played indispensable roles in my life. Without their love, consistent support and understanding, I cannot make it.

Contents

List of Figures

List of Tables

Nomenclature and Acronyms

Nomenclature

C	Morphological element
D	Dilation operation
E	Erosion operation
$\mathbf{H}$	Homography matrix
I	Image intensity
(x, y)	Coordinates of pixel in an image plane
P_Φ	Pixel value
f_α	Average value of orientations of total pixels in an image
Ω	Image region
$\otimes$	Erosion operator
$\oplus$	Dilation operator
$\sigma_w^2(t)$	Intra-class variance
$\bar{e}_k$	Variation of optical flow vector velocity
$\bar{b}_k$	Variation of optical flow vector direction
$u(t)$	Control inputs
θ	Pitch angle
ϕ	Roll angle
ψ	Yaw angle
m	Mass of UQH

$u_z(t)$	Total lift force
$u_\theta(t)$	Applied torque in θ direction
$u_\phi(t)$	Applied torque in ϕ direction
$u_\psi(t)$	Applied torque in ψ direction
$K_n(n=1,...,6)$	Drag coefficients
$u_i(i=1,...,4)$	Thrust of each rotor
L	Centre distance between the gravity of UQH and each propeller
C_m	Thrust-to-moment scaling factor
g	Acceleration of gravity
ω_m	Actuator bandwidth
K_m	A positive gain
$u_{ci}(i=1,...,4)$	Pulse width modulation signals distributed to each rotor

Acronyms

ANNs	Artificial Neural Networks
CCD	Charge-Coupled Device
DC	Direct Current
DDDAS	Dynamic Data-Driven Application System
EKF	Extended Kalman Filter
FD	Flame Detection
GF	Geometry Feature
GNC	Guidance, Navigation, and Control
GPS	Global Positioning System
GL	Geolocation
HSI	Hue, Saturation, and Intensity (color model)
HSV	Hue, Saturation, and Value (color model)
IMUs	Inertial Measurement Units
IR	Infrared
IV	Indoor Validation
IS	Image Stabilization
LQR	Linear Quadratic Regulator
NASA	National Aeronautics and Space Administration
NIR	Near Infrared
OV	Outdoor Validation
OLV	Offline Validation
OMT	Optimal Mass Transport
PP	Propagation Prediction
PWM	Pulse Width Modulation
RGB	Red, Green, and Blue (color model)
ROS	Rate of Spread

SMC	Sliding Model Control
SVM	Support Vector Machine
UAVs	Unmanned Aerial Vehicles
UAV	Unmanned Aerial Vehicle
UAS	Unmanned Aerial System
UQH	Unmanned Quadrotor Helicopter
USFS	United States Forest Services
VNIR	Visible-Near Infrared
WRAP	Wildfire Research and Applications Partnership
WVDF	West Virginia Department of Forestry

Chapter 1

Introduction

1.1 Motivation

Forests play numerous vital roles in nature. They can fertilize and stabilize the soil, cycle nutrients, moderate climate, purify water and air, store carbon, supply habitats for wildlife and nurture environments rich in biological diversity. In addition, forest products industry offers a vast number of jobs and contributes billions of dollars to a country's economic wealth. Unfortunately, every year millions of hectares of forest are damaged by fires and a great deal of personnels, facilities and money are expended to extinguish these fires [4]. Forest fires have become a severe natural danger which threatens ecological systems, economic properties, infrastructure, and human lives [5]. Take Canada as an example, Canada's forests cover a vast area of land which is more than 10% of the world's forests. How Canada manages its forests is, therefore, a global concern. Unfortunately, more than half of the world's natural forests have been destroyed over the past 50 years due to forest fires and poor management of forests. As reported by the Insurance Bureau of Canada, the estimated total cost reaches $3.58 billion [6] by the forest fire occurred at Fort McMurray, Alberta in May 2016 (as shown in Fig. 1.1). This disaster is considered as the most expensive for insurers in the country's history. Currently, almost all forests are in danger from such natural, human-made, and environmental risks, as well as global warming and extreme climate

change. Fighting forest fires is thereby seen as one of the most important issues in the natural resources protection and preservation [5]. In particular, because the fast convection propagation and long combustion period of forest fires, early detection of forest fires is considered to be a prominent way of minimizing the destruction that fires may cause [1, 7].

Figure 1.1: Forest fire occurred in Alberta, Canada in May 2016.

Massive efforts (see Fig. 1.2) have been devoted to the detection of forest fires before they develop into uncontrollable. Traditional forest fire surveillance and detection methods employing watchtowers and human observers to monitor the surroundings usually require extensive labour forces, are subject to the spatio-temporal limitations, and potentially threaten personnel safety. Along with the new development of technologies, in the past decades, monitoring of forests and detection of forest fires primarily rely on ground fire surveillance systems, manned aircraft, and satellites. However, different technological and practical problems exist in each of these systems. Ground surveillance system is normally fixed in a specific place and may suffer from limited surveillance ranges. Manned aircraft is usually large and expensive; meanwhile, the hazardous environments, harsh weather, and operator fatigue can potentially threaten the life of the pilot. Satellite systems are typically expensive for launching and less flexible for deployment and technology updates; moreover, their spatio-temporal resolutions sometimes may be difficult to meet the requirement of detailed data capture and operational forest fire detection [1, 8–10].

There is an urgent need for developing new tools for a better decision making and management of forests through fast and low-cost data acquisition, measuring and monitoring of forests fires and inventories. As a promising substitution of traditional and current forest fire detection approaches, the integration of unmanned aerial vehicles (UAVs) with remote sensing techniques serving as a
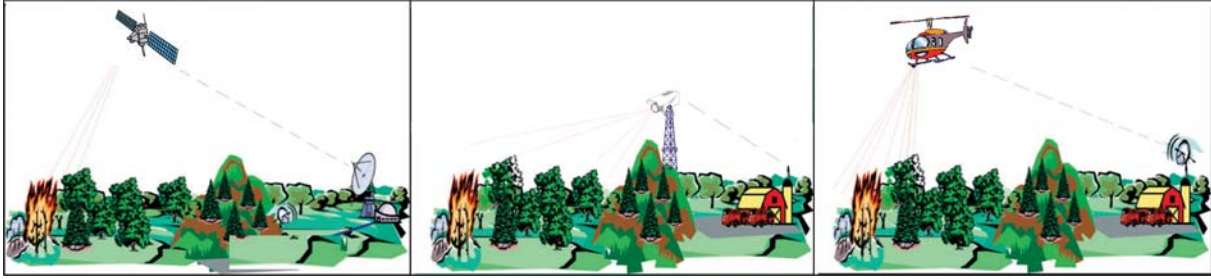
Figure 1.2: The existing forest fire surveillance and detection methods: satellite (left), watchtower (middle), and manned aircraft (right).

powerful tool for operational forest fire detection applications has attracted worldwide increasing attention [1, 11, 12]. The deployment of UAVs offers tremendous benefits:

(1) cover wide areas, in all kinds of weather;

(2) work at day time, night, with long duration;

(3) will not disturb animals during the flight;

(4) easily recoverable and relatively cost-effective compared to other methods;

(5) in the case of electric UAV, is also a benefit to the environment;

(6) carry large and different payloads for different missions even within one flight benefited from the space and weight saving comparing with manned vehicles since there is no need for pilot related life-guard equipment and devices;

(7) be able to cover larger and specific target area efficiently.

UAVs with computer vision based remote sensing systems onboard have been an increasingly realistic choice by providing low-cost, safe, rapid, and mobile characteristics for forest fire surveillance and detection. They are capable of meeting the crucial spatio-temporal and spectral resolution requirements [12]. They can also enable the execution of long-term, dull, and repetitive missions beyond human capabilities. In addition, vision-based detection technique can capture and deliver intuitive and highly real-time information as well as cover a wide viewing range conveniently with reduced development cost. Conventional point-sensors are very useful for indoor

3

fire detection by detecting heat or smoke particles. However, they are not suitable in large open spaces, such as in forests. Rapid development in electronics, computer science and digital camera technologies have made computer-vision-based systems a promising technique for fire monitoring and detection [8]. Vision-based system has become an essential component in the UAVs based forest fire detection system [13]. Accordingly, a great number of research activities, in recent years, have been carried out for UAV-based forest fire monitoring and detection applications [4, 14–32].

1.2 Background and Literature Review

1.2.1 Background: General System Design Architecture and Requirements

The basic components of a general UAV-based forest fire surveillance system can be described in Fig. 1.3, which fulfills the tasks of monitoring (searching a potential fire), detection (triggering an alarm to firefighting staffs or initializing further diagnosis and prognosis), diagnosis (localizing the fire and tracking its evolution), and prognosis (predicting the evolution of the fire with the real-time information of wind and firefighting conditions) [1]. These tasks can be carried out using either a single UAV or a team of UAVs (with different kinds of sensors) as well as a central ground station. The goals are to use UAVs to provide real-time information to human firefighters and/or to send alarm and aid firefighting.

In order to achieve the successful applications, UAV-based forest fire surveillance system typically contains the following components:

- UAV frames (fixed-wing and rotary-wing types) carrying the necessary payloads (remote sensing sensors for day-time, night-time, all weather conditions) for fire surveillance and detection. A variety of sensors, including global positioning system (GPS) receivers, inertial measurement units (IMUs), and cameras (visual and infrared cameras), all of which aid in fire surveillance and detection;

- Remote sensing technologies for fires monitoring and detection;
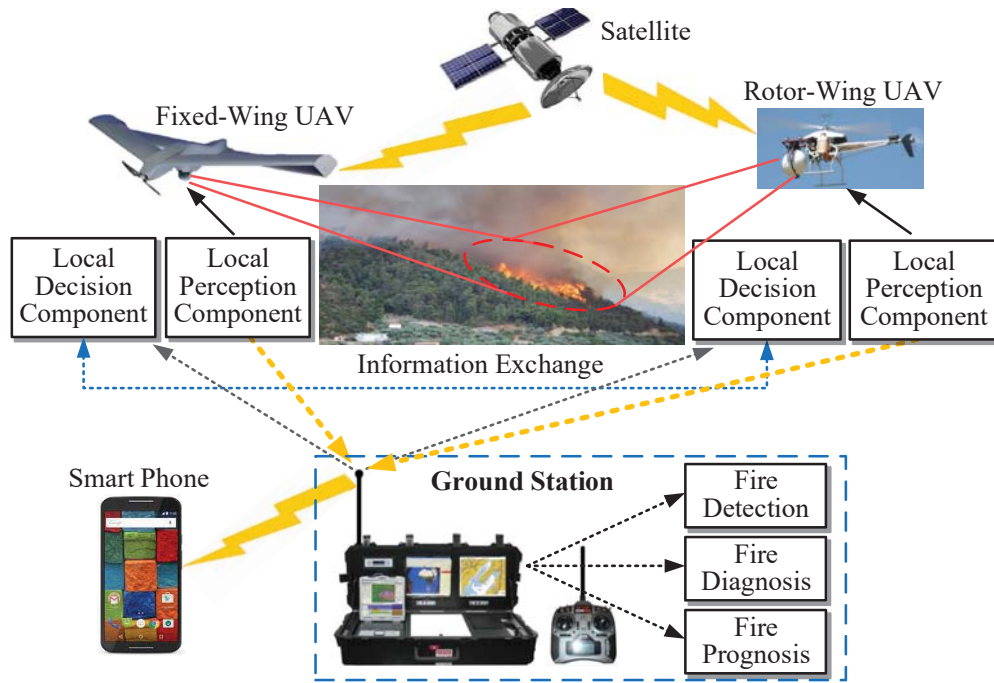
Figure 1.3: Illustration of UAV-based forest fire surveillance system [1].

- Sensors fusion and image processing techniques for rapid and accurate fire detection, decision-making, and localization;

- Guidance, navigation, control (GNC) algorithms of both single and multiple UAV fleets for monitoring, tracking and prediction of fire development, and fire extinguishing operation;

- Cooperative localization, deployment, and control strategies of UAVs for optimal coverage of fire areas for precise and rapid fire tracking, prediction, and assistance/guidance of fire-fighting. Such systems are based on the real-time data supplied by the onboard sensors and their related signal processing algorithms;

- Autonomous and reliable path planning and re-planning strategies before and after fire being detected based on fire development situations;

- Ground station for ground computation, image processing, visualization for fire detection, tracking, and prediction with automatic fire alarm and for safe and efficient operation of the

UAVs system during the mission.

Forest fire monitoring and detection mission can generally be broken down into one of three stages: fire search, fire confirmation, and fire observation [33].

In the fire search stage, the ground control station assigns the task to each UAV according to the characteristics of terrain, and functions of individual UAVs including their onboard payloads. After that, either a single UAV or a fleet of homogeneous/heterogeneous (fixed-wing and rotary-wing) UAVs [34, 35] is/are commanded to patrol the surveillance region along respective pre-planned paths for searching the potential fire.

The fire confirmation stage starts when a fire is detected. The ground control station sends the UAV which has detected the fire to hover near the detected fire spot with a safe distance, while other UAVs are also commanded to fly to the fire spot for the further fire confirmation based on their individual detection results.

The fire observation stage begins if the fire is determined to be true; otherwise the fire search stage is resumed. In the fire observation stage, UAVs are designated to synchronously collect images and data about the fire from different perspectives. These gathered information are finally delivered to operators at ground station or firefighting managers, and deploy service UAVs to assist firefighting operations.

1.2.2 Review on UAV Based Forest Fire Monitoring and Detection Systems

Recent decades have seen many advances in the field of UAV-based automatic firefighting technologies. A majority of research has been conducted in the North America and Europe. Table 1.1 provides a brief summary of existing UAV-based forest fire surveillance systems [1].

The earliest application of UAVs for collecting data on forest fires can be dated back to 1961 by the United States Forest Services (USFS) Forest Fire Laboratory [36]. In 1996, a Firebird 2001 UAV with a camera based imaging system was adopted for gathering forest fire images in Missoula, Montana [29]. Later on, during the period of 2003 to 2010, a Wildfire Research and Applications

6

Partnership (WRAP) project was carried out by the USFS and National Aeronautics and Space Administration (NASA), with the purpose of increasing under-served forest fire applications [26, 37]. In 2006, the NASA Altair and the Ikhana (Predator-B) UAVs accomplished their near-real-time wild fire imaging assignments in the western United States [26]. In 2011, with the collaboration of the West Virginia Department of Forestry (WVDF) and NASA, a research group from the University of Cincinnati utilized the Marcus Zephyr UAV to test the performance of its designed forest fire detection scheme [38]. Furthermore, a First Response Experiment (FiRE) project [39] demonstrated the effectiveness of using Unmanned Aerial System (UAS) for real-time wild fire information collection. The total processing time of data collection, telemetry, geo-processing, and delivery was within fifteen minutes by using this system. Instead of a single powerful UAV with sophisticated sensors used by the FiRE project, another project undertaken in Europe applied a team of low-cost UAVs with onboard visual and infrared cameras as local sensors for collecting images and data within close ranges. Experiments adopting multiple UAVs for patrolling, detection, localization, and propagation prediction of forest fires have also been conducted [19, 31, 40, 41]. Additionally, in 2004, the first regulated utilization of a UAV in fire service was developed in Hungary to test the systems function of forest fires detection [42]. Pastor *et al.* demonstrated a Sky-Eye UAV system to detect forest fires in Spain [43]. In 2011, two UAVs with visual and infrared cameras were designed to validate their abilities of fire detection and localization in the Netherlands [44].

Except for the practical use of UAVs, there has also been some simulated researches on UAV-based forest fire surveillance and detection. Casbeer *et al.* [45, 46] verified the efficacy of using several low altitude, low endurance UAVs for cooperative surveillance and tracking of large forest fires propagation. A numerical propagation model for forest fire detection was validated in simulation environment with a six degree-of-freedom dynamic UAV model. Yuan *et al.* [14–17] conducted experiments using an unmanned quadrotor helicopter (UQH) for searching and detecting a fire simulator in lab environment so that verify the efficacy of their proposed UAV based forest fire detection methods.

Although current research demonstrates the feasibility of using UAVs to detect forest fires, the development of automatic forest-fire detection systems, including relevant hardware and software, is still minimal. Further researches on suitable system platforms, remote sensing payloads/sensors, as well as algorithms for GNC and remote sensing are demanded. It is this urgent need that motivates further research and development in this important field.

Table 1.1: Features of reviewed UAV-based forest fire surveillance systems [1].

Test Types	References	UAV Class	Onboard Cameras (Resolution)	Engine Power	Payload Capacity
Near operational	[47]	1 fixed-wing	1 thermal (720×640)	Fuel	$340kg$
Operational	[26]	1 fixed-wing	4 mid-IR (720×640)	Fuel	$> 1088kg$
Near operational	[48]	2 rotary-wing; 1 airship	1 visual (320×240); 1 IR (160×120)	Fuel; Electric	$3.5kg$
Operational	[44]	1 fixed-wing; 1 rotary-wing	1 visual; 1 IR	Fuel	—
Near operational	[37]	1 fixed-wing	1 visual; 1 IR	Fuel	$< 34kg$
Near operational	[29]	2 fixed-wing	1 visual; 1 IR; 1 visual (1920×1080)	Fuel	$25kg$; $250kg$
Near operational	[49]	2 fixed-wing	1 thermal (160×120); 1 NIR (752×582); 1 VNIR (128×128)	Electric	$< 2.6kg$
Near operational	[50, 51]	1 fixed-wing	1 visual (720×480)	Gas	$0.68kg$
Near operational	[43]	1 rotary-wing	2 visual (4000×2656; 2048×1536); 1 thermal (320×240)	Fuel	$907kg$
Near operational	[42]	1 fixed-wing	1 visual	Electric	—
Near operational	[38]	1 fixed-wing	1 visual (656×492)	Electric	$5.5kg$

Note: (-) not mentioned; IR: Infrared; NIR: Near IR; VNIR: Visible-NIR.

1.2.3 Review on Vision Based Automatic Forest Fire Detection Techniques

The advantages of vision-based techniques have made them a major research topic in the field of forest fire monitoring and detection [13]. As outlined in Table 1.2, a sequence of near-operational field tests have been carried out in the past decade using vision-based UAV systems for forest fire detection, though practical firefighting tests are still rare.

Moreover, there are many research works using other platforms and offline videos to monitor and detect fires, as shown in Tables 1.3 and 1.4. Although these approaches are not originally designed for UAV application, they still can supply some inspiring insights into UAV-based forest

Table 1.2: UAV-based forest fire detection methods in near-operational field [1].

Detection Method	Spectral Bands	Resolution	Used Features	FD	SD	GL	PP	IS	References
Georeferenced uncertainty mosaic	IR	320×240	Color	√	×	√	√	√	[28]
Statistical data fusion	Visual Mid-IR	752×582 256×256	Color	√	×	√	√	√	[27]
Training method	IR	160×120	Color	√	×	×	×	√	[52]
Training method	Visual Far-IR	320×240 —	Color	√	×	√	×	√	[53, 54]
Training method	Visual Far-IR	320×240 —	Color	√	×	√	√	√	[19, 33]
—	Visual IR	720×640 —	Color	√	×	√	×	—	[39, 47]
Genetic algorithm	IR	320×240	Color	√	×	×	×	×	[55]
Training method	Visual IR	752×582 160×120	Color	√	×	√	×	—	[48, 56]
Training method	Visual IR	— —	Color	√	×	√	×	—	[40, 57]

Note: (√) considered; (×) not considered; (FD) Flame Detection; (SD) Smoke Detection; (GL) Geolocation; (PP) Propagation Prediction; (IS) Image Stabilization.

fire detection systems due to their common properties utilizing vision-based technologies in fire detection. For the purpose of saving the cost of devices development and personnel employment, as well as experimental time, the validity of various fire detection methodologies are usually tested and verified on forest fire videos in advance.

Over the last decade, a variety of vision-based techniques primarily focus on image/video processing algorithms. According to the spectral range of the camera used, vision-based fire detection technologies can generally be classified into either visual fire detection or IR fire detection systems [58]. Most of all, the *color* and *motion* of fire form the two dominant characteristic features for vision-based fire detection [59].

1.2.3.1 Fire Detection with Visual Images

In Tables 1.3 and 1.4, the color and motion features of the detected fire are usually utilized in the present studies, while discriminative properties in color spaces are commonly employed as a pre-processing step in the segmentation of fire regions in the images [60, 61]. In addition, most of researchers prefer to combine the color and motion features to offer more reliable fire detection

results, rather than only use color feature. As illustrated in Table 1.3, major efforts have been devoted into the investigation of offline video-based fire detection. Chen *et al.* [62] make use of color and motion features in a red, green, and blue (RGB) model to identify real fire and smoke in video sequences. The disordered characteristic of flame is as well dynamically analyzed to confirm the fire occurrence. Töreyin *et al.* [63] design a real-time scheme combining motion and color clues with fire flicker analysis on wavelet domain to do video fire detection. In [64], a common chromatic model based on RGB color model, motion information, and Markov process-enhanced fire flicker analysis are merged to build a whole fire detection system. Subsequently, the same fire detection approach is also adopted to distinguish potential smoke pixels in video samples for early fire alarm [65]. In [66], a rule-based generic color model for flame pixel classification is described, with test results demonstrating great improvement in detection performance. In [67], a method comprising four sub-algorithms for wildfire detection at night is presented and an adaptive active fusion approach is utilized to linearly form decisions from sub-algorithms. Continuing with previous work, Gunay *et al.* [68] design and apply an entropy-functional-based online adaptive decision fusion frame to discover the wildfires in video. A real-time fire detection approach utilizing an adaptive background subtraction algorithm is devised in [69] in order to distinguish foreground information; a statistical fire color model is then applied to check the occurrence of fires. In [70], a color-lookup table is employed with a great number of training images to identify the existence of suspicious fire regions and a temporal variation is also used to differentiate fires from fire color analogous objects. A support vector machine (SVM) based fire detection approach, which adopts a luminance map to eliminate non-fire pixels regions, is introduced in [71]. Moreover, a two-class SVM classifier with a radial basis function kernel is devised for the verification of fire presence in [71]; but it is difficult to make this classifier in real-time because of its excessive demand for computation time. Yuan *et al.* [14–16] address methods intended to successfully extract fire-pixels by taking the advantages of Lab color model capable of revealing fire color feature obviously, while in [14, 16] optical flow method is used to conduct motion detection and motion analysis for fire pixels confirmation; experimental results verify that the designed method can effectively

identify forest fire pixels. In [72], a benchmarking of state of the art color-based fire segmentation algorithm is proposed using a newly introduced fire dataset. According to the principal color of the fire, the luminosity, and the presence of smoke in the fire area, all images are characterized to determine the efficiency of algorithms on different kind of images. [73] presents a novel fire detection methods based on machine learning techniques and using all the rules as features; this method provides a very interesting tool for the future development of fire detection methods for unstructured environments.

Majority of the researches detect forest fires by flame, whereas smoke is also a prominent characteristic used in alarming the presence of forest fires. Tables 1.3 and 1.4 present some investigations that revolve around smoke detection. Chen *et al.* [74] combine a color-based static decision rule and a diffusion-based dynamic characteristic decision rule to extract smoke pixels. Experimental results validate that this method can offer an robust and cost-efficient solution for smoke classification. In [75], a real-time smoke detection method making use of texture analysis is investigated, while a back-propagation neural network is used as a distinguishing model. Experiments have verified that the devised algorithm is able to differentiate smoke and non-smoke images with a quick and low rate of false fire alarm. [76] proposes a smoke detection strategy adopting an accumulative motion model on whole images by smoke motion orientation estimation. Since the estimation accuracy can influence subsequent critical decisions, smoke orientation is accumulated over time as compensation for inaccuracy so that false alarm rate is reduced. [77] develops a real-time fire alarm system employing spectral, spatial, and temporal features of smoke, and utilizing fuzzy logic for extracting smoke. Experimental validations indicate that smoke can be successfully discriminated in different circumstances. However, further development to integrate such findings with existing surveillance systems and implement them in actual operations is still demanded. A scheme taking advantage of static and dynamic characteristic analysis for forest fire smoke detection is presented in [78]. Zhang *et al.* [79] use an Otsu-based strategy to segment both fire and smoke together. Yu *et al.* [80] adopt both color-based decision rules and optical flow technique to extract the color and motion features of smoke. Experiments prove that video detection accuracy

11

has been significantly improved. Although a variety of forest fire detection techniques have been developed experimentally, currently only several studies have been conducted in near operational environments (as shown in Table 1.2). Most of these research have been carried out by a research group from the University of Seville in Spain. These tests utilize multiple UAVs and make use of color feature to detect forest fires.

In recent years, intelligent methods have been widely adopted to lower false alarm rates. As presented in Table 1.3, the commonly used algorithms [69,77,80,81] are artificial neural networks (ANNs), fuzzy logic, and fuzzy neural networks. Experimental validations indicate that these methods can effectively detect fires, but most of them have not been evaluated on UAVs or in practical forest fire scenarios.

1.2.3.2 Fire Detection with Infrared Images

Since infrared (IR) images can be captured in either weak or no light situations while smoke is transparent in IR images, it is therefore applicative and practical to detect fires in both daytime and nighttime. Tables 1.2 and 1.4 list fire detection studies done by IR cameras. [48,53] take advantage of a training-based threshold selection method [52] to obtain binary images containing fire pixels from IR images. The false alarm rates are significantly reduced, since the appearance of fire is a high intensity region in IR images. Bosch *et al.* [30] detect the occurrence of forest fires in IR images by using decision fusion. Various useful information for the fire detection can be acquired by this method. Pastor *et al.* [82] use linear transformations to precisely calculate the rate of spread (ROS) of forest fires in IR images, while a threshold-value-searching criterion is applied to locate the flame front position. Ononye *et al.* [83] illustrate a multi-spectral IR image processing method which is capable of automatically obtaining the forest fire perimeter, active fire line, and fire propagation tendency. The proposed method is developed based on a sequence of image processing tools and a dynamic data-driven application system (DDDAS) concept. Huseynov *et al.* [84] devise a multiple ANNs model for distinguishing flame in IR images. The experimental results show that the proposed approach can reduce training time and improve the success rate of classification.

One issue related to processing images collected by IR cameras is that miniaturized cameras still have low sensitivity [48]. This phenomenon demands an augment in detector exposure periods to produce higher-quality images. In addition, the high frequency of vibration of UAV can lead to blurring images, which remains a major difficulty in their development.

1.2.3.3   Fusion of Visual and Infrared Images

At present, it is confirmed that visual and IR images can be fused together to improve the accuracy, reliability, and robustness of fire detection algorithms, while reducing the rate of false alarms. These improvements are achieved by making use of fuzzy logic, intelligent, probabilistic, and statistical methods (as described in Tables 1.2 and 1.4).

Arrue *et al.* [85] develop a system comprised of IR image processing, ANNs, and fuzzy logic to decrease the false alarm rate. In their research, matching the information excessiveness of visual and IR images is used to confirm forest fires. [56] adopts both IR and visual cameras for fire front parameter estimation through visual and IR image processing techniques, whereas experimental tests are only carried out in a laboratory. After that, Martinez-de Dios *et al.* [4] illustrate a forest fire perception system using computer vision techniques. Visual and IR images are fused to compute a three-dimensional fire perception model so that the fire evolution can be visualized through remote computer systems.

Although various image fusion approaches have been proposed in the existing research, how to optimize the number of features that are used in fire detection remains a challenging problem. Solving this problem can not only decrease the computation burden of onboard computers, but also lower both the cost of hardware and the rate of false alarms.

Table 1.3: Offline video fire detection methodologies using visual cameras [1].

Detection Method	Resolution	Color	Motion	Geometry	FD	SD	References
Statistic method	320×240 400×255	√	×	×	√	×	[86]
Fuzzy logic	256×256	√	×	×	√	×	[59]
SVM	—	√	√	√	√	×	[87]
Fuzzy logic	320×240	√	√	√	×	√	[77]
Wavelet analysis	320×240	√	√	√	√	×	[64]
Computer-vision	320×240	√	√	×	√	×	[88]
Wavelet analysis	320×240	√	√	×	√	×	[63]
Rule-based video processing	—	√	√	×	√	√	[62]
Fourier transform	—	√	√	×	√	×	[89]
Bayes and fuzzy c-means	—	√	√	×	√	×	[90]
Adaptable updating target extraction	—	√	√	×	√	×	[91]
Histogram based method	—	√	√	×	√	×	[92]
Fuzzy-neural network	—	√	√	×	√	×	[93]
Statistical method	176×144	√	×	×	√	×	[69]
Fuzzy finite automata	—	√	√	×	√	×	[81]
Gaussian mixture model	320×240	√	√	×	√	×	[94]
Histogram back projection	—	√	×	×	√	×	[95]
Wavelet analysis	—	√	√	×	×	√	[65]
Adaptive decision fusion	—	√	√	×	×	√	[68]
Accumulative motion model	—	×	√	×	×	√	[76]
Image processing method	—	√	√	×	×	√	[78]
Neural network	320×240	√	√	×	×	√	[80]

Note: (√) considered; (×) not considered; (—) not mentioned; (FD) Flame Detection; (SD) Smoke Detection.

1.3 Problem Formulation

Many techniques have been used for forest fire detection. However, the existing approaches still have various practical issues for their use in operational conditions. Using UAV-based systems to detect forest fire can provide rapid and low-cost way to satisfy the critical requirements of forest fire fighting, as they can avoid the drawbacks of systems based on satellites, manned aerial vehicles and ground equipments. Although the existing research demonstrates the possibility and potential benefits of using UAVs to detect forest fires, development of such systems, including related hardware, software and application strategies, is still minimal in the previous limited number of research works. Further investigation is demanded on all aspects of their use, including suitable system platforms, remote sensing payloads/sensors, and algorithms for GNC, as well as remote sensing techniques. Moreover, the combination of UAV and remote sensing techniques is also particularly challenging.

Table 1.4: Fire detection methodologies using visual and IR cameras [1].

Detection Method	Spectral Bands	Resolution	OV	IV	OLV	CF	MF	GF	FD	SD	PP	GL	References
Training method	Visual Mid-IR	752×582 256×256	×	√	×	√	×	×	√	×	√	√	[56]
Training method	Visual Mid-IR	— —	√	×	×	√	×	×	√	×	√	√	[4]
Images matching	Visual IR	— —	√	×	×	√	√	√	×	√	×	√	[22, 85]
Data fusion	Visual IR	— —	×	√	×	√	—	—	√	√	×	×	[30]
Neural networks	IR	—	×	√	×	√	√	√	×	×	×	×	[84]
Dynamic data-driven	Multi-spectral IR	—	×	×	√	√	×	√	√	×	√	×	[83]

Note: (√) considered; (×) not considered; (—) not mentioned; (OV) Outdoor validation; (IV) Indoor validation; (OLV) Offline validation; (CF) Color feature; (MF) Motion feature; (GF) Geometry feature; (FD) Flame Detection; (SD) Smoke Detection; (GL) Geolocation; (PP) Propagation Prediction; (IS) Image Stabilization.

In addition, UAV-based forest fire detection remains difficult, given highly complex, non-structured environments of forest, the chance of smoke blocking the images of the fire, or the chance for analogues of flame characteristics, such as sunlight, vegetation, and animals, or the vibration and motion of cameras mounted on UAVs, either false alarms or alarm failures are often caused. How to reduce false alarm rates, increase high detection probability, and enhance adaptive capabilities in various kinds of environmental conditions to improve the reliability and robustness of forest fire detection are all worth further investigation.

Although the few existing researches have verified that the fusion of IR and visual images can contribute to the accuracy of forest fire detection with high detection probability, how to decrease false alarm rates and improve adaptability in a variety of environmental circumstances are still challenging issues which need to be further studied, in particular for the situation with application to UAV systems.

In general, the developed vision-based fire detection methods are applied with stationary cameras by separating fires from the static backgrounds. However, the techniques using/involving motion features of fire for fire detection may fail to perform as expected when cameras are attached to UAVs which are moving during the entire operation period. Under this circumstance,

objects (including the interested objects and background) in the captured images are all moving, which is the primary cause of the failure in fire detection.

1.4 Objectives of This Thesis

In order to achieve the goals of automatic forest fire detection using UAVs, this thesis aims to design and develop novel vision-based forest fire detection schemes that are capable of effectively detecting and alarming forest fires with application to UAV-based forest fire surveillance systems. In particular, this thesis is organized for the following research objectives:

- Design and develop effective forest fire detection techniques based on visual images.

- Design and develop effective forest fire detection techniques based on IR images.

- Investigate information fusion (including visual and IR images) schemes/strategies to improve the reliability and accuracy of fire detection so as to significantly reduce the rate of false fire alarm.

- Design and develop smoke detection schemes to achieve earlier fire detection so as to further improve the reliability and robustness of fire detection as well as save more time for firefighting and reduce property losses.

To sum up, this thesis (as shown in Fig. 1.3) is primarily intended to propose advanced fire monitoring and detection techniques which in turn can guarantee the reliable and satisfactory performance of forest fire detection at both visual and IR levels with application to UAV-based forest fire surveillance system. The schemes and strategies developed in this thesis are verified by a series of aerial images/videos in the presence of forest fire scenarios and indoor simulation with a real UAV system.

1.5   Contributions of This Thesis

Although a variety of fire detection methodologies have been developed and proposed, only several research studies have considered forest fire scenarios and few relative experiments have been conducted for detecting forest fires using UAVs. The merits of this research can be reflected by significant contributions to the realization of a new concept and technology of UAV-based forest fire surveillance. The main contributions of this thesis can be categorized into the following major aspects:

(1) *Reliable fire detection using visual images with application to UAV system*

    (a) Design of a fire detection scheme using fire color feature in visual images.

    (b) Design of a fire detection scheme using fire motion feature in visual images.

    (c) Design of a fire detection scheme using both color and motion features in visual images.

(2) *Reliable fire detection using IR images with application to UAV system*

    (a) Design of a fire detection scheme using fire brightness feature in IR images.

    (b) Design of a fire detection scheme using fire motion feature in IR images.

    (c) Design of a fire detection scheme using both brightness and motion features in IR images.

(3) *Reliable smoke detection using visual images with application to UAV system*

(4) *Fusion of visual and IR images*: Using common information in the segmented visual and IR images to improve the detection performance.

(5) *UAV experimental platform development*: Development and system integration of UAV and computer vision system.

In addition, the knowledge and experience gained in this thesis can be not only used in forest fire detection for UAV-based fire surveillance, but also transferable towards other firefighting applicaiton such as fire suveilliance of oil fields, pipelines, electric power lines and nuclear

power plants, and public area which significantly contribute to infrastructure and public safety. Although the tasks and objectives of this thesis are targeted mainly for UAV-based forest fires detection, the developed technologies and techniques can be straightforwardly adopted for other manned/unmanned mobile forest fire detection platforms. To sum up, the outcome of this thesis in the long-term is expected to evolve into innovative inventions enhancing natural resources and environmental sustainability and protection, safety and security of society, reduce the economic losses, and save more lives from forest fires.

1.6 Organization of This Thesis

The remainder of this thesis is organized as follows:

- Chapter 2 provides an overview of some preliminary knowledges which will facilitate the reading of this thesis.

- Chapter 3 addresses a novel method of UAV-based forest fire detection in visible range images. In order to improve the accuracy of fire detection, both color and motion features are adopted to process images captured from a camera installed on a UAV which is moving during the entire mission period. First, a color-based detection rule is designed for isolating fire-colored pixels by using fire chromatic characteristics in the so-called Lab color model. Then two types of optical flow algorithms are combined to further analyse the isolated fire-colored regions from color-based detection, one is a classic artificial optical flow for estimating the motion of camera, while the other one is based on the optimal mass transport theory for fire detection.

- Chapter 4 introduces the proposed fire detection algorithm dealing with IR images, this algorithm takes advantages of both brightness and motion features of fire for achieving good detection performance. In addition, the data fusion technique combining information from both visual and IR cameras is illustrated as well.

- Chapter 5 presents a new learning-based fuzzy smoke detection methodology using color feature of smoke and an extended Kalman filter for training the fuzzy smoke detection rule, an effective early fire detection is expected.

- Chapter 6 presents conclusions of the conducted research works, and summarizes several predominant ideas for the future developments of the thesis's outcomes.

1.7 Publications During the Thesis Work

- Journal Papers

  (1) Chi Yuan, Youmin Zhang, & Zhixiang Liu (2015). A survey on computer vision based technologies for automatic forest fire detection using UAVs and remote sensing techniques. *Canadian Journal of Forest Research*, 45(7): 783-792. DOI: 10.1139/cjfr-2014-0347.

  (2) Chi Yuan, Zhixiang Liu, & Youmin Zhang (2017). Forest fire detection in aerial images for firefighting using optical remote sensing techniques and unmanned aerial vehicles. *Journal of Intelligent and Robotic Systems*, First Online: 05 January 2017. DOI:10.1007/s10846-016-0464-7.

  (3) Chi Yuan, Zhixiang Liu, & Youmin Zhang (2017). Automatic fire detection in aerial images for UAV-based forest fire surveillance. *International Journal of Wildland Fire* (To be submitted).

  (4) Chi Yuan, Zhixiang Liu, & Youmin Zhang (2017). Smoke detection for UAV-based forest fire surveillance using computer vision techniques. *Canadian Journal of Forest Research* (To be submitted).

  (5) Zhixiang Liu, Youmin Zhang, Xiang Yu, & Chi Yuan (2016). Unmanned surface vehicles: An overview of developments and challenges. *Annual Reviews in Control*, 41: 71-93. DOI:10.1016/j.arcontrol.2016.04.018.

(6) Zhixiang Liu, Chi Yuan, Youmin Zhang, & Jun Luo (2015). A learning-based fault tolerant tracking control of an unmanned quadrotor helicopter. *Journal of Intelligent and Robotic Systems*, 84(1): 145-162. DOI: 10.1007/s10846-015-0293-0.

(7) Zhixiang Liu, Chi Yuan, Xiang Yu, & Youmin Zhang (2016). Leader-follower formation control of unmanned aerial vehicles in the presence of obstacles and actuator faults. *Unmanned Systems*, 4(3): 197-211.

(8) Zhixiang Liu, Chi Yuan, & Youmin Zhang (2017). Active fault-tolerant control of unmanned quadrotor helicopter using linear parameter varying technique. *Journal of Intelligent and Robotic Systems*, First Online: 29 March 2017, DOI: 10.1007/s10846-017-0535-4.

(9) Zhixiang Liu, Chi Yuan, & Youmin Zhang (2016). Reliable and safe line-of-sight path following control of unmanned surface vehicle. *IEEE Transactions on Control Systems Technology* (Under review).

(10) Zhixiang Liu, Chi Yuan, & Youmin Zhang (2016). Adaptive fault-tolerant tracking control of an unmanned quadrotor helicopter considering actuator dynamics. *International Journal of Robust and Nonlinear Control* (Under review).

- Conference Papers

(1) Chi Yuan, Zhixiang Liu, & Youmin Zhang (2017). Fire detection using infrared images for UAV-based forest fire surveillance. *The International Conference on Unmanned Aircraft Systems (ICUAS 2017)*, June 13-16, 2017, Miami, FL, USA (Accepted on April 12, 2017).

(2) Chi Yuan, Zhixiang Liu, & Youmin Zhang (2016). Vision-based forest fire detection in aerial images for firefighting using UAVs. *The International Conference on Unmanned Aircraft Systems (ICUAS 2016)*, June 7-10, 2016, Arlington, VA, USA.

(3) Chi Yuan, Khaled A. Ghamry, Zhixiang Liu, & Youmin Zhang (2016). Unmanned aerial vehicle based forest fire monitoring and detection using image processing technique. *The IEEE Chinese Guidance, Navigation and Control Conference (CGNCC 2016)*, August 12-14, 2016, Nanjing, Jiangsu, China.

(4) Chi Yuan, Zhixiang Liu, & Youmin Zhang (2015). UAVs based forest fire detection and tracking using image processing techniques. *The International Conference on Unmanned Aircraft Systems (ICUAS 2015)*, June 9-12, 2015, Denver, CO, USA.

(5) Chi Yuan, Youmin Zhang, & Zhixiang Liu (2014). Automatic vision-based forest fire detection technologies for unmanned aerial vehicles: A review. *The International Conference on Intelligent Unmanned Systems (ICIUS 2014)*, September 29 - October 1, 2014, Montreal, QC, Canada.

(6) Zhixiang Liu, Laurent Ciarletta, Chi Yuan, Youmin Zhang, & Didier Theilliol (2017). Path following control of unmanned quadrotor helicopter with obstacle avoidance capability. *The International Conference on Unmanned Aircraft Systems (ICUAS 2017)*, June 13-16, 2017, Miami, FL, USA (Accepted on April 12, 2017).

(7) Zhixiang Liu, Chi Yuan, & Youmin Zhang (2016). Adaptive fault-tolerant control of unmanned quadrotor helicopter using linear parameter varying control technique. *The International Conference on Unmanned Aircraft Systems (ICUAS 2016)*, June 7-10,

2016, Arlington, VA, USA.

(8) Zhixiang Liu, Chi Yuan, & Youmin Zhang (2016). Linear parameter varying control of unmanned quadrotor helicopter with mass variation and battery drainage. *The IEEE Chinese Guidance, Navigation and Control Conference (CGNCC 2016)*, August 12-14, 2016, Nanjing, Jiangsu, China.

(9) Zhixiang Liu, Chi Yuan, & Youmin Zhang (2016). A hybrid collision avoidance method for unmanned surface vehicle considering international maritime regulation. *The International Conference on Intelligent Unmanned Systems (ICIUS 2016)*, August 23-25, 2016, Xi'an, Shaanxi, China.

(10) Zhixiang Liu, Xiang Yu, Youmin Zhang, Chi Yuan, & Jun Luo (2015). Active disturbance compensating tracking control of an unmanned quadrotor helicopter. *The ASME 2015 International Design Engineering Technical Conferences & Computers and Information in Engineering Conference (IDETC/CIE 2015)*, August 2-5, 2015, Boston, MA, USA.

(11) Zhixiang Liu, Xiang Yu, Chi Yuan, & Youmin Zhang (2015). Leader-follower formation control of unmanned aerial vehicles with fault tolerant and collision avoidance capabilities. *The International Conference on Unmanned Aircraft Systems (ICUAS 2015)*, June 9-12, 2015, Denver, CO, USA.

(12) Zhixiang Liu, Youmin Zhang, Chi Yuan, & Jun Luo (2015). An adaptive linear parameter varying fault tolerant control scheme for unmanned surface vehicle steering control. *The 34th Chinese Control Conference and SICE Annual Conference (CCC&SICE 2015)*, July 28 - 30, 2015, Hangzhou, Jiangsu, China.

(13) Zhixiang Liu, Chi Yuan, & Youmin Zhang (2015). Linear parameter varying adaptive control of an unmanned surface vehicle. *The 10th IFAC Conference on Manoeuvring and Control of Marine Craft (MCMC 2015)*, August 22-26, 2015, Copenhagen, Denmark.

(14) Zhixiang Liu, Youmin Zhang, & Chi Yuan (2015). Active fault tolerant control of an unmanned surface vehicle. *The 15th International Conference on Control, Automation and Systems (ICCAS 2015)*, October 13-16, 2015, Busan, Korea.

(15) Zhixiang Liu, Youmin Zhang, & Chi Yuan (2015). A survey of recent developments and challenges on unmanned surface vehicles. *The 2015 Unmanned Systems Canada Annual Conference*, November 3-5, 2015, Halifax, NS, Canada.

(16) Zhixiang Liu, Chi Yuan, Youmin Zhang, & Jun Luo (2014). A learning-based fuzzy LQR control scheme for height control of an unmanned quadrotor helicopter. *The International Conference on Unmanned Aircraft Systems (ICUAS 2014)*, May 27-30, 2014, Orlando, FL, USA.

(17) Zhixiang Liu, Xiang Yu, Youmin Zhang, Chi Yuan, & Jun Luo (2014). Straight line following active disturbances attenuation control of an unmanned surface vehicle. *The International Conference on Intelligent Unmanned Systems (ICIUS 2014)*, September 29 - October 1, 2014, Montreal, QC, Canada.

(18) Youmin Zhang, Didier Theilliol, Xiang Yu, Chi Yuan, & Zhixiang Liu (2015). New development and applications on sense & avoid, fault-tolerant & cooperative control of unmanned systems (Pre-conference Workshop Presentation). *The International Conference on Unmanned Aircraft Systems (ICUAS 2015)*, June 9-12, 2015, Denver, CO, USA.

Chapter 2

Preliminaries

Vision-based fire detection mainly depends on the image segmentation techniques by making use of fire characteristics shown in the images captured from cameras. Color and motion features, which are the primary features of fire, have been widely used in image segmentation. The main objective of image segmentation is to differentiate fire pixels from background pixels. The techniques that are commonly applied for image segmentation can be chosen according to the type of image: visual or infrared (Figs. 2.1 and 2.2 show visual and infrared images taken by a UAV and its corresponding segmented images).

Figure 2.1: Segmentation of visual image: original (left) and segmented (right) images [2].
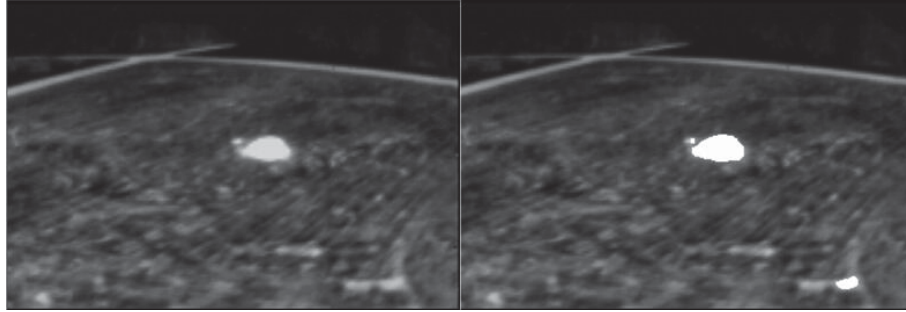
Figure 2.2: Segmentation of infrared image: original (left) and segmented (right) images [2].

2.1 Color Models

As a dominant feature of fire, color is the earliest and most popularly used feature in the development of detection techniques adopted in the vision-based forest fire detection applications [58]. The color information is usually used as a pre-processing step in the detection of potential fire. A variety of algorithms taking advantage of the discriminative properties in color space are developed to obtain fire regions in the image. Generally, the decision rules are built in specified color space to represent fire colors in the image and then thresholding technique is used to segment fire regions based on such rules.

A color space (also called color model), which is a specification of a coordinate system, aims to establish the specification of colors in a standard and commonly accepted way [3]. In the field of digital image processing, RGB color model, hue, saturation and intensity (HSI) color model, hue, saturation and value (HSV) color model, and Lab color model are the predominant models for image processing. They have been widely adopted to represent images in corresponding color spaces. Figs. 2.3 and 2.4 display fire in each channels of different color models.

2.1.1 RGB Color Model

The RGB color model is an additive color model in which three spectral components (red, green and blue) are mixed together in various means to reform a broad array of colors. The prime function of the RGB color model is for the perception, representation, and display of images in electronic systems, such as computers, televisions, and mobile phones.

25
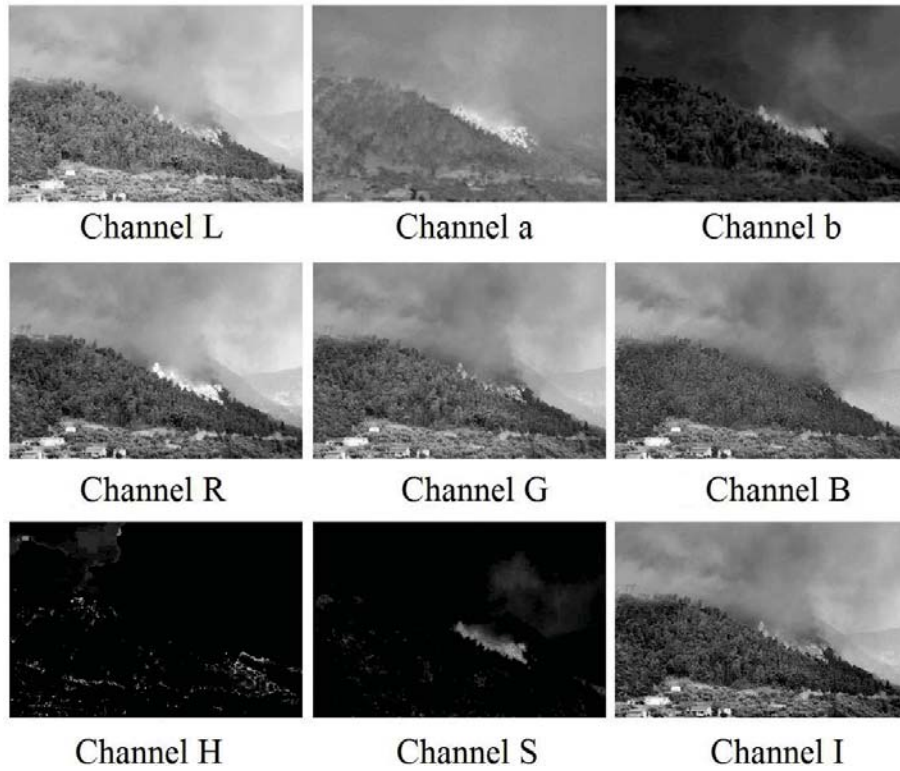
Figure 2.3: Forest fires display in different color channels (Scenario 1).
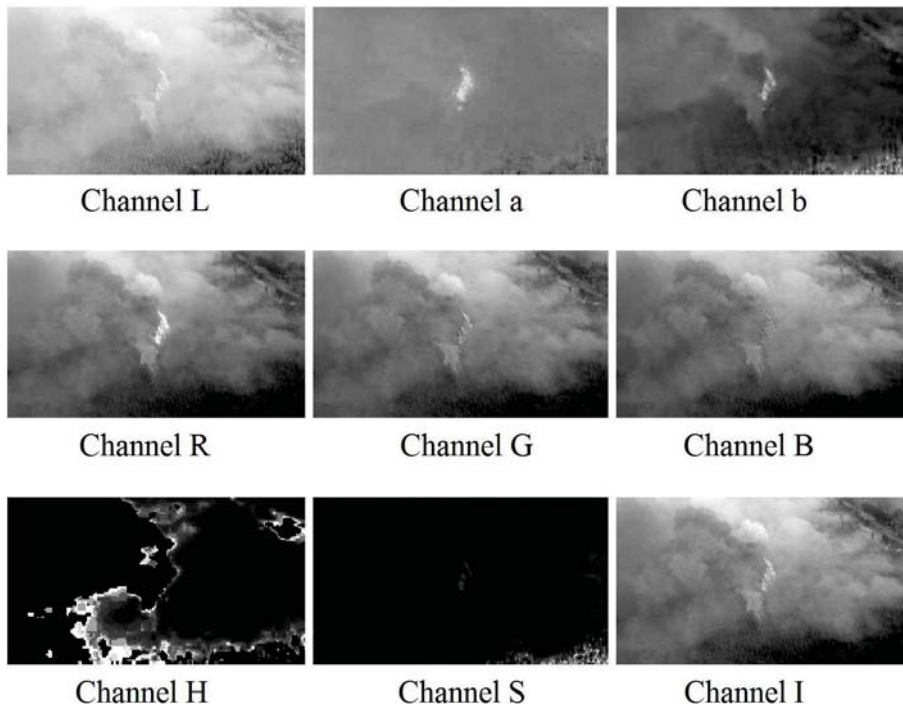
Figure 2.4: Forest fires display in different color channels (Scenario 2).
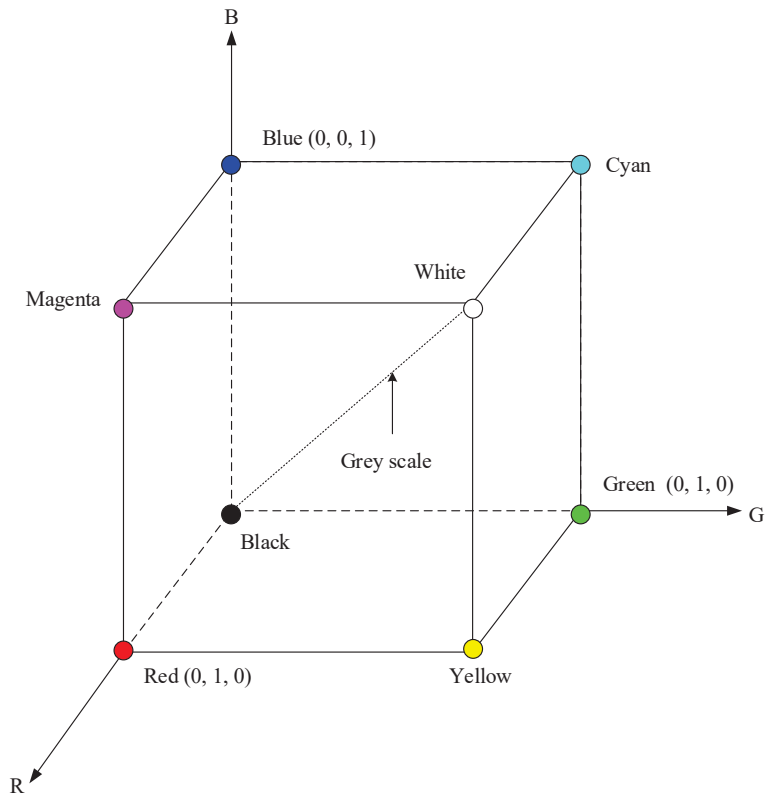
Figure 2.5: Illustration of RGB color model [3].

The RGB color model is built upon a Cartesian coordinate system as shown in the cube of Fig. 2.5. In this cubic model, the values of R, G, and B are coordinate axes and the range of values is assumed to be normalized within $[0, 1]$; each color can be described as a point in or on the cube by the coordinates of three components R, G, and B; the primary colors red, green, and blue are at three corners $(1, 0, 0), (0, 1, 0), (0, 0, 1)$; three other corners $(0, 1, 1), (1, 0, 1), (1, 1, 0)$ denote secondary colors cyan, magenta, and yellow, respectively; black is at the origin $(0, 0, 0)$, while white is at the corner $(1, 1, 1)$; the gray scale which are points of equal R, G, B values spread from black to white along the line jointing the origin and the corner farthest from the origin.
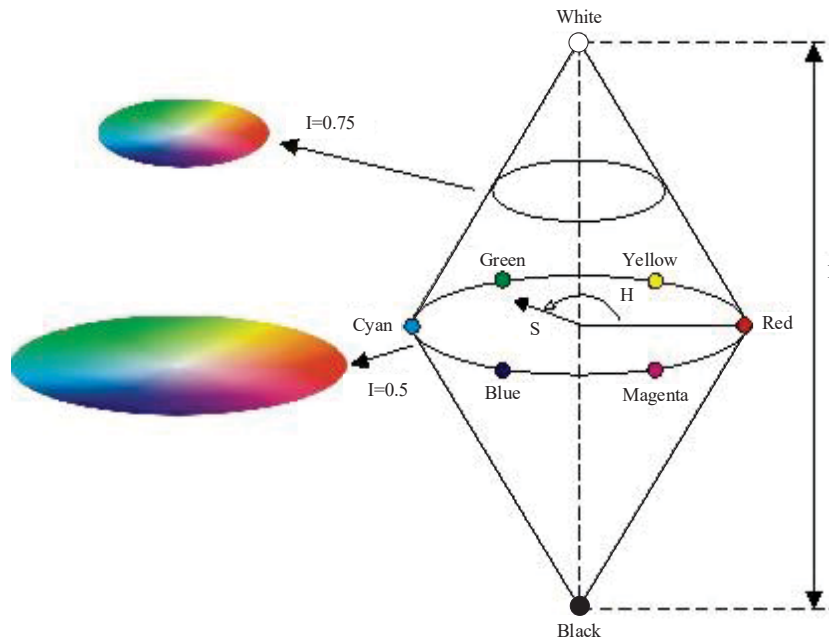
Figure 2.6: Illustration of HSI color model [3].

2.1.2 HSI Color Model

The HSI color model is a very important and attractive model for developing image processing algorithms due to the fact that the color definitions in HSI color model are intuitive, natural, and ideal to human. When human observe a color object, hue, saturation, and brightness are used to describe it. Similar to the way of human interpretation, the HSI color model defines every color with three elements: hue, saturation, and intensity. Fig. 2.6 illustrates the representation of colors in HSI color model.

The hue component H illustrates the chrominance itself in the form of an angle ranging from $0°$ to $360°$. The primary colors (red, green, and blue) are divided by $120°$ and the secondary colors cyan, magenta, and yellow are $60°$ from primary colors, respectively. In other words, $0°$, $120°$, and $240°$ denote red, green, and blue while $60°$, $180°$, and $300°$ denote cyan, magenta, and yellow. The saturation component S represents how much the color is mixed with white color. The range of the S component is normalized in $[0, 1]$. The intensity component I also ranges during $[0, 1]$. Value 0

means black and value 1 signals white.

Since digital cameras are typical RGB input devices, images obtained from cameras are usually represented by RGB format. Given an image in RGB format, it can be converted to HSI space by the following equation [3]:

$$
\begin{aligned}
H &= \begin{cases} \Theta, & \text{if } (B \leqslant G) \\ 360 - \Theta, & \text{if } (B > G) \end{cases} \\
I &= \frac{R + G + B}{3} \\
S &= 1 - \frac{3}{(R + G + B)} \min(R, G, B) \\
\Theta &= \cos^{-1} \left(\frac{\frac{1}{2}((R - G) + (R - B))}{[(R - G)^2 + (R - B)(G - B)]^{\frac{1}{2}}} \right)
\end{aligned}
\tag{1}
$$

where R, G, and B are the values of red, green, and blue in RGB color model, respectively.

2.1.3 HSV Color Model

Hue, saturation, and value (HSV) color model is one of the most common cylindrical-coordinate representations of points in an RGB color space. HSV stands for its three components: hue, saturation, and value. Similar to HSI color space, it rearranges the geometry of RGB to become more intuitive and perceptual than the Cartesian (cube) representation.

In the cylinder (as shown in Fig. 2.7), hue, saturation, and value are represented by the angle around the central vertical axis, the distance from the axis, and the distance along the axis respectively. In this cylindrical geometry, hue starts at the red primary at $0°$, wrapping through the green primary at $120°$ and the blue primary at $240°$. The central vertical axis is consisted of the neutral, achromatic, or gray colors, ranging from the bottom (black at value 0) to the top (white at value 1).

As aforementioned, most cameras output RGB images, there is also a necessity to covert RGB
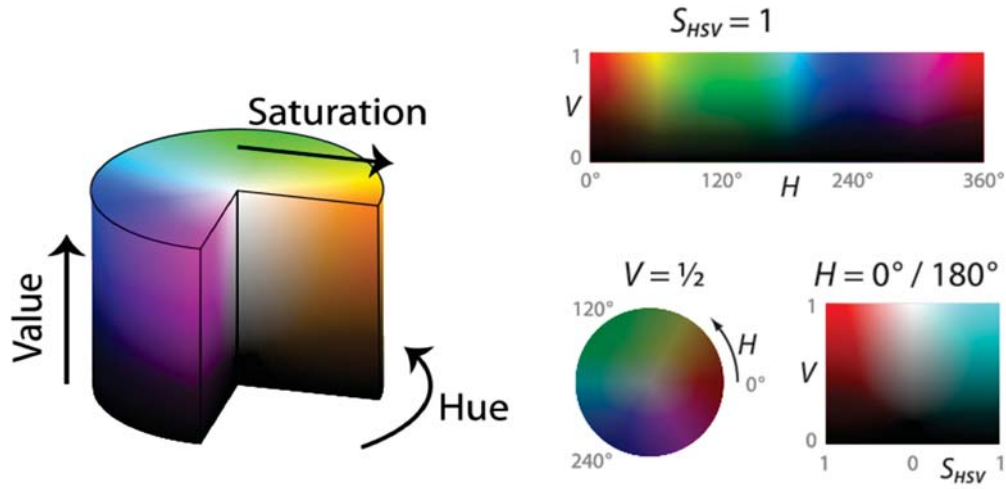
Figure 2.7: Illustration of HSV color model.

color model to HSV color model. The conversion principle can be formulated as follows:

$$V = \max(R, G, B)$$

$$S = \begin{cases} 0, & \text{if } (\max(R,G,B) = 0) \\[2mm] \frac{\max(R,G,B) - \min(R,G,B)}{\max(R,G,B)}, & \text{otherwise} \end{cases}$$

$$H = \begin{cases} \text{undefined}, & \text{if } (S = 0) \\[2mm] 60 \times \frac{G-B}{\max(R,G,B) - \min(R,G,B)}, & \text{if } (\max(R,G,B) = R) \& (G \geqslant B) \\[2mm] 60 \times \frac{G-B}{\max(R,G,B) - \min(R,G,B)} + 360, & \text{if } (\max(R,G,B) = R) \& (G < B) \\[2mm] 60 \times \frac{B-R}{\max(R,G,B) - \min(R,G,B)} + 120, & \text{if } (\max(R,G,B) = G) \\[2mm] 60 \times \frac{R-G}{\max(R,G,B) - \min(R,G,B)} + 240, & \text{if } (\max(R,G,B) = B) \end{cases} \tag{2}$$

2.1.4 Lab Color Model

The Lab color model is designed to approximate all perceivable colors of human vision, which means its gamut outweighs those of the RGB and HSI color models as well. Unlike the RGB and HSI color models, Lab color model is an absolute color space which does not depend on devices such as cameras, monitors and printers. The merit of device independence is that Lab color model
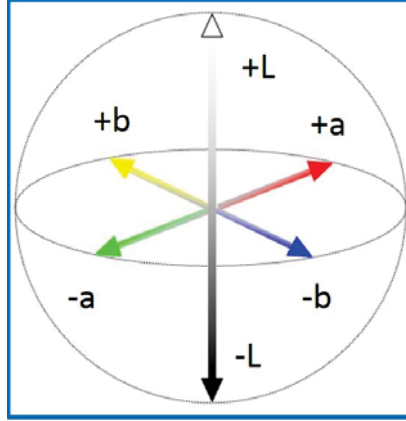
Figure 2.8: Illustration of Lab color model.

can define colors accurately without the influence of their nature of creation or the device they are displayed on.

As presented in Fig. 2.8, the Lab color model comprises three portions: the luminance L, the chrominance a, and the chrominance b. Luminance L represents the intensity ranges from the darkest black to the brightest white. The scaling of L values run in the range from 0 to 100. Chrominance a denotes that the color varies from red to green, with red at positive a value and green at negative a value. Chrominance b indicates the color changes from yellow to blue, with yellow at positive b value and blue at negative b value. The scale of a and b values are normally confined in $[-128, 127]$.

In order to covert RGB color model to Lab color model, the following rules can be used:

$$
\begin{aligned}
L =& 116 \times (0.299R + 0.587G + 0.114B)^{1/3} - 16, \\
a =& 500 \times [1.006 \times (0.607R + 0.174G + 0.201B)^{1/3} - (0.299R + 0.587G \\
& + 0.114B)^{1/3}], \\
b =& 200 \times [(0.299R + 0.587G + 0.114B)^{1/3} - 0.846 \times (0.066G + 1.117B)^{1/3}].
\end{aligned}
\tag{3}
$$

2.2 Moving Object Segmentation

The first step of automatic vision-based surveillance is to segment interesting objects in the field of view of the camera. The interesting objects are defined as potential targets of detection which are context dependent. For a general detection system, the moving zones of the video sequence, such as people and vehicles, are mostly treated as the interesting areas. Segmentation of interesting areas is an essential and crucial assignment, as faults made at this step are difficult to correct in subsequent processing including object tracking and classification [96]. In other words, accurate segmentation can produce more precise results of detection.

Many motion detection methods have been extensively investigated. At present, most of the existing motion segmentation methods adopt either temporal or spatial video information and can be summarized into four major categories: temporal differencing, background subtraction, statistical analysis, and optical flow [96].

2.2.1 Temporal Differencing

Temporal differencing is a direct motion detection method by making use of temporal difference of consecutive frames in video sequence. The absolute difference of each pixel between two or three consecutive frames can be computed and a threshold is utilized to obtain the motion object, such as a three-frame-difference algorithm used in [97].

Temporal differencing is simple to implement and highly adaptive to dynamic environments, but it is not so effective to extract the whole region or the complete shapes of the moving objects, especially does poor job in segmenting the inner part of the moving object.

2.2.2 Background Subtraction

Background subtraction is a frequently used approach for motion segmentation, particularly in the situation when the background is relatively static. In this method, stationary pixels in the image are defined as the background since the background can be seen as temporally static part

of the image. If the background scene is observed for a period, then pixels constituting the whole background can be calculated and modelled. For instance, the background can be estimated by averaging consecutive initialization frames, because moving regions and objects occupy only some parts of the background scene in the image and their effect is counteracted over time by averaging. After the background model is known, the moving pixels are determined if the pixel-by-pixel difference between previous and current frames exceeds a threshold.

Although background subtraction techniques are good at isolating the relevant pixels of moving regions in most cases, they become vulnerable when the scene is more complex, for example there are dynamic changes, such as moving leaves or sudden illumination changes. Since it is assumed that the camera is stationary, background model cannot represent the background very well if the background is changing as well.

2.2.3 Statistical Based Methods

Statistical based methods utilizing the statistical characteristics of individual pixels have been investigated to improve the basic background subtraction with more reliability in complex scenes that contain noises, illumination changes and shadow. Inspired by the background subtraction methods, advanced statistical approaches gather and dynamically update statistics of the pixels that belong to the background so that achieving the goals of overcoming the weakness of background subtraction methods. Foreground pixels (moving pixels in the images) are distinguished by matching each pixel's statistics with that of the improved background model.

Because the statistical methods are based on the principle of background subtraction, they perform well in the situation that the surveillance camera is static.

2.2.4 Optical Flow

Optical flow is described as the two-dimensional distribution of apparent motion velocities of brightness patterns in an image plane. This feature can be applied to estimate local image pixel's movement and specify the velocity of each image pixel between adjacent images. Each pixel in

the image corresponds to one velocity vector, and these velocity vectors compose an optical flow field. In brief, optical flow is capable of converting image information into estimated motion fields for a more advanced analysis.

The key idea of this technique is based on a brightness constancy conception. If the movement is comparatively small and illumination of the circumstance remains uniform in space and steady during a period, it is presumed that the brightness of a particular point maintains constant in time of the movement. The brightness consistency assumption is mathematically represented by the following equation:

$$\frac{d}{dt}I = \frac{\partial I}{\partial x}u + \frac{\partial I}{\partial y}v + \frac{\partial I}{\partial t} = I_x u + I_y v + I_t = 0, \tag{4}$$

where $I(x, y, t)$ is a function of image intensity of spatial coordinates (x, y) and time t. The flow vector $(u, v) = (x_t, y_t)$ directs to the motion direction of pixel (x, y).

Obviously, only one equation is not sufficient to compute the two unknowns in (u, v), which is known as the "aperture problem", additional constraints are demanded. Various optical flow techniques have been proposed to solve the aperture problem, such as matching, differential, energy-based methods. Horn and Schunck algorithm [98] and Lucas and Kanade algorithm [99] are two classical calculation methods which are widely used in motion detection.

2.2.4.1 Horn and Schunck Optical Flow

Horn and Schunck algorithm [98] hypothesizes that the optical flow is smooth over the entire image and adds an additional constraint with (4) to compute the velocity (u, v) by minimizing:

$$\int \int (I_x u + I_y v + I_t)^2 dxdy + \alpha(||\nabla u||_2^2 + ||\nabla v||_2^2)dxdy, \tag{5}$$

where the constant α regularizes the smoothness term, ∇u and ∇v denote the Laplacians of u and v, respectively, which are defined as follows:

$$\nabla^2 u = \frac{\partial^2 u}{\partial^2 x} + \frac{\partial^2 u}{\partial^2 y} \quad \text{and} \quad \nabla^2 v = \frac{\partial^2 v}{\partial^2 x} + \frac{\partial^2 v}{\partial^2 y}. \tag{6}$$

Then (u, v) can be obtained by minimizing (5) and solving the following two iterative equations:

$$
\begin{aligned}
u_{x,y}^{n+1} &= \bar{u}_{x,y}^{n} - \frac{I_x[I_x \bar{u}_{x,y}^{n} + I_y \bar{v}_{x,y}^{n} + I_t]}{\alpha^2 + I_x^2 + I_y^2}, \\
v_{x,y}^{n+1} &= \bar{v}_{x,y}^{n} - \frac{I_y[I_x \bar{u}_{x,y}^{n} + I_y \bar{v}_{x,y}^{n} + I_t]}{\alpha^2 + I_x^2 + I_y^2},
\end{aligned}
\tag{7}
$$

where n denotes the iteration integer, $[u_{x,y}^{n}, v_{x,y}^{n}]$ denotes the velocity estimates for the pixel at (x, y) and for $n = 0$, the initial velocity is zero, and $[\bar{u}_{x,y}^{n}, \bar{v}_{x,y}^{n}]$ is the neighbourhood average of $[u_{x,y}^{n}, v_{x,y}^{n}]$.

2.2.4.2 Lucas-Kanade Optical Flow

In terms of the principles introduced by Lucas and Kanade [99], an additional constraint is combined with the classical optical flow (4) for estimating velocities of optical flow. This constraint supposes that the flow (u, v) is locally constant in a small neighborhood Ω. Within this region, the following term can be minimized:

$$\sum_{(x,y) \in \Omega} W^2(x)(I_x u + I_y v + I_t)^2, \tag{8}$$

where $W(x)$ is a window function that favors the center section of Ω.

The solution to (8) then gives:

$$\begin{bmatrix} \sum W^2 I_x^2 & \sum W^2 I_x I_y \\ \sum W^2 I_y I_x & \sum W^2 I_y^2 \end{bmatrix} \begin{bmatrix} u \\ v \end{bmatrix} = - \begin{bmatrix} \sum W^2 I_x I_t \\ \sum W^2 I_y I_t \end{bmatrix}. \tag{9}$$

Although optical flow method is computationally complex, it is capable of fulfilling successful motion detection with the presence of camera motion or background changing. It can detect the motion precisely even without knowing the background [96].

2.3 Object Classification

Typically, the scenes captured by a camera comprise various objects such as animals, plants, vehicles and fires. To further track target objects and analyze their behavior, it is required to exactly differentiate them from other objects. Thus object classification which categorizes the type of detected objects from the segmentation step is appeared to achieve this task.

Currently, a variety of approaches towards object classification have been proposed and they can be generally classified into three types: training-based classification, statistical-based classification, and rule-based classification.

Take fire detection for example, training-based methods such as SVM, fuzzy logic, and neural networks are the most popularly adopted methods for fire classification. In addition, statistical-based classification (like Bayesian classifiers [100,101], Markov models [102,103]) and rule-based classification are also applied.

2.4 Data Fusion of Multiple Cameras

The fusion of information from multiple cameras is an indispensable techniques for a more advanced detection system. Although many missions of object detection can be carried out by adopting a single camera, multiple cameras can offer an effective solution to overcome a variety

of difficulties with respect to improving the accuracy, reliability and robustness of detection. In addition, systems with multiple cameras can expand the entire range of view, handle the presence of occlusions and enable three-dimensional (3D) localization of objects via observation of different perspectives or diverse images (when using different types of cameras) [96]. However, multiple camera systems also have to confront with lots of practical and technical problems produced by the growing costs and complexity related to the development of hardware and software.

According to the camera configurations, multi-camera systems are classified into two categories: multi-view camera system and multi-modal camera system [96].

2.4.1 Multi-View Camera System

The multi-view camera system combines different detection results from multiple viewpoints to improve results of object detection and localization. It can be grouped into two types, one is system with spatially non-overlapping camera views, while the other one is system with overlapping camera views [104]. The non-overlapping type performs well for covering wide range of views. On the contrast, overlapping type makes use of the redundant information obtained simultaneously from different cameras observing the same scene to increase the accuracy in the object detection and the computation of the object's position and size [105]. In the application of UAVs-based fire detection, multi-view methods are widely adopted for cooperative detection, confirmation and positioning of fire with multiple UAVs.

2.4.2 Multi-Modal Camera System

The multi-modal camera system intelligently fuses different types of imagery sensors such as visual and IR cameras to supply enriched information of monitored scene so that the detection performance and behavior analysis can be improved. Compared with multi-view detection, multi-modal detection mainly concentrates on the simultaneous analysis of different kinds of images in which sight lines are near to each other. By employing images produced by various imaging sensors, multi-modal camera system can successfully detect and analyze activity in the scenario

37

with lower faults, because fusion of these kinds of imagery is capable of providing informative details of the scene. Moreover, as each type of sensor can overcome other type sensors' technical limitations, errors caused by one sensor can be modified by the other sensors. Owing to these advantages, the fusion of multiple sensor data is considered as a well-known solution to be used for enhancing the reliability and robustness of fire detection.

Chapter 3

Forest Fire Detection Using Visible Range Images

Although numerous researches of fire detection have been conducted, only minority of them have considered forest fire scenes and few relevant experiments have been carried out for monitoring and detecting forest fires using UAVs [4, 14–17, 19, 22–29, 31, 32]. Generally, the existing vision-based fire detection methodologies are developed with stationary cameras through isolating fires from the static backgrounds. However, the techniques taking advantage of fire motion features for fire detection may fail to accomplish tasks as expected when cameras are installed on UAVs which are moving in the whole operation process. Under this condition, objects (including the interested objects and background) in the captured images are all moving, which is the main reason leading to false alarms of forest fire [106].

To overcome this barrier, several techniques are developed by researchers. In [107], a background subtraction algorithm is employed with integration of intensity thresholding, motion compensation, and pattern classification. [108] describes an accumulative frame differencing approach for extracting the moving pixels and integrating the homogeneous areas of these pixels in the frame after the step of image segmentation. As one of the most important and promising motion

analysis techniques, optical flow is widely adopted in the computer vision based detection studies [109, 110]. In spite of this, the motion of camera is usually presumed to be *a priori* known in these studies. More superior online motion estimation strategies are urgently needed.

For the purpose of solving the problems stated above, the research in this thesis investigates a novel vision-based forest fire detection method using UAVs. In order to improve the accuracy of fire detection, both color and motion features are employed to process images gathered from the camera mounted on a UAV which is moving during the entire mission period. The proposed method comprises a two-layered system architecture. In the first layer, a color-based fire detection algorithm with light computational requirement is designed to segment fire-colored pixels as candidate fire regions for further analysis by making use of chromatic feature of fire. As the changeable pose and low-frequency vibrations of UAV make all objects and background in the images are moving, it is difficult to distinguish fires depending on a single motion based method. In the second layer, the motion-based fire detection algorithm utilizing two types of optical flow is designed to further analyse and segment the candidate fire regions. Consequently, fires are anticipated to be identified from other fire analogues based on their motion features.

This design philosophy aims to greatly reduce the computation burden without decreasing the accuracy of forest fire detection. The good performance is expected to significantly improve the reliability of forest fire detection and reduce false alarm rates without increasing much computation efforts. The overall process procedure of this research can be described as follows: 1) for the color-based detection approach, chromatic characteristics in the so-called Lab color model is employed for isolating fire-colored pixels and removing non-fire colored pixels; 2) regarding the motion-based detection method, two types of optical flow algorithms are combined to further analyse the isolated fire-colored regions from the color-based detection, one is a classic artificial optical flow [98] for calculating the motion vectors (both orientation and velocity) of camera; the other optical flow is based on a newly investigated technique taking advantage of optimal mass transport theory in [110] for fire detection; 3) at last, the fire pixel candidates are further classified through a relatively empirical discrimination rule. Once the fire pixels are verified, the binary feature images

can be obtained via thresholding and performing morphological operations on the motion vectors. A blob counter method is then adopted to track the fire regions in each binary feature image. Experimental validations on aerial video sequences of forest fires and indoor tests with charge-coupled device (CCD) camera onboard UAV are both conducted to verify the effectiveness of the proposed forest fire detection method.

The rest of this chapter is organized as follows. Section 3.1 provides descriptions of the proposed forest fire detection method in twofold steps: 1) color-based candidate forest fire pixels extraction method using chromatic features in Lab color model, and 2) the motion-based forest fire detection algorithm with two types of optical flow techniques. Section 3.2 illustrates the control strategies that are designed to assign the UAV for the tasks of fire search and detection. At last, Section 3.3 presents the scenarios illustration and results discussion of the conducted experiments.

3.1 Vision Based Forest Fire Detection

The proposed forest fire detection methodology, which combines both color and motion features of fire, is intended to greatly improve the accuracy and reliability of forest fire detection. Color-based decision making rules are used to extract color features, while motion features are analyzed by optical flow which is an important technique for motion estimation in computer vision applications. The flowchart of the proposed forest fire detection technique is shown in Fig. 3.1, which comprises three steps: color detection, motion detection, and fire classification.
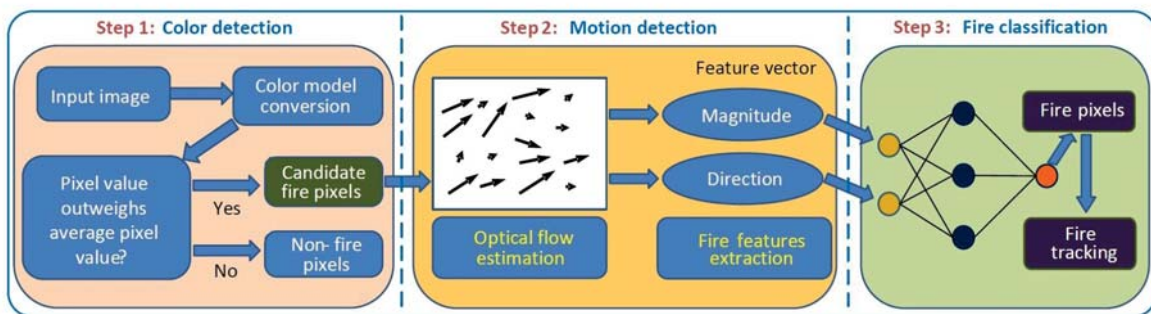
Figure 3.1: Illustration of the proposed forest fire detection architecture.

Specifically, Fig. 3.1 can also be introduced as follows:

(1) The captured RGB images are first transformed into Lab color model, a subsequent image processing technique is utilized to segment the potential fire regions.

(2) A motion-based fire detection approach is then applied to perform a further confirmation of these segmented pixels.

(3) Finally, the confirmed fire regions are to be tracked by a blob counter scheme and fire alarms along with potential fire images are transmitted to the ground station and firefighters for succeeding operations; otherwise, the onboard camera continues to capture new images for processing.

3.1.1 Color Based Forest Fire Detection

Color detection is one of the first detection techniques used in vision-based fire detection and is still popular by far in almost all detection methods [58]. It is obvious that color cannot be used by itself to detect fire because lots of false alarms will be caused by the similar color objects. However, the color information can be used as a part of a more sophisticated system. In this research, the color-based image processing algorithms applied for automatic forest fire detection contain image collection, image preprocessing (including image enhancement, color model conversion), and threshold segmentation. The organization of these algorithms can be summarized in Fig. 3.2. An instance of the proposed color-based fire detection results is also presented in Fig. 3.3 for offering readers a clearer picture.

3.1.1.1 Fire Color Features

In the point of general fires [111], the fire usually shows reddish color. In addition, fire color will vary with the temperature. If the fire temperature is low, the color ranges from red to yellow, and it may become white if the temperature gets higher. This indicates that low-temperature fires
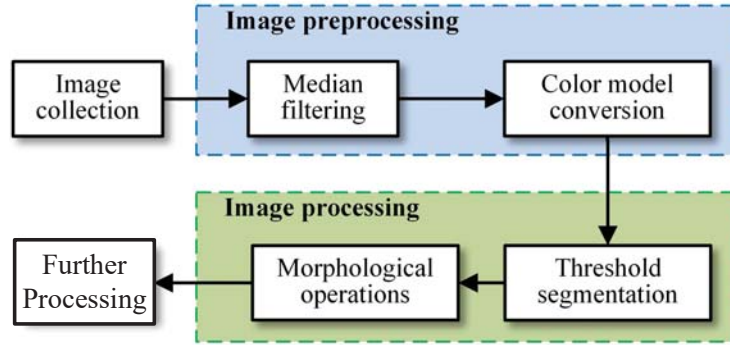
Figure 3.2: Flowchart of color based detection algorithms.
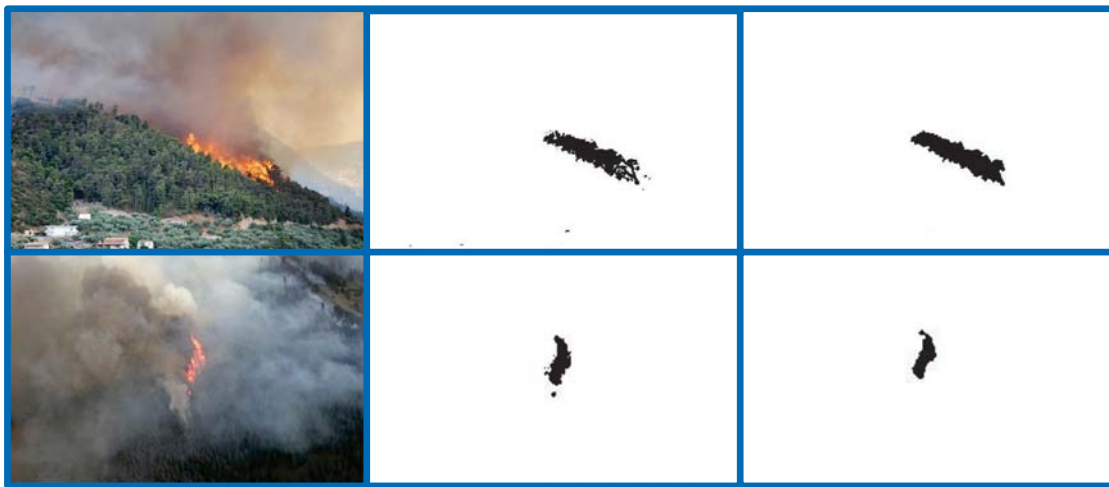
Figure 3.3: Color-based fire segmentation.

present high saturation colors while high-temperature fires display low-saturation colors. More-
over, the color of fires in the daytime or with the extra light source has a heavier saturation than
that of no light source [62].

Usually, fire flames show reddish colors, which varied from red to yellow in the burning pro-
cess [62]. Therefore, the variation of fire color can be represented as discrete values between red
and yellow in color models. Generally, different segmentation results can be obtained using dif-
ferent color models. Based on this phenomenon, most of the existing color-based fire detection
approaches utilize RGB color model or combine it with HSI model as well [62, 68, 88, 94]. RGB
model is popularly used mainly because that almost all visible range cameras output video in RGB
format. It is reported in [112] that RGB values of fire pixels in red-yellow color range indicate the

rule $(R > G > B)$, while the red to yellow range colors in HSI color model can be represented as follows:

$$
\begin{cases}
\text{Condition 1:} & 0^o \leq H \leq 60^o; \\
\text{Condition 2:} & \text{Brighter environment: } 30 \leq S \leq 100, \\
& \text{Darker environment: } 20 \leq S \leq 100; \\
\text{Condition 3:} & 127 \leq I \leq 255,
\end{cases}
\tag{10}
$$

where H, S, and I are the hue, saturation and intensity values of a specific pixel, respectively.

An option of using the color-based fire detection rules is proposed in this thesis by using the Lab color model to determine the zones of candidate fire pixels. This is owe to the fact that, according to the findings and experiences of the author, the fires in Lab model are more visible than that in other color models (it can also be observed from Figs. 2.3 and 2.4).

3.1.1.2 Flame Color Based Decision Rules

In this research, the color-based decision rules are designed in Lab model to determine candidate fire regions. There are three components (luminance "L", chrominance "a", and chrominance "b") which constitute the Lab color model. As described in Fig. 2.8, the model reveals that the higher value of each component, the more they are close to brightest white, red and yellow respectively. Since fire color usually owns features that are close to red and yellow, and possesses high luminance, it is reasonable to assume that the values of fire pixels in each channel of Lab color model should be larger than that of other non-fire color pixels. Fig. 3.4 provides an example of fire appearance in each component of Lab model which reveals this phenomenon as well. On the basis of this assumption, the color decision making rules in Lab color model then can be established in the following sequence.

| Original image | Component L | Component a | Component b |
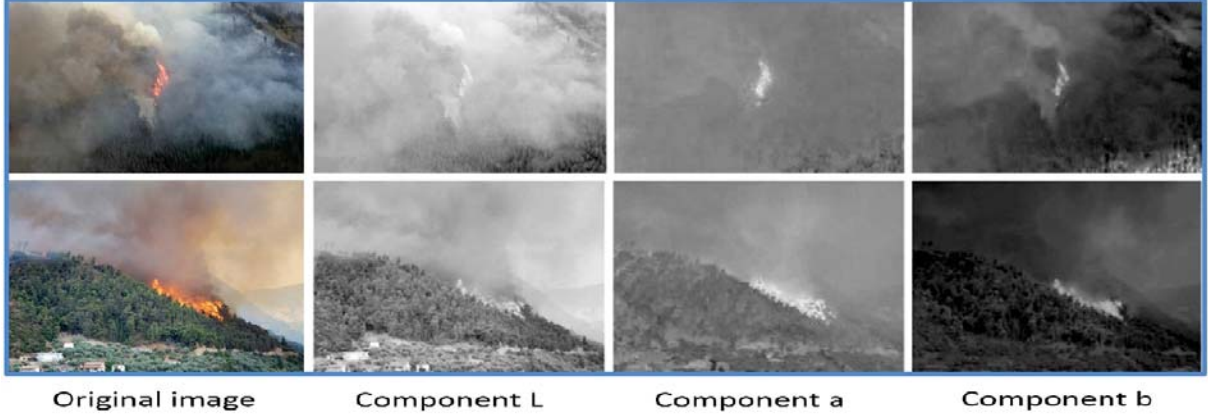
Figure 3.4: Flame appearance in each component of Lab model.

In each frame, the average value $\bar{A}_I$ of pixels is computed as follows:

$$\bar{A}_I = \frac{1}{N} \sum_{(x,y) \in I} P_\Phi(x, y), \tag{11}$$

where $P_\Phi(x, y)$ is the pixel value at position (x, y) for three components (L, a, b) in the image plane I, N represents the total number of pixels in the image.

Finally, the decision making rules (P_{FC}) for the fire-colored pixels are formulated as follows:

$$P_{FC} = \begin{cases} 1, & \text{if } (P_\Phi(x, y) > \bar{A}_I), \\ 0, & \text{otherwise,} \end{cases} \tag{12}$$
$$\bar{A}_I = \frac{1}{N} \sum_{(x,y) \in I} P_\Phi(x, y).$$

It is worth-mentioning that the pixel is treated as a fire-colored pixel if $P_\Phi(x, y)$ exceeds the threshold $\bar{A}_I$, and meanwhile P_{FC} is set to be 1, which means that the pixel is preserved as the candidate fire pixel for further processing by motion detection approach. Otherwise, the pixel is set to be 0 which indicates that the pixel is rejected for further analysis.

3.1.2   Motion Based Forest Fire Detection

Generally, the detection approaches solely paying attention to objects displaying flame color are considered as unreliable and tending to raise false alarm rates, additional fire characteristics analysis and more effective techniques are thereby highly demanded to achieve more accurate and reliable detection systems. Fires show dynamic features with changeable shapes since the airflow produced by wind can result in dramatic oscillation and sudden movement of the fire [62]. These dynamic features make the motion detection techniques being widely applied in fire detection for isolating the moving objects, while discarding the stationary non-fire pixels from images. Some early studies simply consider fire-colored moving objects as fire but this method causes lots of false alarms, because fire-colored moving objects such as waving leaves in autumn or reddish/yellowish animals, may all be wrongly identified as fire. To judge whether the motion is induced by fire or a non-fire moving object, further analysis of moving regions in video sequence is essential.

Therefore, optical flow is adopted in this thesis due to its advantages in fulfilling motion detection tasks with further dynamic analysis of moving regions so that non-fire moving objects can be eliminated. Particularly, the camera utilized for capturing images is installed on the UAV, which has movement during the whole assignment. This special condition can severely degrade the performance of fire detection, since all objects in the field of view of the camera are moving. In order to solve this challenging and practical problem, this research proposes a new solution to distinguish the variations in the images caused by the motion of the UAV from those caused by fire.

The main idea of the proposed method is the estimation of the discrepancies between an artificial optical flow and an optimal mass transport (OMT) optical flow [110], and extraction of the fire pixels from the estimated discrepancies. The design architecture of the proposed approach is presented in Fig. 3.5.

3.1.2.1   Optimal Mass Transport Optical Flow

Classical optical flow models are insufficient to represent the external of fire because they highly depend on the brightness constancy ($\frac{d}{dt}I = 0$). This problem is induced by two reasons

46
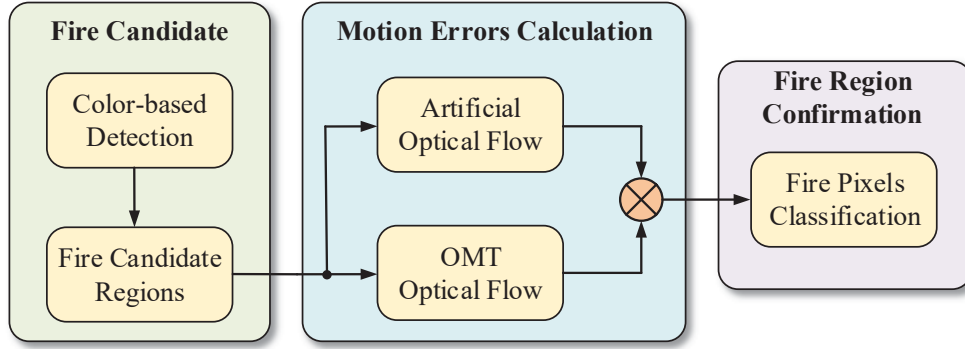
Figure 3.5: Design architecture of the motion-based fire identification methodology.

[110]:

- Because of the fast pressure and heat dynamics, rapid variation of intensity exists in the combustion process, therefore the hypothesis of intensity constancy in Eq. (4) cannot be applied.

- Chaotic motion (non-smooth motion field) produced by air turbulence may make smoothness regularization counter-productive to the calculation of fire motion.

Taking the above-mentioned situations into consideration, the OMT optical flow tends to be a suitable option for the fire detection applications. In OMT, the optical flow problem is regarded as a generalized mass (which stands for image intensity I in this research) transport problem, where a mass conservation is performed by the data term. The conservation law can be formulated as below [110]:

$$I_t + \nabla \cdot (\vec{\mathbf{u}}I) = 0, \tag{13}$$

where $\vec{\mathbf{u}} = (u, v)^T$. The intensity I is substituted by mass density.

Similar to the classical optical flow, the OMT optical flow model solves the aperture problem by minimizing the total energy according to:

$$\min_{\vec{\mathbf{u}}} \frac{1}{2} \int_\Omega \int_0^T (I_t + \nabla \cdot (I\vec{\mathbf{u}}))^2 + \alpha ||\vec{\mathbf{u}}||_2^2 I dt dx dy, \tag{14}$$

and subjects to the boundary conditions $I(x, y, 0) = I_0(x, y)$ and $I(x, y, 1) = I_1(x, y)$, where I_0 and I_1 are given gray-scale frames. The transport energy $||\vec{u}||_2^2 I$, which is the operation demanded to transfer mass from one location at $t = 0$ to another at $t = 1$, denotes the regularization term in Eq. (14). The solution to this minimization problem can be acquired via discretizing Eq. (14):

$$\min_{\vec{u}} \frac{\alpha}{2}(\vec{u}^T \hat{I} \vec{u}) + \frac{1}{2}(I_t + [D_x I D_y I]\vec{u})^T (I_t + [D_x I D_y I]\vec{u}), \tag{15}$$

where $\vec{u}$ is a column vector composed of u and v, and $\hat{I}$ is a matrix including the mean intensity values $(I_0 + I_1)/2$ on its diagonal. The derivatives are discretized by $I_t = I_1 - I_0$ and the central-difference sparse-matrix derivative operators D_x and D_y.

Eq. (15) can be rewritten as:

$$\min_{\vec{u}} \frac{\alpha}{2}(\vec{u}^T \hat{I} \vec{u}) + \frac{1}{2}(A\vec{u} - b)^T (A\vec{u} - b), \tag{16}$$

where $A = [D_x I \; D_y I]$ and $b = -I_t$.

Then the solution of Eq. (16) is obtained as [110]:

$$\vec{u} = (\alpha \hat{I} + A^T A)^{-1}(A^T b). \tag{17}$$

Additionally, the generalized mass of a pixel can be described by its similarity to a center flame color in the HSV color model ($H, S, V \in [0, 1]$). The center flame color can be properly selected as $H_c = 0.083$, $S_c = V_c = 1$ [110], which represents a fully color-saturated and bright orange. Then, the generalized mass can be calculated as:

$$I = f(\min\{|H_c - H|, 1 - |H_c - H|\}) \cdot S \cdot V, \tag{18}$$

where f can be written into the logistic function as below:

$$f(x) = 1 - (1 + \exp(-a \cdot (x - b)))^{-1}, \tag{19}$$

where $a = 100$ and $b = 0.11$.

3.1.2.2 OMT Optical Flow Feature Extraction

As this work mainly concentrates on the pixels in movement, thus these essential pixels ($\Omega_e \subset \Omega$) are defined as:

$$\Omega_e = \{(x, y) \in \Omega : ||\vec{u}(x, y)||_2 > c \cdot \max_{\Omega} ||\vec{u}||_2\}, \tag{20}$$

where $0 \le c < 1$ is selected so that adequate number of pixels can be reserved, $\Omega \subset \Re^2$ represents an image region.

In this study, two features $f_i : \vec{u} \mapsto \Re, i = 1, 2$ defining the two dimensional feature vector $F = (f_1, f_2)^T$ are selected to carry out feature extraction. More specifically, the feature of magnitude f_1 measures mean magnitude, while the directional feature f_2 is used for analysis of motion directionality.

Consequently, given the image region Ω and the OMT optical flow field in this region, the magnitude and directional characteristics are chosen through the following procedures [110].

(1) OMT Transport Energy:

$$f_1 = \underset{\Omega_e}{Mean} \left(\frac{I}{2} ||\vec{u}_{OMT}||_2^2 \right), \tag{21}$$

this feature is to estimate the mean OMT transport energy per pixel in a subregion.

(2) OMT Source Matching: For rigid movement, the flow field tends to be composed of parallel vectors implying rigid translation of mass. This feature is devised to quantify how well an ideal source flow template matches the estimated OMT flow field, which is formulated as:

$$\vec{u}_T(x, y) = \begin{bmatrix} u_T(x, y) \\ v_T(x, y) \end{bmatrix} = \exp\left(-\sqrt{x^2 + y^2}\right) \begin{bmatrix} x \\ y \end{bmatrix}. \tag{22}$$
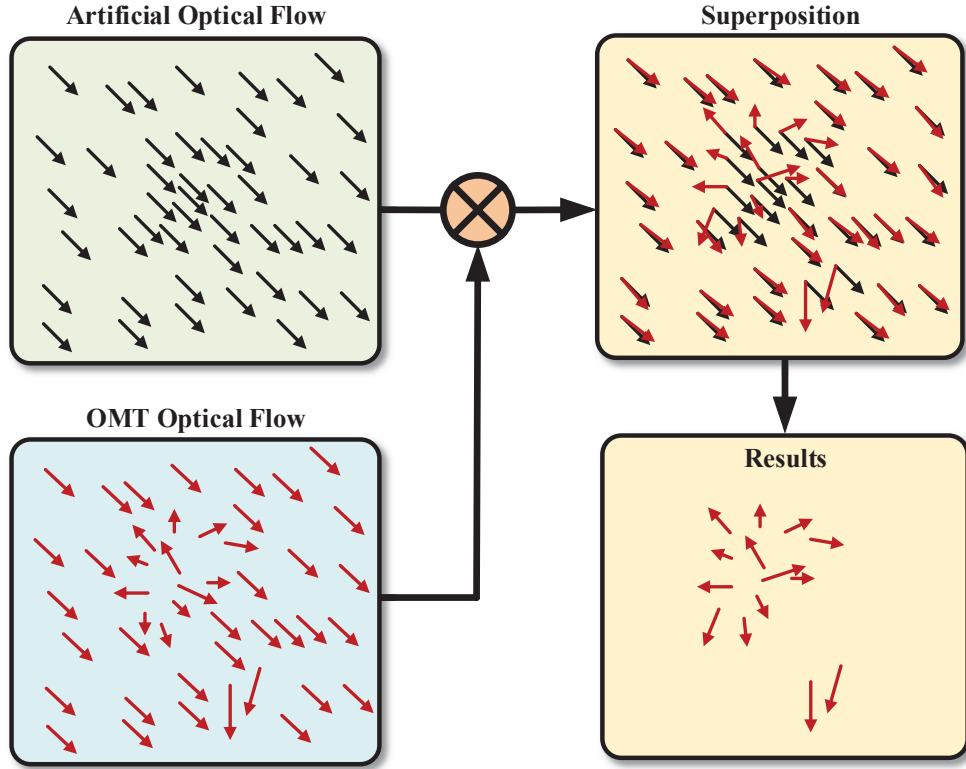
Figure 3.6: Illustration of the fire pixels identification.

Then, the best match can be computed by:

$$f_2 = \max_{\Omega} \left| (u_T * \frac{u_{OMT}}{||\vec{\mathbf{u}}_{OMT}||_2}) + (v_T * \frac{v_{OMT}}{||\vec{\mathbf{u}}_{OMT}||_2}) \right|, \tag{23}$$

where $*$ means convolution.

3.1.2.3   Motion Errors Calculation

After computing two optical flows (one is artificial optical flow for calculating the movements of camera and the other one is OMT optical flow for estimating the motion of pixels in the whole image), a succeeding step is to compare these two achieved optical flows and figure out their differences.

As illustrated in Fig. 3.6, the artificial optical flow evaluates the identical moving direction of

the view in the image, meanwhile the OMT optical flow estimates the motion of each pixel in the image. Afterwards, two optical flows are incorporated together in the same image. Since there is a presence of fire in this scene, the OMT optical flow shows some obvious distinctions of movements among pixels. This circumstance is generated by the intrinsic properties of fire, such as oscillation and sudden movements with irregular shapes and velocities.

3.1.2.4 Motion Based Fire Regions Classification and Tracking

To classify fire pixels from background, or other uninterested moving objects in the image, the following detailed fire identification procedure is needed:

(1) On the basis of the estimated moving orientation of each pixel (f_{OMT}) utilizing the OMT optical flow and the calculated moving orientation of the camera (f_α) using the artificial optical flow, the residual between them can be acquired by $\Delta f = |f_\alpha - f_{OMT}|$. It is worth-mentioning that f_α is chosen as the average value of orientations of total pixels in the image so as to decrease the disturbance of noises and some unexpected errors.

(2) This thesis suggests a feasible but relatively simple approach of identifying fire pixels, which is to compare the angle deviations of each pixel with a properly chosen threshold. A pre-defined decision making rule is accordingly made for filtering the background and isolating the candidate fire pixels. This rule is designed as follows:

$$P_{FM} = \begin{cases} 1, & \text{if } \Delta f > \bar{f}, \\ 0, & \text{otherwise}, \end{cases} \tag{24}$$

where P_{FM} is the binarized values of pixels obtained by applying the fire moving pixels decision making rule. If Δf outweighs the threshold $\bar{f}$, the pixel is classified as fire pixel and is set to 1, otherwise the pixel is set to 0. The threshold value can be settled on the basis of the practical condition or by using advanced artificial intelligent methods, such as SVM, neural network, and fuzzy logic.

51

In order to get rid of the existing small unconcerned objects after the aforementioned proce-dures and enhance the ultimate fire detection performance, this research suggests to make use of the morphological operations to remove the small irrelative objects in the thresholding images.

Morphological operations, which can perform well at eliminating small uninterested objects in the thresholding images, cover a sequence of operators, such as dilation, erosion, opening, and closing. This thesis employs the dilation operation after erosion operation. The erosion operation E can wipe off pixels on the object boundaries, while the dilation operation D can add pixels on the contrary. These two operations can be described as follows:

$$
\begin{aligned}
E &= I \otimes C = \{(i,j)|C_{ij} \subseteq I\} \\
D &= I \oplus C = \{(i,j)|[(\hat{C})_{ij} \cap I] \neq \Phi\},
\end{aligned}
\tag{25}
$$

where symbols $\otimes$ and $\oplus$ represent the erosion operator and dilation operator, respectively. (i,j) denotes the coordinates of pixel, I is image set, and C is morphological element.

Blob counter approach is adopted in this study for fire tracking owing to its merit of simplicity and effectiveness in image processing applications. Taking advantages of blob counter can track the number and direction of blobs passing through a specific passage/entrance per unit time, the general working principle is illustrated as follows:

- Images are transformed to binary images after the fire is eventually identified and segmented from the background.

- Subsequently, the objects are to be identified based on the pixel connectivity. After that, a specific region of interest is produced for each object which is labelled and assigned with a set of coordinates.

- At last, the tracked objects are distinguished from the image, their number and position information are all achievable, and the fire areas are effectively tracked and located in images [113].

3.2 Control Rules Design for Unmanned Aerial Vehicle

In order to search potential forest fires in a specific terrain and capture the aerial images by the onboard camera(s), the UAV is required to be deployed for accomplishing these tasks. Thus a well devised control deployment is also demanded for the operation of UAV. In this work, an integration of sliding mode control (SMC) and linear quadratic regulator (LQR) is proposed for the control of UAV. The designed UAV's control architecture can be separated into two loops, the inner-loop and outer-loop. The LQR is utilized in the outer-loop to control the positions of UAV, while the sliding mode control, which is in charge of the attitude stabilization, is used in the inner-loop. In addition, as a category of nonlinear controller, the utilization of SMC combining with the UAV's nonlinear dynamics is aimed to improve the system accuracy and robustness. A brief introduction of the control system is presented in Fig. 3.7.
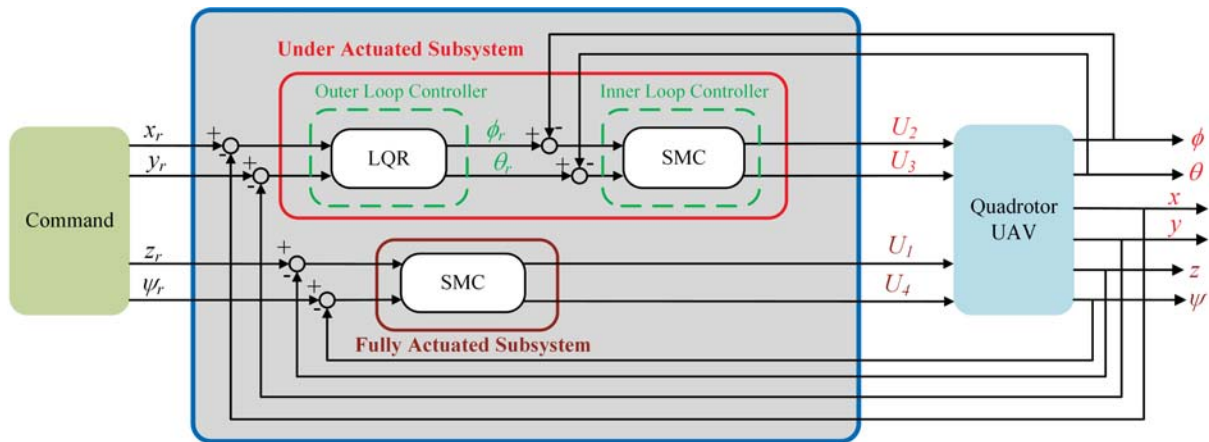
Figure 3.7: Block diagram of the employed UAV control system.

3.2.1 Modelling of Unmanned Quadrotor Helicopter

Fig. 3.8 illustrates a typical unmanned quadrotor helicopter (UQH), which is cooperatively operated via four direct current (DC) motor-driven propellers fixed at the front, rear, left, and right corners, respectively. Thrusts u_1, u_2, u_3, and u_4 are produced by these four propellers. The front and rear propellers spin clockwise, while the right and left propellers rotate counter-clockwise.
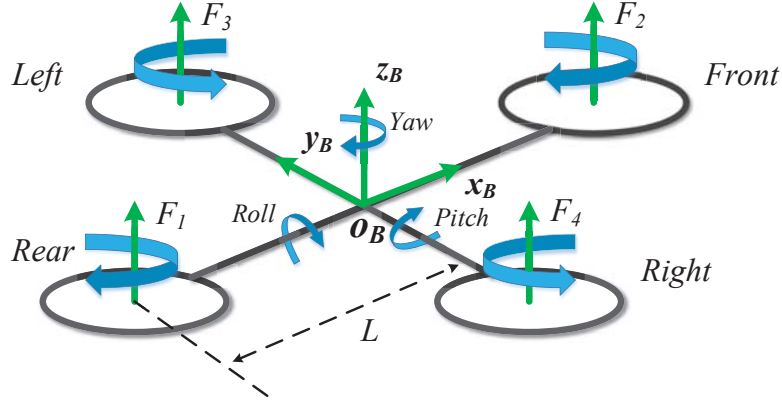
Figure 3.8: Schematic diagram of a general UQH.

The entirely created thrusts point upward along the z_B-direction all the time. Consequently, the vertical translation is accomplished by straightforwardly distributing same amount of control signal to each motor, while the horizontal translation is performed by allocating a distinctive amount of control signals to the opposite motors, so that the UQH is capable of rolling/pitching towards the slowest motor, the lateral/forward movement can be enforced afterwards [20].

As introduced in [20], a representative UQH dynamic model in relation to the earth-fixed co-ordinate system can be described as:

$$
\begin{aligned}
\ddot{x} &= \frac{(sin\psi sin\phi + cos\psi sin\theta cos\phi)u_z(t) - K_1\dot{x}}{m} \\
\ddot{y} &= \frac{(sin\psi sin\theta cos\phi - cos\psi sin\phi)u_z(t) - K_2\dot{y}}{m} \\
\ddot{z} &= \frac{(cos\theta cos\phi)u_z(t) - K_3\dot{z}}{m} - g \\
\ddot{\phi} &= \frac{u_\phi(t) - K_4\dot{\phi}}{I_x} \\
\ddot{\theta} &= \frac{u_\theta(t) - K_5\dot{\theta}}{I_y} \\
\ddot{\psi} &= \frac{u_\psi(t) - K_6\dot{\psi}}{I_z}.
\end{aligned}
\tag{26}
$$

Table 3.1: Nomenclature (earth-fixed coordinate system).

Symbols	Explanation
x, y, z	Coordinates of UQH at center of mass
θ	Pitch angle
ϕ	Roll angle
ψ	Yaw angle
$u_z(t)$	Total lift force
$u_\theta(t)$	The applied torque in θ direction
$u_\phi(t)$	The applied torque in ϕ direction
$u_\psi(t)$	The applied torque in ψ direction
$K_n \ (n = 1, 2, ..., 6)$	Drag coefficients
$u_i(t) \ (i = 1, 2, 3, 4)$	Thrust of each rotor
L	Center distance between the gravity of UQH and each propeller
C_m	Thrust-to-moment scaling factor
g	Acceleration of gravity
m	UQH mass
I_x	Moment of inertia along x direction
I_y	Moment of inertia along y direction
I_z	Moment of inertia along z direction
ω_m	Actuator bandwidth
K_m	A positive gain
$u_{ci}(t) \ (i = 1, 2, 3, 4)$	PWM signals distributed to each rotor

Besides, the relationship between accelerations and lift/torques is:

$$\begin{bmatrix} u_z(t) \\ u_\theta(t) \\ u_\phi(t) \\ u_\psi(t) \end{bmatrix} = \begin{bmatrix} 1 & 1 & 1 & 1 \\ L & -L & 0 & 0 \\ 0 & 0 & L & -L \\ C_m & C_m & -C_m & -C_m \end{bmatrix} \begin{bmatrix} u_1(t) \\ u_2(t) \\ u_3(t) \\ u_4(t) \end{bmatrix}. \tag{27}$$

The relationship between the force and its corresponding pulse width modulation (PWM) signal is described as following:

$$u_i(t) = K_m \frac{\omega_m}{s + \omega_m} u_{ci}(t). \tag{28}$$

The definitions of all the above-mentioned symbols are listed in Table 3.1.

3.2.2 Control Schemes Design

In general, making use of nonlinear systems and controllers tends to greatly increase the computation burden; meanwhile, the inherent property of SMC may likewise result in chattering effects to the system. The suggested method, which is intended to decrease the adverse effects of the above-mentioned issues and dramatically make improvement of system performance, combines the linear controller such as LQR with SMC.

In this work, the quadrotor dynamic model [20] is grouped into two subgroups as a result of its nonholonomic characteristics, which can be rewritten as follows:

$$
\begin{bmatrix} \ddot{z} \\ \ddot{\psi} \end{bmatrix} = \begin{bmatrix} \frac{u_z(t)}{m} \cos\theta\cos\phi - g \\ \frac{u_\psi(t)}{I_z} \end{bmatrix},
\tag{29}
$$

and an under-actuated subsystem is defined as:

$$
\begin{bmatrix} \ddot{x} \\ \ddot{y} \end{bmatrix} = \frac{u_z(t)}{m} \begin{bmatrix} \cos\psi & \sin\psi \\ \sin\psi & -\cos\psi \end{bmatrix} \begin{bmatrix} \sin\theta\cos\phi \\ \sin\phi \end{bmatrix},
$$
$$
\begin{bmatrix} \ddot{\phi} \\ \ddot{\theta} \end{bmatrix} = \begin{bmatrix} \frac{u_\phi(t)}{I_x} \\ \frac{u_\theta(t)}{I_y} \end{bmatrix}.
\tag{30}
$$

The target of the fully-actuated subsystem controller is to obtain the minimization of the altitude and yaw angle errors e_z and e_ψ respectively. The SMC applied in this study is expected to complete this objective. The following conditions need to be satisfied:

$$
\lim_{t\to\infty} \|e_z\| = \|z_r - z\| = 0
$$
$$
\lim_{t\to\infty} \|e_\psi\| = \|\psi_r - \psi\| = 0,
\tag{31}
$$

where z_r and ψ_r represent the desired altitude and yaw angle respectively. The control laws for the

altitude and yaw angle can be derived upon classical SMC principle [114]:

$$\hat{u}_z(t) = \left(\frac{m}{\cos\theta\cos\phi}\right)(g + \ddot{z}_r - \lambda_z\dot{e}_z) \tag{32}$$

$$\hat{u}_\theta(t) = I_z(\ddot{\psi} - \lambda_\psi\dot{e}_\psi), \tag{33}$$

where λ_z and λ_ψ denote control gains with $\lambda_z > 0$ and $\lambda_\psi > 0$. A discontinuous term is appended across the surface $s = 0$ to meet the sliding condition such that:

$$U = \hat{U} - ksgn(s), \tag{34}$$

where

$$sgn(s) = \begin{cases} +1 & \text{if } s > 0 \\ -1 & \text{if } s < 0. \end{cases} \tag{35}$$

For the purpose of facilitating the control design procedure, a further simplified model is usually demanded other than the nonlinear model (26). Before performing the model simplification, the following assumptions are essential:

Assumption 1 *It is supposed that the UQH is in hovering situation in the overall flight period [20], which implies $u_z(t) \approx mg$. The deflections of pitch and roll motions are so small that $sin\phi \approx \phi$ and $sin\theta \approx \theta$. There is no yaw movement such that $\psi = 0$. UQH moves with low velocity so that the influences from the drag coefficients are unimportant.*

On the basis of *Assumption 1*, nonlinear model (26) can be reduced into:

$$\ddot{x} = \theta g$$

$$\ddot{y} = -\phi g$$

$$\ddot{z} = u_z(t)/m - g$$

$$I_x\ddot{\theta} = u_\theta(t)$$ (36)

$$I_y\ddot{\phi} = u_\phi(t)$$

$$I_z\ddot{\psi} = u_\psi(t).$$

Due to the time constant of DC motor is much smaller than that of UQH [115], (28) can be further simplified as follows:

$$K_m\frac{\omega_m}{s + \omega_m} \approx K_m.$$ (37)

Hence, combining with (37), (27) can be rewritten as below:

$$\begin{bmatrix} u_z(t) \\ u_\theta(t) \\ u_\phi(t) \\ u_\psi(t) \end{bmatrix} = \begin{bmatrix} K_m & K_m & K_m & K_m \\ K_mL & -K_mL & 0 & 0 \\ 0 & 0 & K_mL & -K_mL \\ K_mC_m & K_mC_m & -K_mC_m & -K_mC_m \end{bmatrix} U_c,$$ (38)

where $U_c = [u_{c1}(t), u_{c2}(t), u_{c3}(t), u_{c4}(t)]^T$.

The goal of the outer-loop controller is to compute the desired position in x and y axes. This is fulfilled by employing a LQR to the following quadrotor linear dynamic model based upon *Assumption 1*:

$$\ddot{y} = -\phi g$$ (39)

$$\ddot{x} = \theta g.$$

Written into state-space representation, the combination of (38) and (39) comes into:

$$\dot{x}(t) = Ax(t) + Bu(t),$$ (40)

where $x(t) = [\dot{x}, \dot{y}]^T \in \Re^n$ is the state vector, $u(t) = [\theta, \phi]^T \in \Re^m$ denotes the control input, and

$$A = \begin{bmatrix} 0 & 0 \\ 0 & 0 \end{bmatrix} \text{ and } B = \begin{bmatrix} g \\ -g \end{bmatrix}.$$

The objective of this controller is to search the feedback control gain K of the optimal control input u such that $u(t) = -Kx(t)$, for the purpose of minimizing the following quadratic cost function:

$$J = \int_0^\infty (x^T Q x + u^T R u) dt, \tag{41}$$

where Q and R denote the weighting matrices with $Q > 0$ and $R > 0$, respectively. K is obtained by solving the Ricatti equation.

Moreover, SMC is adopted in the design of inner-loop control which is intended to produce the control inputs $u_\phi(t)$ and $u_\theta(t)$ to fulfill the requirements of precise quadrotor attitude stabilization. This controller's mission is to converge the actual values of Euler angles ϕ and θ to their desired values ϕ_r and θ_r, which are acquired from the outer-loop controller. The corresponding control laws can be derived as:

$$\hat{u}_\phi(t) = I_x(\ddot{\phi} - \lambda_\phi \dot{e}_\phi) \tag{42}$$

$$\hat{u}_\theta(t) = I_y(\ddot{\theta} - \lambda_\theta \dot{e}_\theta), \tag{43}$$

where λ_θ and λ_ϕ are control gains with $\lambda_\theta > 0$ and $\lambda_\phi > 0$. e_ϕ and e_θ express the errors in roll and pitch angles, $e_\phi = \phi_r - \phi$ and $e_\theta = \theta_r - \theta$. ϕ_r and θ_r signify the desired roll and pitch angles respectively. To meet the sliding conditions, (34) should be put into use.

3.3 Experimental Results

This study selects two groups of videos to verify the effectiveness of the proposed forest fire detection method: one is a recorded aerial forest fire video, and the other one is a real-time fire video

Table 3.2: Specification of adopted camera.

Parameter	Description
Image device	$1/3$-inch Sony color CCD
Resolution	752×582
Auto backlight compensation	On/off switchable
Minimum illumination	$0.1 Lux/F1.2$
S/N ratio	Greater than $48dB$
White balance	Auto tracking
Power supply	$12V/150mA$
Lens	$3.6 - 6mm$

obtained through a UAV in the lab. Both of the experiments are performed in Matlab/Simulink environment. A desktop with Windows 7 operating system, Intel core $i7$ processor and $8GB$ memory is used to conduct image processing and data display.

3.3.1 Scenarios Description

For the purpose of achieving an effective and clear assessment of the developed algorithm, the following scenarios are chosen:

(1) *Scenario 1*: An aerial video recorded with real forest fire scene downloaded from the website (https://www.youtube.com/watch?v=up3kuTwBpsw) is employed for the demonstration of the proposed fire detection method. The resolution of the video is 640×360.

(2) *Scenario 2*: For verifying the validity of the proposed UAV-based forest fire detection method in practical situations, a UAV-based forest fire detection system is designed for the indoor experimental test. The conceptual architecture of the designed single UAV based framework is illustrated in Fig. 3.10. The concept is to use a ground station command a single UAV with different kinds of onboard sensors for searching and observing suspicious forest fires. Once the fire is detected and confirmed, a fire alarm with potential fire images will be sent to both the ground station and mobile devices for firefighters to further check whether fire happens or not.
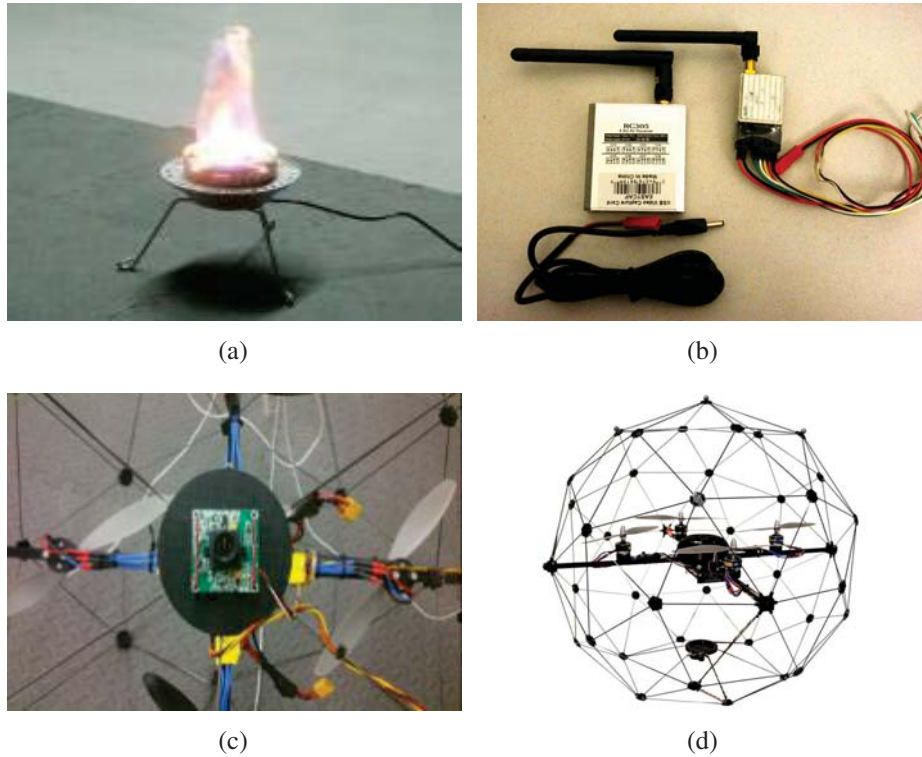
Figure 3.9: Experimental equipments: (a) fire simulator, (b) wireless transmission system, (c) installed camera, and (d) Qball-X4 UAV.

As addressed in Fig. 3.9, several elements are contained in the experimental system:

- For the reason that there is no GPS signal available indoor, a network of cameras system is served as the GPS to supply 3D position information of the UAV.

- A UQH is assigned to carry payload (visual camera) for fire search and detection.

- A visual camera and a wireless communication system (contains a $5.8GHz$ $200mW$ transmitter and a $5.8GHz$ AV receiver) are configured at the bottom of the UQH to obtain and send real-time images to the ground station. Table 3.2 illustrates the specification of the employed camera.

- The simulative fire is seen as the target fire, which is created by a fire simulator.

- A ground station is established to plan and deploy tasks for UQH to implement, as well as display and process real-time images captured from onboard camera.
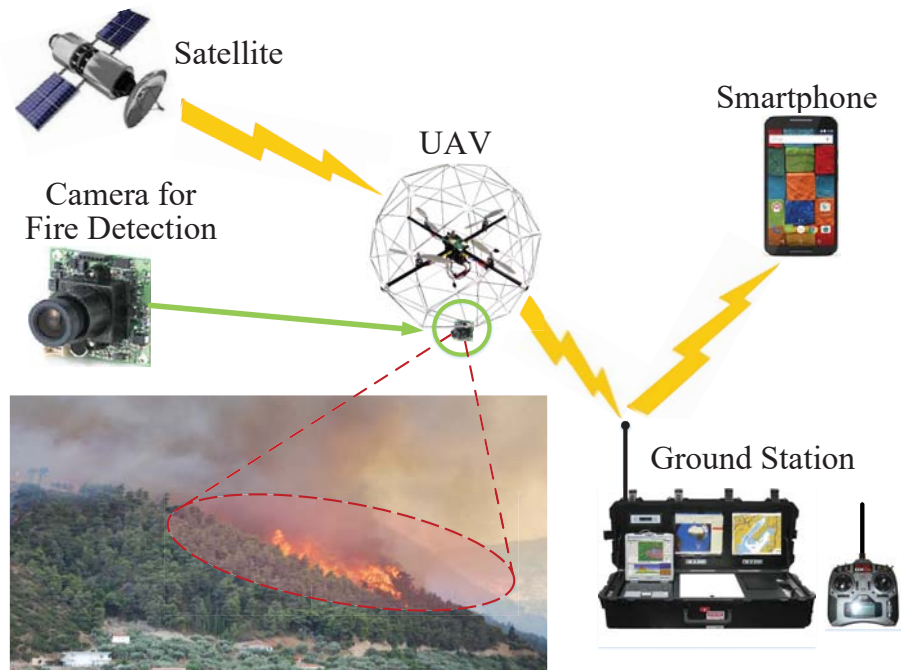
Figure 3.10: General concept of the UAV-based forest fire detection system.

In addition, Fig. 3.11 gives an overview of the used experimental platform and environment. In this experimental test, a single UAV is commanded to patrol a $4m \times 4m$ square field for the purpose of seeking fire spots. As shown in Fig. 3.12, this UAV first begins its mission from the corner of the field; following this, it covers the assigned surveillance area along a predefined trajectory (each trajectory is $1m$ away from its neighbors); a sequence of hovering actions around the possible fire spot (each action lasts $6s$) are to be executed once a potential fire is detected, so as to conduct a further confirmation; the data gathered by the UAV is to be transmitted to the ground station for processing. If the fire is confirmed, a fire alarm is to be triggered, otherwise the fire search mission resumes.

3.3.2   Results of Scenario 1

Figs. 3.13, 3.14, and 3.15 present the results of the proposed fire detection method which is used to process a video captured from a real forest fire scene. Figs. 3.13(a), 3.14(a), and 3.15(a) list the original images; color segmented results are shown in Figs. 3.13(b), 3.14(b), and 3.15(b);
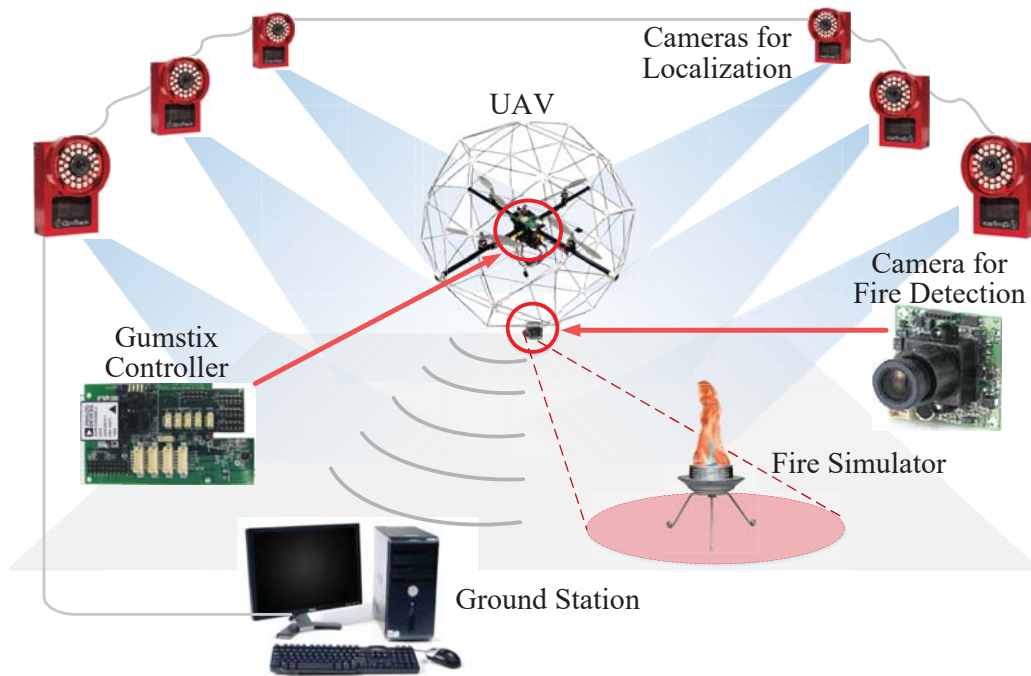
Figure 3.11: Layout of the used UAV-based forest fire search and detection system.

optical flow analysis and morphological operation results are indicated in Figs. 3.13(c), 3.14(c), and 3.15(c); while the final results of fire tracking using the blob counter approach are shown in Figs. 3.13(d), 3.14(d), and 3.15(d), respectively.

From Figs. 3.13(b), 3.14(b), and 3.15(b), it reveals that the majority of non-fire objects are removed such as trees and smoke, while the remainder pixels that have passed through the color-based decision making rule are deemed as candidate fire pixels for further analysis by motion-based detection algorithm adopting optical flow approaches. Figs. 3.13(c), 3.14(c), and 3.15(c) indicate that, after further dealing with the segmentation results using optical flow analysis and morphological operations, the moving/static fire colored analogues such as smoke, houses, and paths in the forest can be eliminated by the moving regions detection rule. At last, fires are successfully tracked by red rectangles through using blob counter, these results can be found in Figs. 3.13(d), 3.14(d), and 3.15(d).
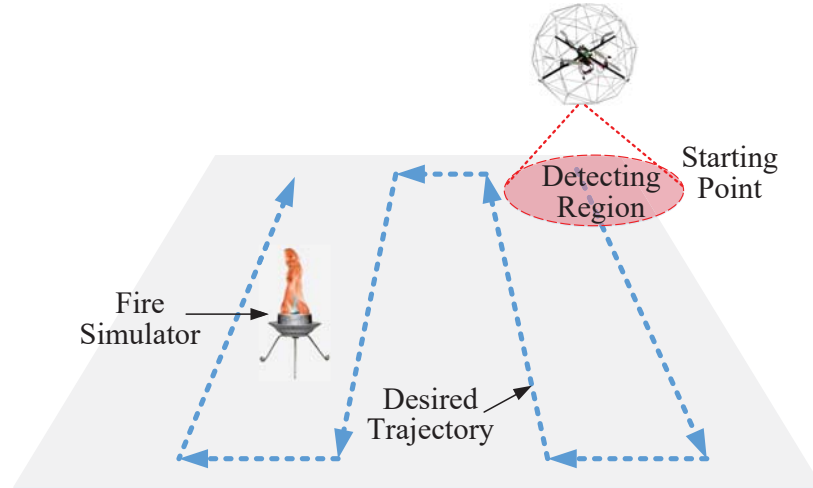
Figure 3.12: General illustration of the conducted fire search and detection experiment.

3.3.3 Results of Scenario 2

Fig. 3.16 presents a scene of conducting the experiment in indoor environment. The real trajectory tracking result of the deployed UAV in 3D is illustrated in Fig. 3.17. The planned trajectory is eventually tracked with satisfactory performance through adopting the designed control method. In order to describe the fire search procedure in a clearer style, Fig. 3.18 and 3.19 are utilized as well. Particularly, Fig. 3.18 reveals that the UAV hovers at three locations during the whole mission period at 62th, 68th, and 74th second, respectively; and every hovering action sustains 6 seconds. As a matter of fact, these three hovering operations are intentional, which exactly illustrate the potential fire detection and further confirmation by commanding UAV to hover at different places to observe the fire from different perspective of views.

Figs. 3.20, 3.21, 3.22, and 3.23 present images captured from UAV and fire detection results of the designed method. Four frames obtained by the UAV at different sites as well as their corresponding image processing results are displayed in Figs. 3.20, 3.21, 3.22, and 3.23. Similar to the layout in Figs. 3.13, 3.14, and 3.15, the original images are shown in Figs. 3.20(a), 3.21(a), 3.22(a) and 3.23(a); Figs. 3.20(b), 3.21(b), 3.22(b) and 3.23(b) list the results of color detection; Figs. 3.20(c), 3.21(c), 3.22(c) and 3.23(c) indicate the optical flow analysis and morphological operation results; final results of fire tracking are presented in Figs. 3.20(d), 3.21(d), 3.22(d) and

(a) Original image   (b) Color detected result

(c) Motion detected result   (d) Tracking result
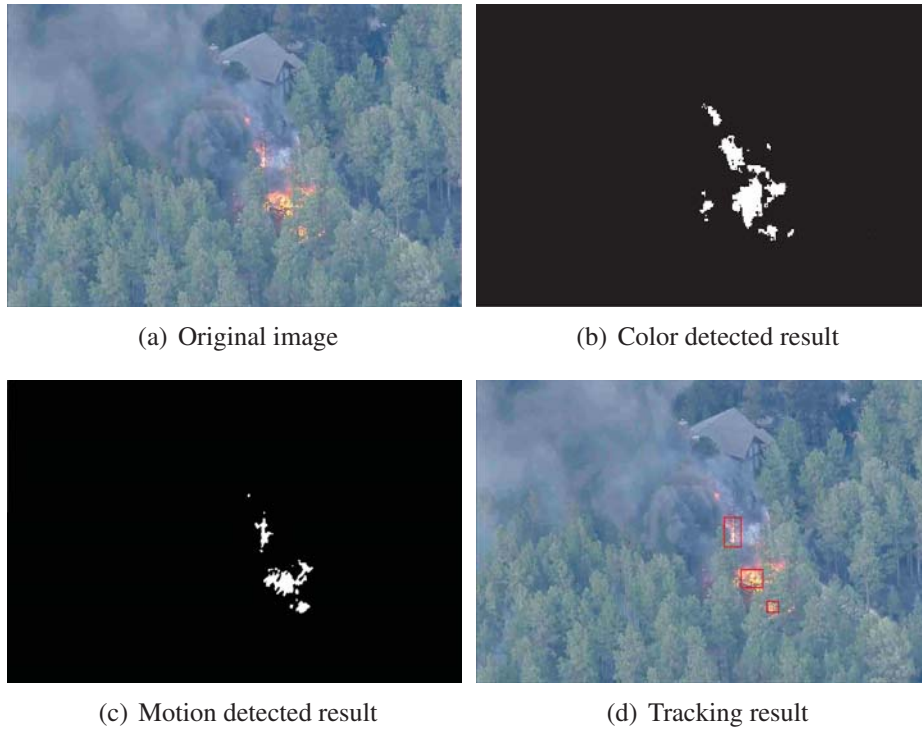
Figure 3.13: Experimental results of sample frame 1.

(a) Original image   (b) Color detected result

(c) Motion detected result   (d) Tracking result
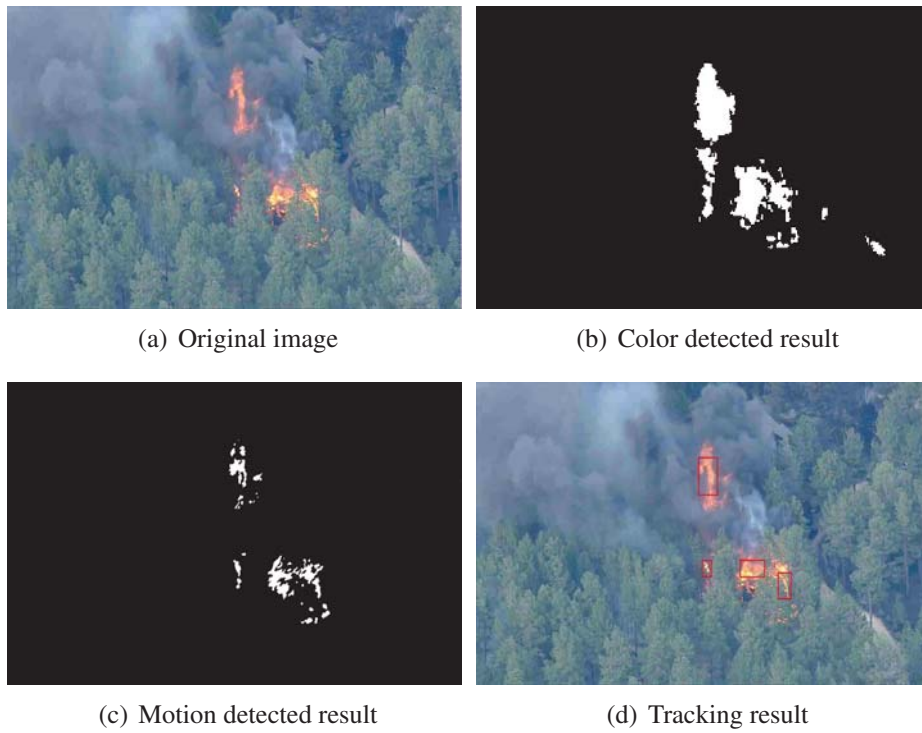
Figure 3.14: Experimental results of sample frame 2.

(a) Original image

(b) Color detected result

(c) Motion detected result

(d) Tracking result
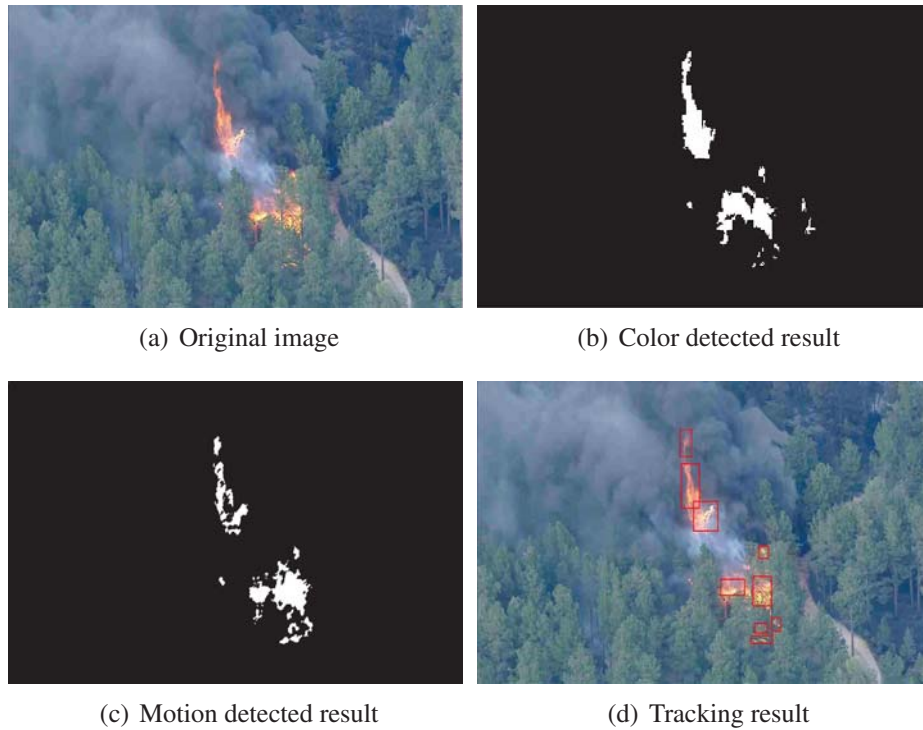
Figure 3.15: Experimental results of sample frame 3.

3.23(d).

From Figs. 3.20(b), 3.21(b), 3.22(b) and 3.23(b), it can be clearly seen that the fire-colored regions have been effectively segmented and extracted, whereas some non-fire regions with similar color of fire, such as the lights and metal parts of the fire simulator which reflect the fire color are also wrongly extracted. The motion-based decision making rules for judging the true fire regions are thereby required to enhance the performance of fire detection. The optical flow features in this study are employed for further analyzing the incorrectly extracted areas. Comparing with Figs. 3.20(b), 3.22(b) and 3.23(b), it obviously indicates that non-fire areas are successfully removed in Figs. 3.20(c), 3.22(c) and 3.23(c).
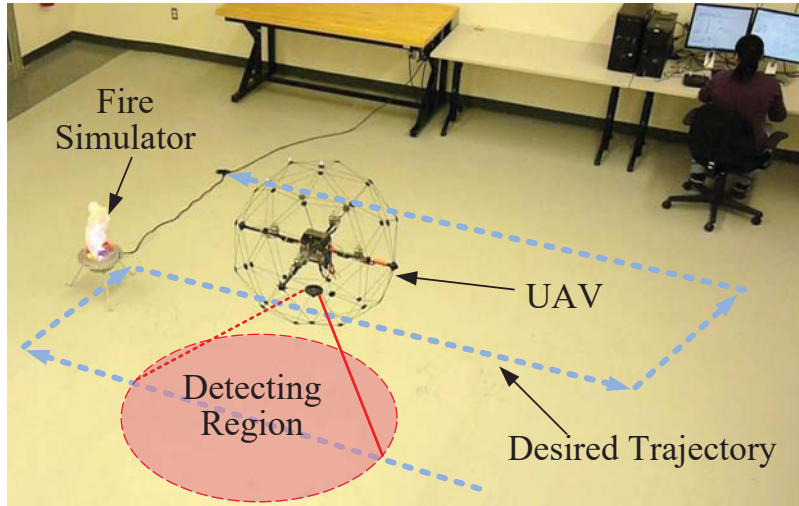
Figure 3.16: Experimental scenario description in practice.
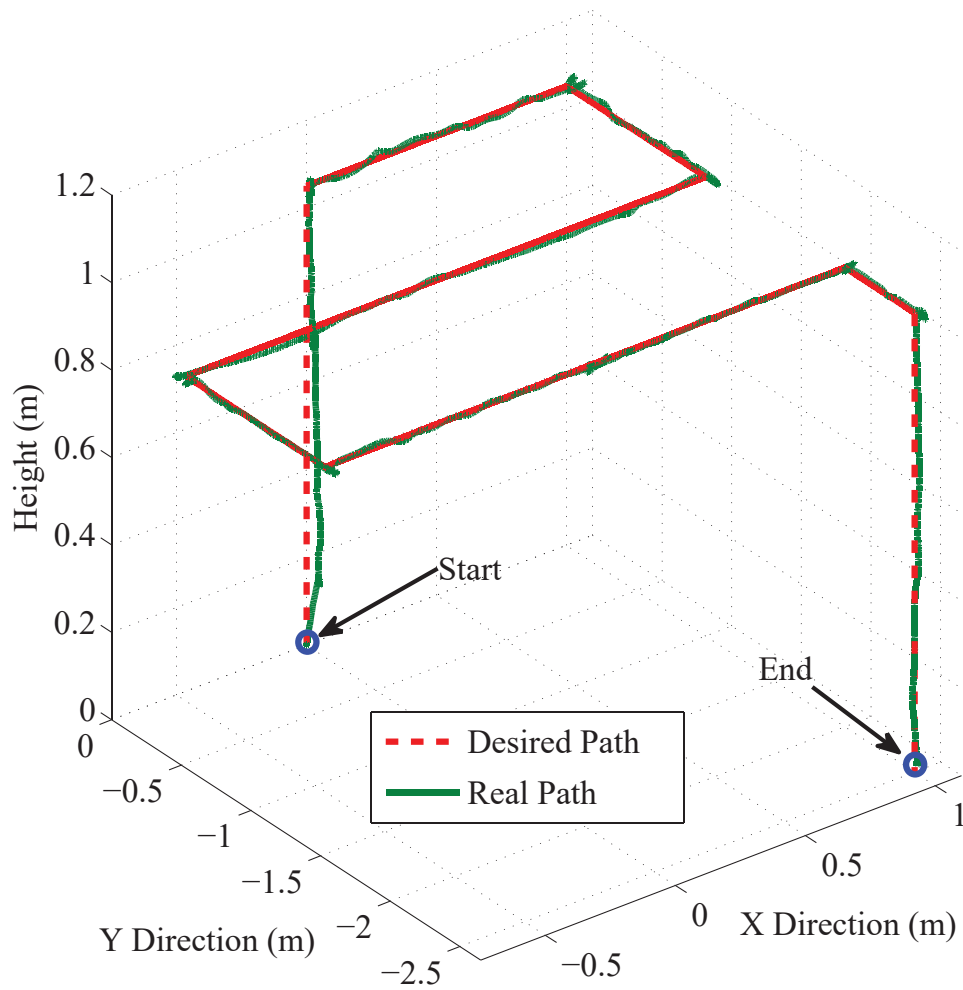
Figure 3.17: Trajectory tracking performance of the UAV displayed in 3D.
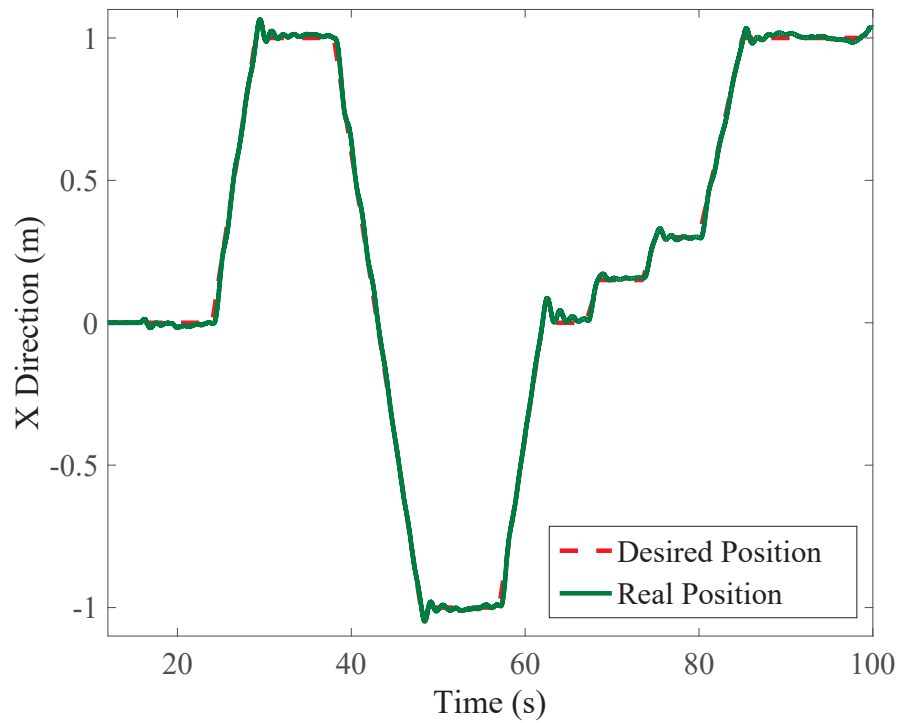
Figure 3.18: Trajectory tracking performance of the UAV along X coordinate.
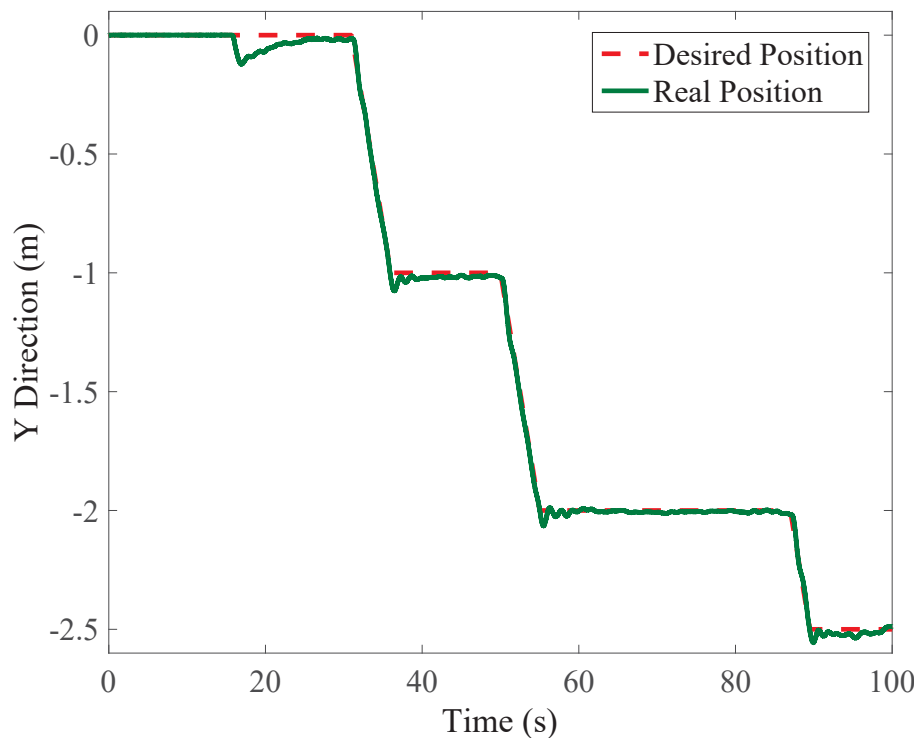
Figure 3.19: Trajectory tracking performance of the UAV along Y coordinate.

(a) Original image

(b) Color detected result

(c) Motion detected result

(d) Tracking result
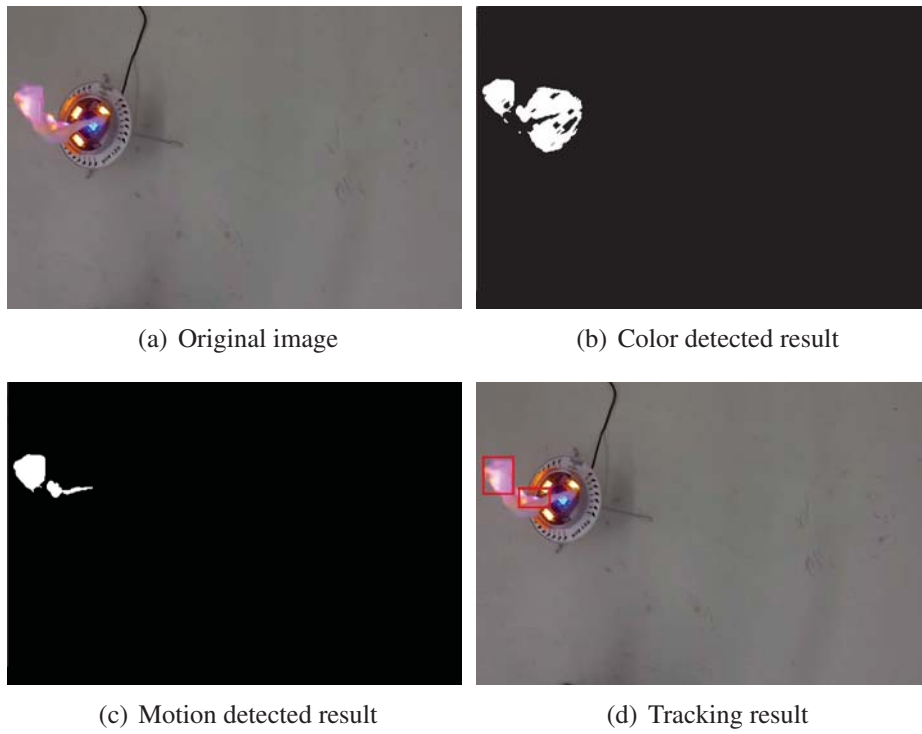
Figure 3.20: Experimental results of sample frame 1.

(a) Original image

(b) Color detected result

(c) Motion detected result

(d) Tracking result
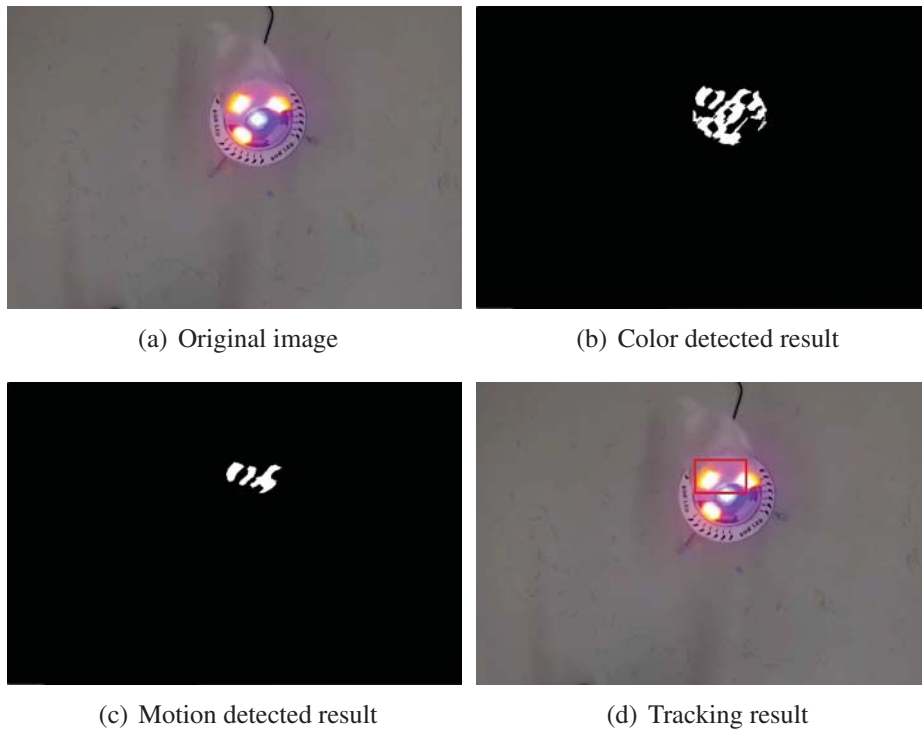
Figure 3.21: Experimental results of sample frame 2.

(a) Original image

(b) Color detected result

(c) Motion detected result

(d) Tracking result
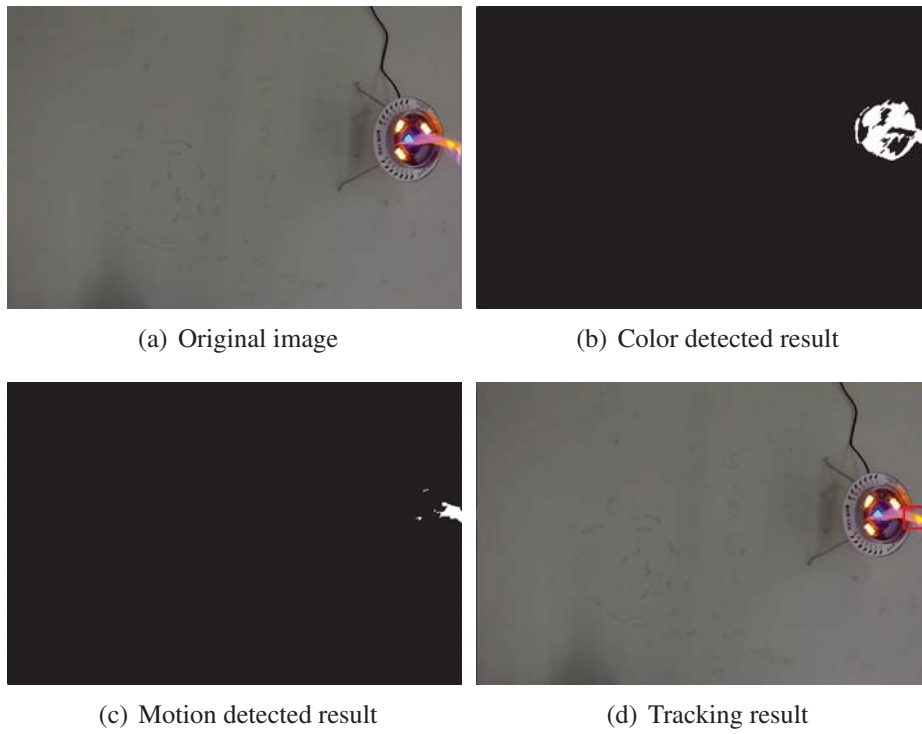
Figure 3.22: Experimental results of sample frame 3.

(a) Original image

(b) Color detected result

(c) Motion detected result

(d) Tracking result
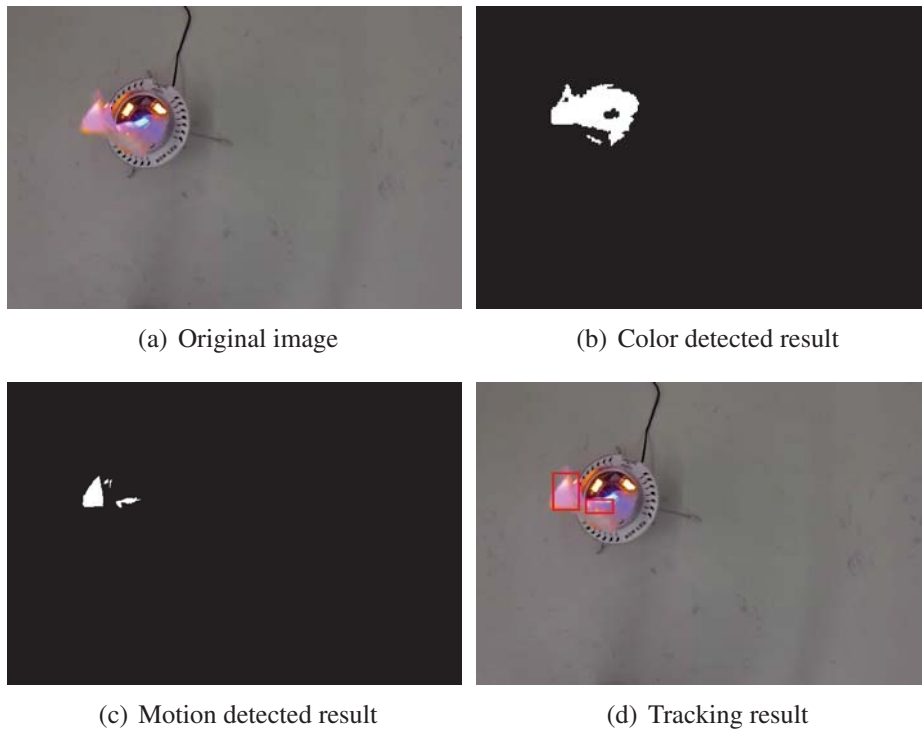
Figure 3.23: Experimental results of sample frame 4.

Chapter 4

Forest Fire Detection Using Visual and Infrared Cameras

In addition to CCD cameras, IR cameras are also frequently mounted on UAVs for forest fire surveillance and detection. Massive efforts have been dedicated to the development of more effective IR images based processing schemes for fire detection. The color and motion features in visual images captured by CCD cameras have been utilized for fire detection. However, the usage of CCD cameras is normally considered as not robust and reliable enough in some outdoor applications. Given highly sophisticated, non-structured environments of forest, the chance of smoke blocking the fire, or the situation for analogues of fire including reddish leaves swaying in the wind and reflections of lights, false fire alarm rate often tends to be considerably high. Due to the fact that IR images can be obtained in either weak or no light conditions, and smoke can be seen as transparent in IR images, IR cameras are thereby widely applied to capture monochrome images in both daytime and nighttime, even though IR cameras are more expensive than CCD cameras. By employing this additional powerful solution in the forest fire detection system design, it is expected to significantly reduce false fire alarm rate and enhance the adaptive capabilities of the forest fire detection system in various environments.

Although many fire detection approaches have been developed for processing IR images [30,

71

48, 82–84], only a few applicable to UAV platforms are designed, and rare application scenarios have been considered forest fire. This chapter first presents a fast fire detection algorithm in IR images, then a fusion detection method combining both IR and visual images together is developed for reducing the false fire detection rate. By taking advantages of both visual and IR based fire detection methodologies, this proposed method is expected to achieve a significant performance improvement of forest fire detection in reducing false fire alarm rate and failure of fire detection. The remainder of this chapter is organized as follows: Section 4.1 introduces the proposed fire detection algorithms dealing with the IR images. Section 4.2 addresses the fusion technique combining information from both CCD camera and IR camera for the application of UAV-based forest fire detection. Experimental results are illustrated and discussed in the last section.

4.1 Fire Detection Using Infrared Images

This section presents a fast fire detection algorithm for the purpose of automatically detecting forest fire in IR images. The proposed fire detection method in this thesis utilizes both brightness and motion features of fire appearance in IR images. The combination of these two characteristics aims to greatly increase the reliability of forest fire detection. Histogram-based segmentation is first adopted to extract hot targets, and optical flow technique is then used to estimate motion features of fire. The purpose of adopting brightness feature is first to distinguish any fire analogues from the background, while the objective of using optical flow is to further confirm the candidate fire from those fire analogues employing the motion feature of fire. The general concept of the proposed method can be briefly illustrated in Fig. 4.1.

To be more specific, the proposed fire detection approach can be further described as follows:

- Hot objects are first detected as candidate fire regions using histogram-based segmentation method, so as to remove the non-fire background.

- The classical optical flow method is then applied to detect moving objects for eliminating stationary non-fire objects in the candidate fire regions.
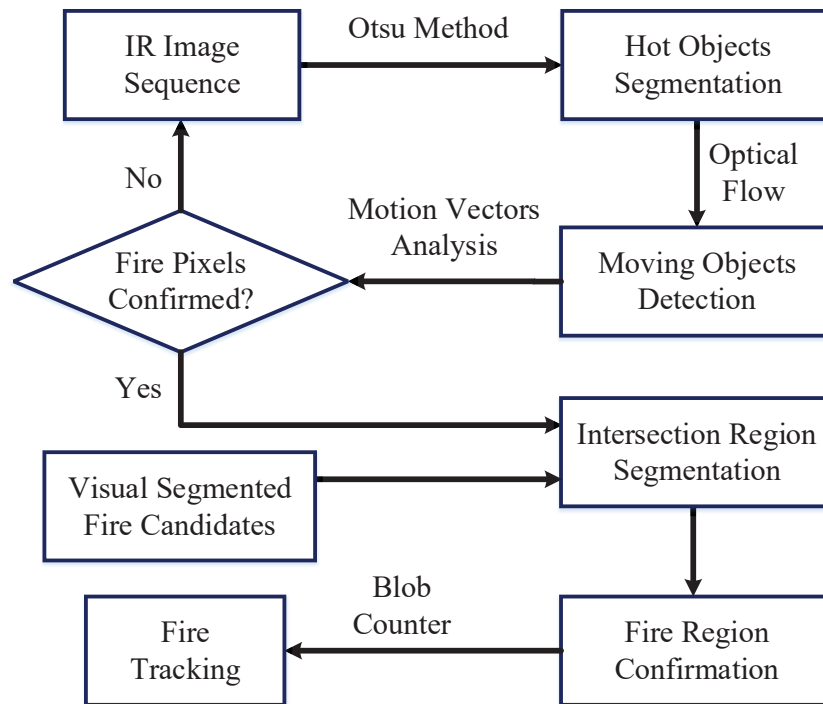
Figure 4.1: Flowchart of fire detection algorithms.

- Next, the motion vectors calculated by optical flow are further analyzed to reduce false fire alarm rates caused by hot moving objects.

- After that, the intersected candidate fire regions of visual and IR images are segmented, the ultimate fire confirmation is based on these pixels in the intersection regions.

- Finally, once the fire regions are confirmed, fire zones are tracked by blob counter scheme.

4.1.1 Hot Object Detection

Most IR cameras measure the heat distribution in the scene and produce single channel images. In IR images, hot objects are represented as bright areas, while cold objects are displayed as dark regions. Therefore, fire pixels appear as high intensity regions, and local maxima of brightness is a dominant clue for fire pixel classification in IR images.

In this study, the histogram-based segmentation method is utilized to extract the hot objects

73

which represent possible fires in the IR image by distinguishing the high brightness objects from the less brightened objects. Only these hot objects are further analyzed by optical flow using the motion features.

The segmentation step takes advantage of Otsu method [116] which is adopted to automatically threshold histogram-based dynamic images. This thresholding method can be generally described in the following. It assumes that the images to be processed contain two types of pixels: foreground pixels and background pixels. The optimum threshold t discriminating those two classes is iteratively computed so that their combined spread (intra-class variance) is minimum, or equivalently, for the purpose of maximizing their inter-class variance.

In order to find the threshold that minimizes the intra-class variance (the variance within each class), it defines in Otsu method that intra-class variance as a weighted sum of variances of foreground pixels and background pixels:

$$\sigma_w^2(t) = \omega_0(t)\sigma_0^2(t) + \omega_1(t)\sigma_1^2(t), \tag{44}$$

where weights ω_0 and ω_1 are the probabilities of the two classes (foreground pixels and background pixels) distinguished by a threshold value t, σ_0^2 and σ_1^2 are variances of these two classes.

The class probabilities $\omega_0(t)$ and $\omega_1(t)$ are calculated through the L histograms:

$$\begin{aligned} \omega_0(t) &= \sum_{i=0}^{t-1} p(i), \\ \omega_1(t) &= \sum_{i=t}^{L-1} p(i). \end{aligned} \tag{45}$$

Otsu minimizes the intra-class variance to maximize inter-class variance:

$$\begin{aligned} \sigma_b^2(t) &= \sigma^2 - \sigma_w^2(t) = \omega_0(\mu_0 - \mu_T)^2 + \omega_1(\mu_1 - \mu_T)^2 \\ &= \omega_0(t)\omega_1(t)\left[\mu_0(t) - \mu_1(t)\right]^2, \end{aligned} \tag{46}$$

where μ represents the class mean, while the class means $\mu_0(t)$, $\mu_1(t)$ and μ_T are defined by:

$$
\begin{aligned}
\mu_0(t) &= \sum_{i=0}^{t-1} i\frac{p(i)}{\omega_0} \\
\mu_1(t) &= \sum_{i=t}^{L-1} i\frac{p(i)}{\omega_1} \\
\mu_T &= \sum_{i=0}^{L-1} ip(i).
\end{aligned}
\tag{47}
$$

The following equations can be obtained:

$$
\begin{aligned}
\omega_0\mu_0 + \omega_1\mu_1 &= \mu_T \\
\omega_0 + \omega_1 &= 1.
\end{aligned}
\tag{48}
$$

By iteratively computing the class probabilities and class means, the threshold t can be achieved.

Let A signify the original image, the isolated binary image α from A can then be represented as follows:

$$
\alpha(x,y) = \begin{cases} 1, & \text{if } (A(x,y) > T), \\ 0, & \text{otherwise}, \end{cases}
\tag{49}
$$

where T is the threshold value obtained by Otsu method, and (x,y) is the pixel position in the image plane A. The pixel values of image A are set to 1 if the pixel value outweighs T; otherwise, the pixel values are set to 0.

In order to separate hot object image β from A, the following description is also utilized:

$$
\beta(x,y) = \begin{cases} A(x,y), & \text{if } (\alpha(x,y) = 1), \\ 0, & \text{if } (\alpha(x,y) = 0). \end{cases}
\tag{50}
$$

Through the above steps, image β is composed of hot object pixels (potential fire pixels) without background, and this image is selected to be further analyzed by motion estimation.

4.1.2 Moving Regions Detection Using Optical Flow

As airflow makes fire moving, in order to improve the fire detection performance, so the motion feature of fire is likewise used in vision-based fire detection methods. Usually, a bright moving region is marked as a potential fire region in the scene captured by the IR camera. Despite this, it may still cause high false fire alarm rates based solely on the clues of brightness. This phenomenon is due to the fact that hot objects other than fire, such as vehicles, animals, and people, may also appear as bright regions. Therefore, in the proposed approach, in addition to the brightness-based detection methods, the motion features of fire are further analyzed in optical flow field to distinguish fires from other moving hot objects.

Compared with ordinary moving objects, fire movement is random, and the shape of fire changes irregularly. This feature can be used to reduce the false alarm rates which may be caused by other ordinary moving hot objects by conducting optical flow analysis.

Through Lucas-Kanade method [99], the computation results of optical flow can be presented as $\{f_i | f_i = [f_{xi}, f_{yi}]^T, i = 0, 1, ..., k\}$, and k is the total number of potential fire pixels which are selected by hot objects detection. The variation of optical flow vectors is utilized to further analyze whether the motion is caused by a fire.

The variation of optical flow vector direction can be written as follows:

$$
\begin{aligned}
\bar{b}_k &= \frac{1}{k-1} \sum_{i=1}^{k} (d_i - \bar{a}_k)^2, \\
\bar{a}_k &= \frac{1}{k} \sum_{i=1}^{k} d_i,
\end{aligned}
\tag{51}
$$

where $\bar{a}_k$ is the average directional angles of velocity and $\bar{b}_k$ denotes the velocity variation, while

d_i is defined by:

$$d_i = \begin{cases} \arctan(\frac{f_{yi}}{f_{xi}}), & \text{for } f_{xi} > 0, f_{yi} > 0 \\[2mm] \pi - \arctan(\frac{f_{yi}}{f_{xi}}), & \text{for } f_{xi} < 0, f_{yi} > 0 \\[2mm] \pi + \arctan(\frac{f_{yi}}{f_{xi}}), & \text{for } f_{xi} < 0, f_{yi} < 0 \\[2mm] 2\pi - \arctan(\frac{f_{yi}}{f_{xi}}), & \text{for } f_{xi} > 0, f_{yi} < 0. \end{cases} \tag{52}$$

The variation of optical flow vector velocity can be represented as:

$$\bar{e}_k = \frac{1}{k-1} \sum_{i=1}^{k-1} (\sqrt{f_{xi}^2 + f_{yi}^2} - \bar{c}_k)^2,$$

$$\bar{c}_k = \frac{1}{k} \sum_{i=1}^{k} \sqrt{f_{xi}^2 + f_{yi}^2}, \tag{53}$$

where $\bar{c}_k$ is the average velocity of flow vector and $\bar{e}_k$ denotes the variation of velocity magnitude.

Since fire oscillates and moves irregularly with a variety of shapes, boundaries, and velocities, it is assumed that the movement of pixel produced by fire outweighs the variation of velocity vector. Fire pixels (F_p) are judged by the following rule:

$$F_p = \begin{cases} 1, & \text{if } (b_i > \bar{b}_k) \& (e_i > \bar{e}_k), \\[2mm] 0, & \text{otherwise,} \end{cases}$$

$$b_i = (d_i - \bar{a}_k)^2,$$

$$e_i = (\sqrt{f_{xi}^2 + f_{yi}^2} - \bar{c}_k)^2. \tag{54}$$

If b_i exceeds the threshold $\bar{b}_k$ and e_i is over the threshold $\bar{e}_k$, then this pixel is classified as the candidate fire pixel and its value is set to be 1, otherwise the pixel value is set to be 0.

4.2 Fire Detection Using Both Infrared and Visual Images

Fire detection systems with single camera suffer from numerous problems in real-world scenes. A number of these practical difficulties are triggered by limitations of the type of camera utilized. In most cases, the specific limitations can be compensated by using different types of cameras. Therefore, instead of managing ever more complicated single-camera fire detection algorithms, investigations of fusing multi-camera information from the different types of cameras are demanded in applications of fire detection.

Developing an accurate fire detection system that solely depends on one type of camera is very challenging. For instance, a visual camera can fail to capture images with satisfactory quality due to noises, illumination changes, shadows, and other visual disturbances, while an infrared camera can be disturbed by reflections or emissivity of non-fire objects. Although several techniques have been proposed to solve these problems using a single camera, most of them cannot be effective under all circumstances. For the purpose of achieving high accuracy system, the combination of multi-type cameras has been a strong demand for many researchers. The combined detection in the IR and visual spectral ranges is very actively used in many applications. In the domain of fire detection, the fusion of visual and IR images has already been conducted as an important way to improve the detection performance.

Regarding the studies on multi-modal forest fire detection, they just started from recent decades and are still with limited number of research works. The majority of existing studies are from Arrue *et al.* [85] and Martinez-de Dios *et al.* [4, 27, 48], where both visual and IR information are used to improve forest fire detection results. Arrue *et al.* [85] propose an IR-visual false alarm rate reduction system which decreases false alarm rates by evaluating the ratio between the alarm regions in visual and infrared images collected by a watching tower. Martinez-de Dios *et al.* [4, 27, 48] make use of the information redundancy from visual and infrared cameras to reduce the false alarms of UAVs-based forest fire detection system. This is also the idea borrowed for the multi-modal fire detection proposed in this chapter. However, compared to the work of Arrue *et al.*, this study does not take advantage of extra data from meteorological sensors or a geographical

information database. Similar to the method of Martinez-de Dios *et al.* [48], this thesis introduces how potential fire alarms from both IR and visual images can be fused to provide more reliable fire detection performance.

4.2.1 Registration of Infrared and Visual Images

In order to fuse the data from multi-modal cameras, the corresponding objects in the view are required to be registered. Therefore, an important step before fusing detection results of different types of cameras is image registration which is used to align the corresponding objects in the scene. The function of registration is to set up geometric correspondence between the multi-type images so that they may be transformed, compared, and analyzed in a uniform reference frame [117].

The registration methods can be divided into automatic and manual registration. Since manual registration is labor intensive and it is required to repeat when the background changes or the camera has movement, automatic registration is thus preferred by the researchers.

As for automatic registration methods, it can be divided into region, line and point feature-based methods [118]. It is usually required to adopt features that are stable with respect to the sensors. For the registration of the multi-modal images, Martinez-de Dios *et al.* [48] take advantage of a homography based method to estimate the transformation parameters by using a calibration grid. This thesis borrows their registration approach using the same technique.

Assume that both cameras configured in the system share the centre of projection and the geometry of this configuration is shown in Fig. 4.2.

Let $q_{IR} = [x \ y \ 1]^T$ and $q_{Vis} = [x' \ y' \ 1]^T$ denote the images at the same moment of a point X in homogeneous pixel coordinates of the infrared and visual images, respectively. Assume the centres of projection of both cameras are coincident at point P, the rigid transformation relation between the two type images is illustrated as follows:

$$sq_{IR} = \boldsymbol{H}q_{Vis}, \tag{55}$$
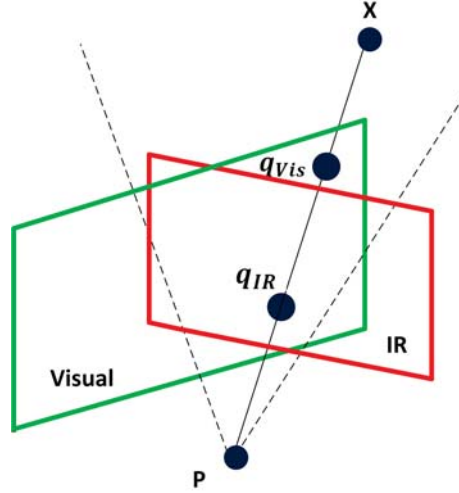
Figure 4.2: Geometry of cameras configuration.

where $\boldsymbol{H}$ represents the homography which is a 3×3 matrix and s is a scale factor.

As described in [119], $\boldsymbol{H}$ can be obtained by:

$$\boldsymbol{H} \cong W_{IR} R W_{Vis}^{-1}, \tag{56}$$

where W_{IR} and W_{Vis} denote the internal calibration matrices of both IR and visual cameras, respectively. R represents the rotation matrix associated with the camera centered coordinate systems. Therefore, $\boldsymbol{H}$ can be calculated if the cameras are calibrated and their related frame transformation is known. In addition, $\boldsymbol{H}$ can be computed by at least four known correspondences among lines or points in both images as well.

There are various techniques have been developed to compute $\boldsymbol{H}$ though it is more challenging to cope with images captured by different type of sensors. For the works presented in [48], the calibration is conducted by making use of a known and visible pattern on both types of cameras; while [120] proposes another approach estimating $\boldsymbol{H}$ on the image plane without requirement of calibration when both cameras are fixed closely together and are moved jointly in space. After $\boldsymbol{H}$ is calculated out, the two type images can be aligned, which means that the detected suspicious fires in the visual image can be transformed into the IR image plane.

80

4.2.2 Information Fusion

The primary advantage of fusing multi-modal image information is that unreliably extracted regions from one camera might be reliably extracted from the other type camera. The fusion of imageries in visible and IR ranges produces informative data about the scene, such as color, motion, and thermal detail. Using such information to successfully detect and analyze fire activity in the scene with lower false alarm rates has become popular to improve the performance of fire detection. The majority of existing researches in multi-modal video fire detection focus on the fusion of infrared and visual images, and it has been demonstrated that combining these two types of images would be beneficial for better detection in different environments.

Similarly to the existing multi-modal techniques, this thesis focuses on the combined analysis of IR and visual flame features. Because corresponding objects in different type images may have different properties such as size, shape, position and intensity, an appropriate image representation is needed to display the common information between the two type of images, while suppress the non-common data [121].

This study proposes a simple way of segmenting the common fire analogous regions of IR and visual images which have been individually processed. After that, the intersected pixels from two images are segmented. Thus, the mathematic morphological operations are further employed for removing the unconnected and irrelevant pixels/regions, while preserving the consecutive regions. Ultimately, the blob counter method is used to track the segmented fire regions.

4.3 Experimental Results

The proposed fire detection algorithms are developed in MATLAB environment. A desktop with Windows 7 operating system, Intel Core $i7$ processor and $8GB$ memory is adopted for image display and processing. In this work, a database from the website (http://cfdb.univ-corse.fr/index.php?menu=1) is used for verifying the effectiveness of the proposed fire detection approach. The images are captured by near infrared (NIR) camera and their resolutions are

1024×768.

4.3.1 Infrared Images Segmentation Results

Figs. 4.3, 4.4, 4.5 and 4.6 present the experimental results of the proposed method that is tested on video sequences of the database. Figs. 4.3(a), 4.4(a), 4.5(a) and 4.6(a) list the raw IR images; Figs. 4.3(b), 4.4(b), 4.5(b) and 4.6(b) are the segmentation results of hot object; Figs. 4.3(c), 4.4(c), 4.5(c) and 4.6(c) show the motion detection results processed by the optical flow analysis.

In Figs. 4.3(b), 4.4(b), 4.5(b) and 4.6(b), it can be clearly seen that high intensity regions which represent hot objects have been effectively extracted from the image background by using the Otsu method, but some non-fire hot regions with motion are also wrongly extracted (as shown in Fig. 4.5(b)). This phenomenon is caused by the heat radiation and light reflection of fires or lights. Therefore, in order to improve the accuracy of fire detection, the motion feature analysis utilizing optical flow for finding accurate fire regions is also employed to further check the extracted candidate areas.

Figs. 4.3(c), 4.4(c), 4.5(c) and 4.6(c) show the thresholding results after the further image processing using optical flow. From these figures, one can obviously observe that the non-fire hot regions are all removed.

The experimental results demonstrate that the proposed method is capable of detecting the fires with satisfactory performance, while the false alarms potentially caused by the fire analogues in IR images are significantly reduced as well.

4.3.2 Infrared and Visual Images Matching Results

Figs. 4.7(a), 4.8(a), 4.9(a) and 4.10(a) list the original visual images; Figs. 4.7(b), 4.8(b), 4.9(b) and 4.10(b) display the segmentation results in visual images; Figs. 4.7(c), 4.8(c), 4.9(c) and 4.10(c) show the motion detection results processed by the optical flow analysis in IR images; and Figs. 4.7(d), 4.8(d), 4.9(d) and 4.10(d) are the images (segmented visual and IR images) matching results after intersection and morphological operations.
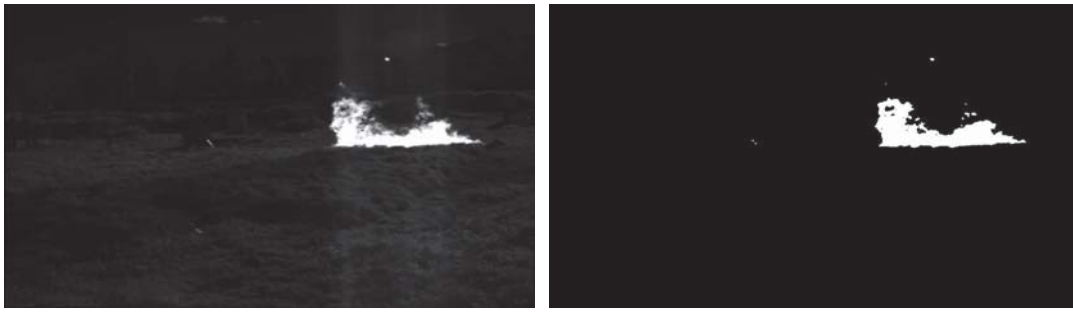
(a) Original IR image

(b) Otsu segmentation

(c) Motion detected result

Figure 4.3: Experimental results of sample frame 1.
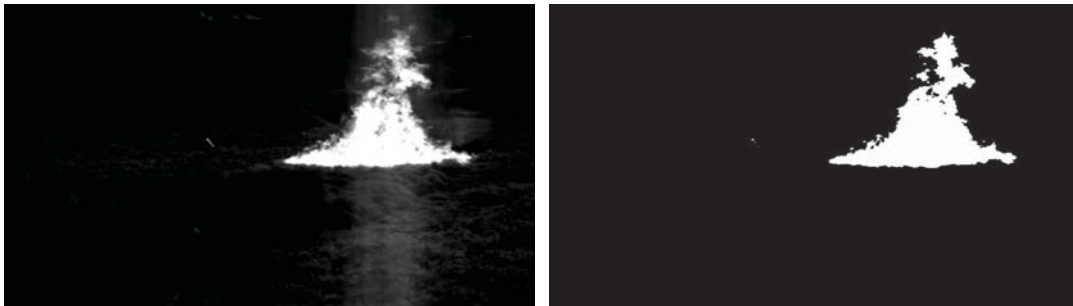
(a) Original IR image

(b) Otsu segmentation

(c) Motion detected result

Figure 4.4: Experimental results of sample frame 2.

(a) Original IR image   (b) Otsu segmentation

(c) Motion detected result

Figure 4.5: Experimental results of sample frame 3.
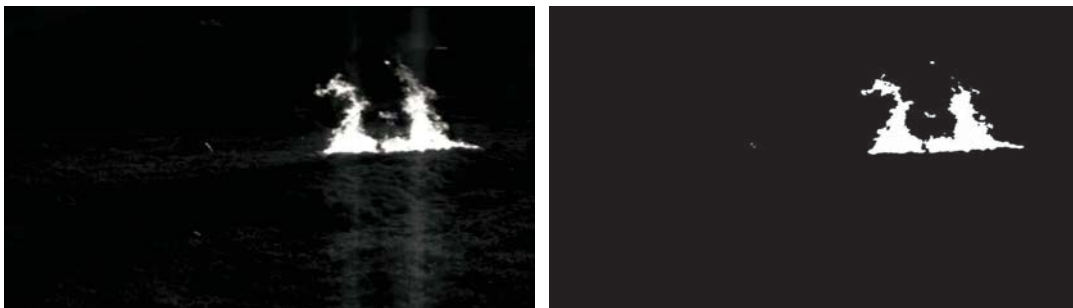
(a) Original IR image   (b) Otsu segmentation

(c) Motion detected result

Figure 4.6: Experimental results of sample frame 4.

(a) Original visual image

(b) Detection result in visual image

(c) Motion detected result in IR image

(d) IR and visual images fusion result
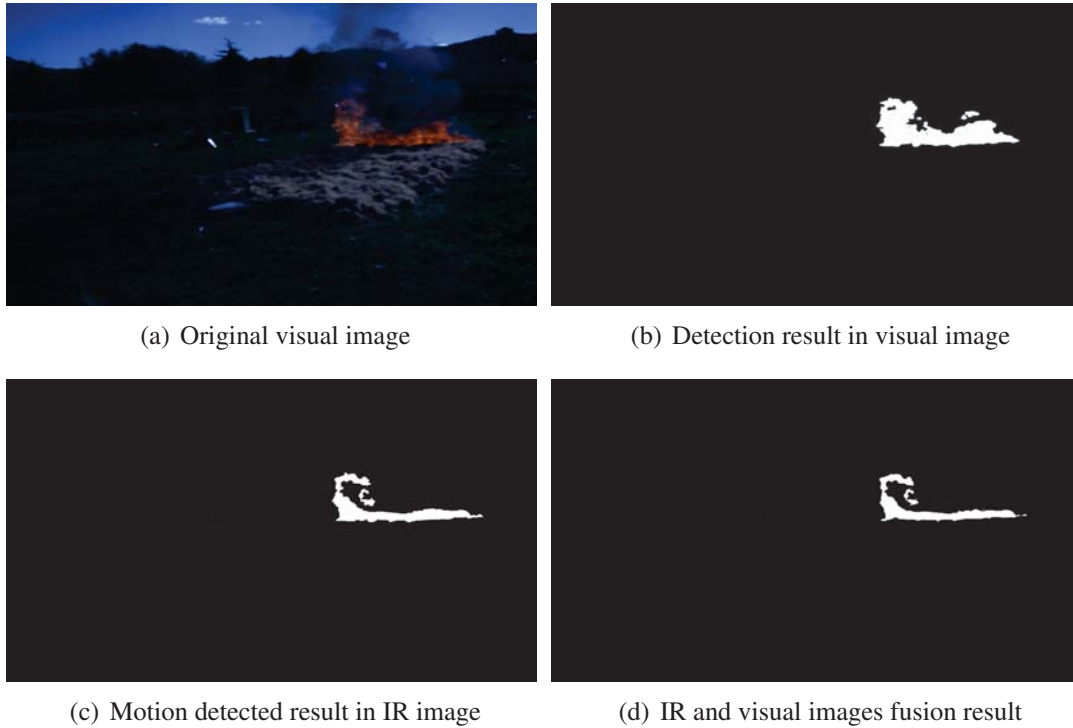
Figure 4.7: Experimental results of sample 1.

From Figs. 4.7(d), 4.8(d), 4.9(d) and 4.10(d), one can observe that the candidate fire regions segmented in IR and visual images are matched, the intersected regions with higher possibility of fire are further segmented by using the proposed method. Then the intersected regions are tracked by blob counter in the images, as shown in Fig. 4.11. This fusion processing procedure provides a drastically reduced number of false detection rates, which results in a significant improvement of fire detection performance.

(a) Original visual image

(b) Detection result in visual image

(c) Motion detected result in IR image

(d) IR and visual images fusion result
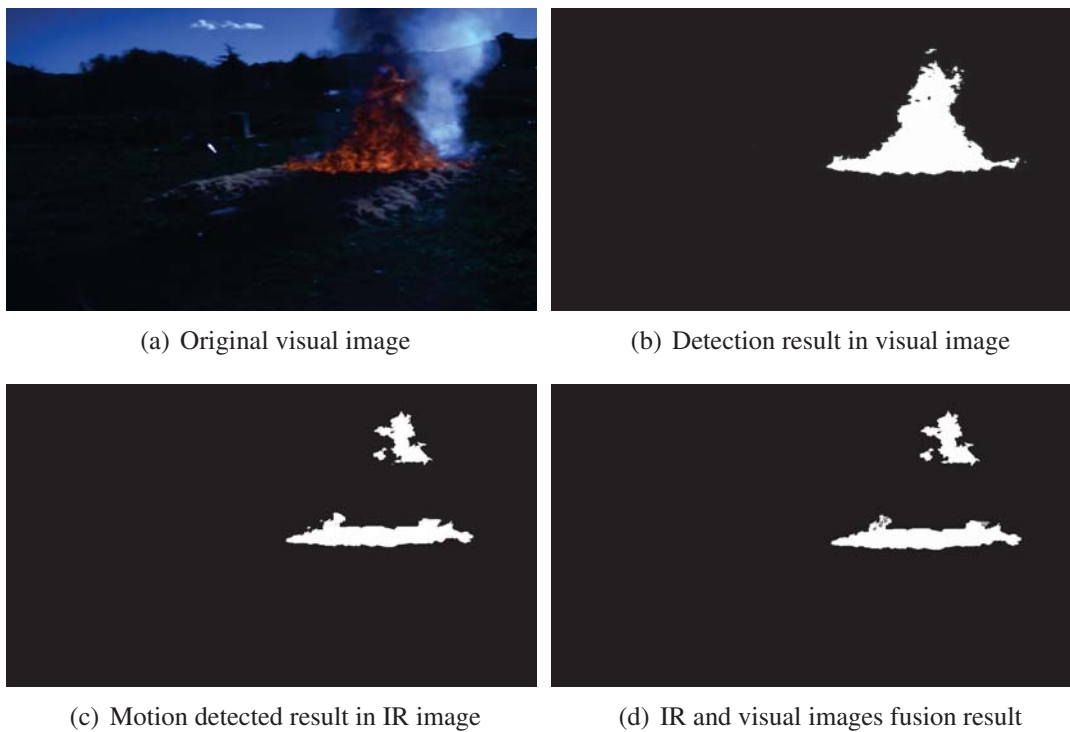
Figure 4.8: Experimental results of sample 2.

(a) Original visual image

(b) Detection result in visual image

(c) Motion detected result in IR image

(d) IR and visual images fusion result
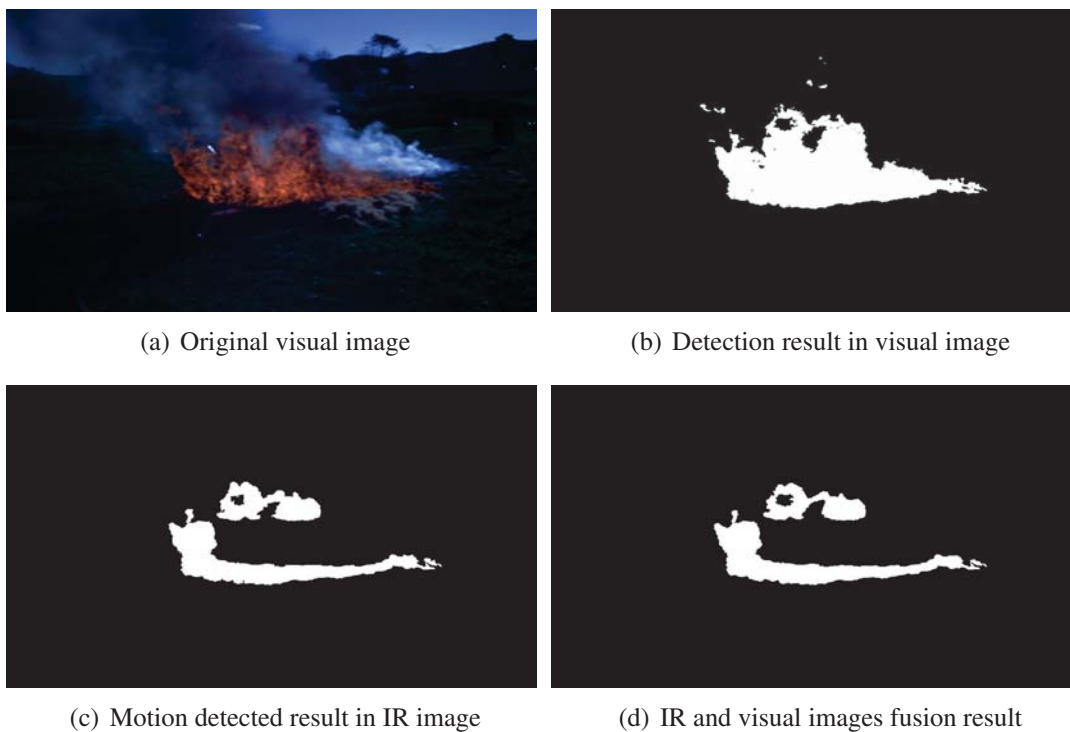
Figure 4.9: Experimental results of sample 3.

(a) Original visual image

(b) Detection result in visual image

(c) Motion detected result in IR image

(d) IR and visual images fusion result
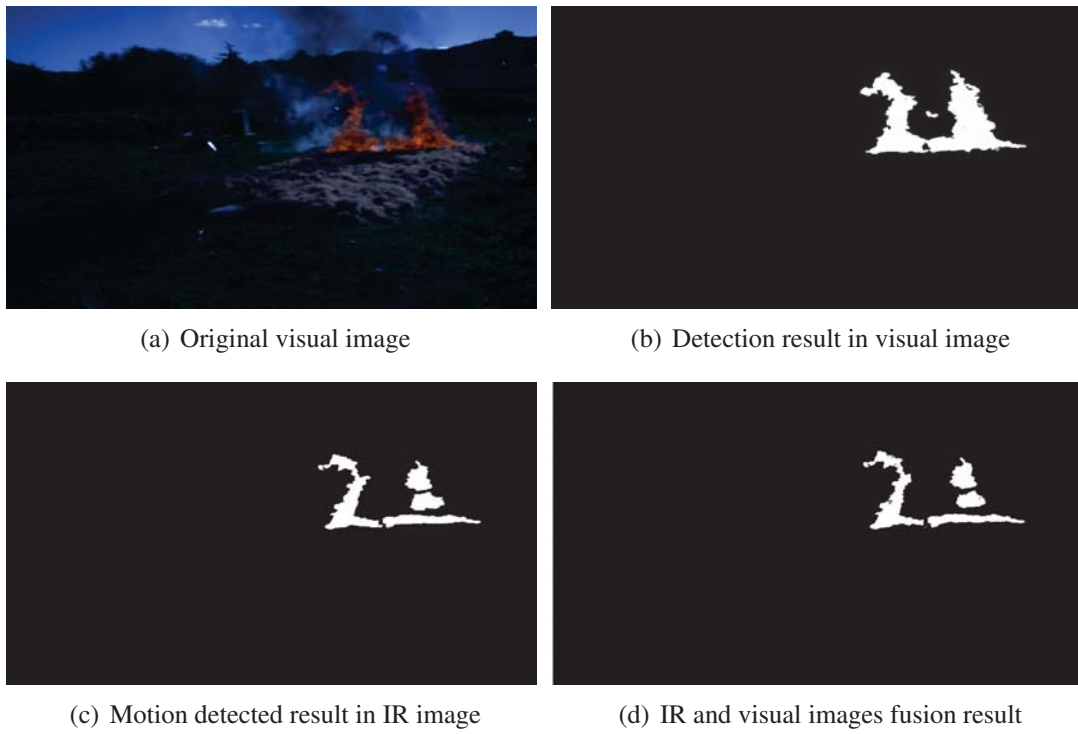
Figure 4.10: Experimental results of sample 4.

(a) Sample 1

(b) Sample 2

(c) Sample 3

(d) Sample 4
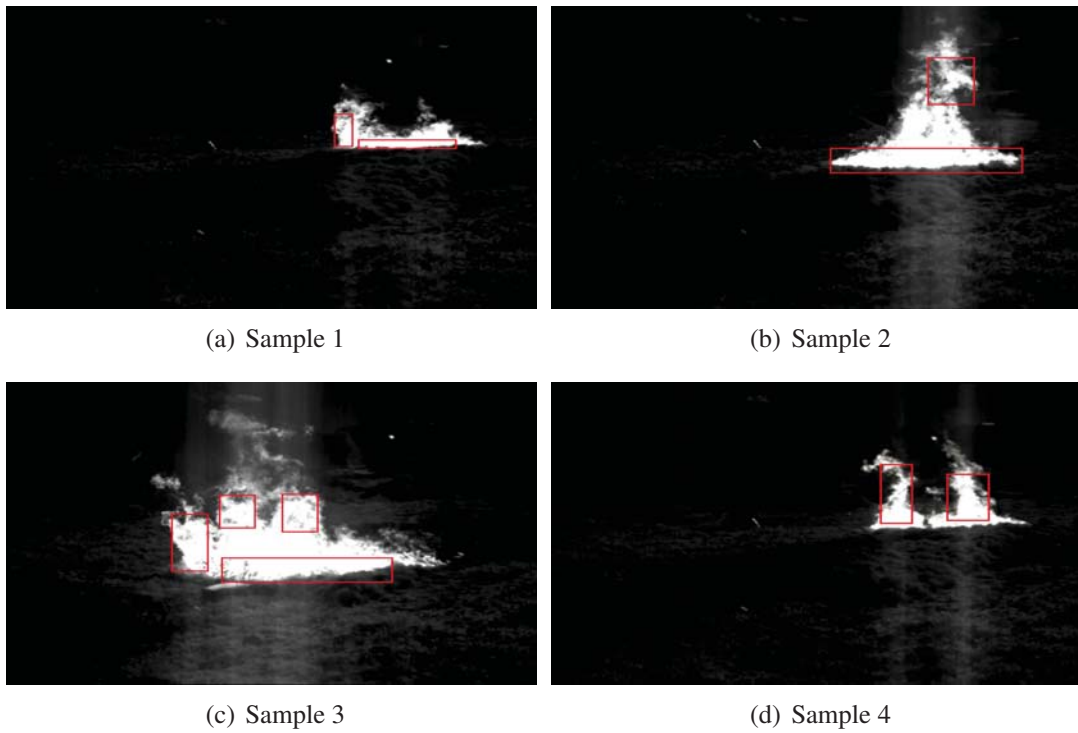
Figure 4.11: Experimental results of fire tracking.

Chapter 5

Learning Based Smoke Detection for UAV Based Forest Fire Surveillance

The existing forest fire detection approaches based on the characteristics of fire (including color and motion) have demonstrated their efficacy. However, to detect forest fire effectively based solely on the information of fire flame is not always enough, or to some extent, not early enough for fire-fighting. Normally, forest fire includes the following six phases of development: 1) incipient, 2) growth (pre-flashover), 3) flashover, 4) fully developed (post-flashover), 5) decay, and 6) extinction [122]. The incipient period (see Fig. 5.1), which is the very early stage of forest fire development, is dependent on a variety of factors, such as the quantity of available oxygen, the effect of wind, temperature, as well as the chemical component and humidity of trees. Early fire detection at this stage can prevent the fire developing into uncontrollable and avoid significant losses by following a timely response from qualified fire-fighting professionals.

Forest fire can be easily covered by smoke, especially in its early period, this phenomenon can seriously degrade the performance of flame-based fire detection approaches. Furthermore, smoke can be identified earlier than fire, and the area of smoke can also be much larger than that of fire flames. Therefore, as an important early sign of fires, smoke, which is compounded with hydrogen, carbon, and oxygen, has been seen as a critical forecasting symbol of fire [123]. Normally, it is
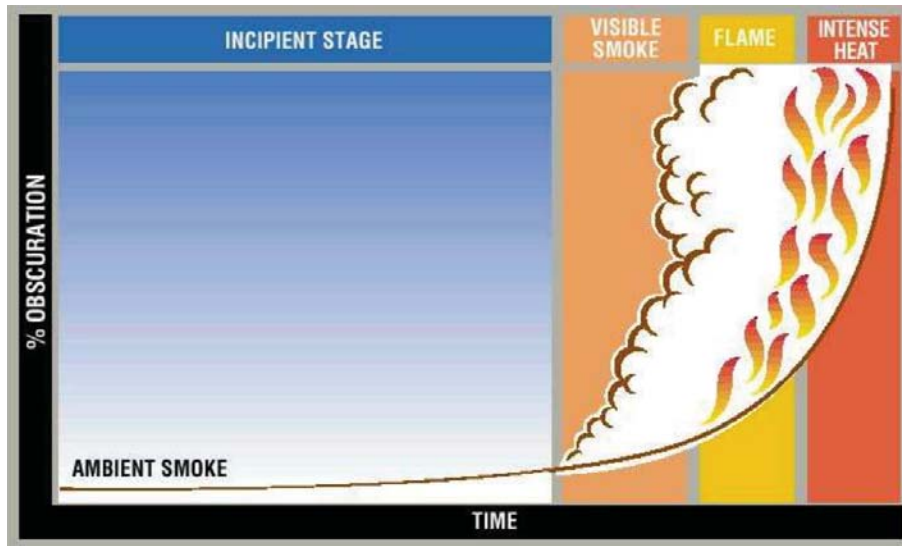
Figure 5.1: Duration of the incipient period of forest fire.

difficult to identify the visual pattern of smoke, and the density of smoke also varies with the surroundings. But smoke from the fire can be easily observed even if the flames are invisible, so that the fire can be detected earlier before it develops into uncontrollable. Thus, it is highly attractive to apply smoke detection in forest fire detection applications.

Traditional smoke detection methods mainly rely on the particle sampling. This requires close proximity to the source of smoke. Fire alarm is raised only when the particles reach and activate smoke detecting sensors. Moreover, the traditional smoke detection methods are difficult to detect smoke in open/large spaces and provide additional descriptive information of smoke including its location, size, orientation, and process of burning. In addition, smoke detection with significantly low false alarm rate remains a challenging issue for the application in open/large spaces with disturbances (own analogous features to smoke including color, motion or texture) from environment, such as specific species of the tree, special ground features, lighting variations caused by the changes from climate, weather, and time of the day. Meanwhile, comparing with fire flame, the visual characteristics of smoke including color and texture are less trenchancy. These phenomena make it rather difficult and more complicated to extract smoke from disturbances and background.

To solve the above-mentioned problems and achieve an effective detection performance, recently, visual-based (using camera) smoke detection techniques have been paid much attention due

to their effectiveness for open and large spaces, and low cost in development. Since the features of smoke including color, motion, motion orientation and texture, based on human's experience, are important to distinguish between smoke and non-smoke regions; investigation of these characteristics thereby plays a critical role in the development of visual-based smoke detection systems. The color of smoke changes from bluish-white to white with low temperature, while ranges from greyish-black to black along with the rise of temperature, then a fire ignites when the temperature reaches a specific level. When fire happens, the smoke usually rises from that site, diffusing upwards, may also spread to other directions when winds act on it. The smoke regions generally vary in area, size and number from one frame after another with rough and coarse surface and boundary [124].

Numerous smoke detection methods have been developed. They can be generally classified into four groups based on the ways adopted for the detection: 1) histogram-based methods, 2) temporal-analysis-based approaches, 3) rule-based techniques, and 4) a combination of techniques. In [125], two decision rules are used for smoke detection, one is the chromatic decision rule for analyzing the color of smoke, while the other one is the diffusion-based dynamic decision rule based on the spreading attributes of smoke. A fast and accumulative motion model is proposed in [76] for video-based smoke detection. This model employs both chrominance and motion orientation features of smoke for achieving effective detection results, but lack of precision presents when the smoke is affected by winds. A target-tracking-based smoke detection method is presented in [126], in addition to the combination of temporal and spatial features of smoke, both static and dynamic visual characteristics of smoke are also adopted, while the brightness consistency of smoke is well assessed. In [127], a visual-based smoke detection method is developed using the SVM. Several features of smoke including the changing unevenness of the density distribution and irregularities of the contour are utilized. After the extraction of these features, SVM is then employed to distinguish between smoke and non-smoke regions. But the color feature is overlooked as a distinguishing feature of smoke in this research. An efficient smoke detection algorithm using wavelets method and a SVM classifier is designed in [128]. In [129], the feature of partial transparency of

smoke is used for the development of smoke detection approach, which is then implemented using the wavelet theory to extract the edge blurring values of background object. After that, the system devised in [129] is then enhanced in [65] by employing the contour characteristics of smoke. A single stage wavelet energy and a back-propagation neural network are selected in [130], these two algorithms are then used on a small data set for smoke detection. In [80], the background estimation and color-based decision rules are adopted, combining with optical flow method for calculating the candidate smoke regions. [131] presents a clustered motion based smoke detection method. [132] proposes an approach considering both smoke and flame as turbulent phenomena, then using the dimensionless edge/area or surface/volume measure to characterize the shape complexity of these turbulent phenomena. The tree-structured wavelet transform and gray level co-occurrence matrices are combined in [133] for the analysis of the texture feature of smoke. But this method requires a high computational cost for processing, which is not available for the generally used surveillance systems with CCD cameras. In general, the developed algorithms can be classified into the following three aspects: 1) combine the rules associated to smoke features; 2) utilize color-based techniques for extracting smoke color attributes; and 3) extract smoke from moving objects.

In order to achieve an effective performance of smoke detection, this thesis proposes a new learning-based fuzzy smoke detection algorithm considering color feature of smoke. All images are captured from visual cameras which are mounted on the bottom of UAV and orientate to the anterior inferior direction with a specified pitch angle. The benefit of this configuration is capable of concentrating on the information of forests and greatly reducing the adverse effects from cloud (which, to some extent, shares the similar features with smoke in color and shape) in the sky. The design procedure of the proposed method can be addressed as follows: 1) first, the visual images are captured by the camera installed on the bottom of UAV; 2) then, a fuzzy smoke detection rule is designed, selecting the RGB difference and intensity as the inputs and smoke likelihood as the output; 3) next, an extended Kalman filter (EKF) is designed based on both the inputs and output of fuzzy smoke detection rule to provide it with additional regulating flexibility by reshaping its fuzzy membership functions and rules on-line; and since it may produce nonconnected (nonconvex

or concave) segments which are distorted by noises and textures after image processing, the morphological operation is then adopted to remove these imperfections; 4) eventually, the smoke can be effectively segmented from the background by the reconfigured smoke detection law regardless of the variation of environmental conditions.

According to the grayscale of segmented area, the fuzzy rules will be changed by EKF. Then the grayscale of smoke also changes. Therefore, the proposed method can offer the following benefits to smoke detection: 1) due to its simplicity, light-computational requirements, and adaptability to system variations, fuzzy logic method is employed for making the smoke segmentation rules; 2) without rich experience of smoke detection skills, an effective smoke detection rule is achievable after training the fuzzy logic based smoke detection scheme by using EKF owing to its system variation learning capabilities; 3) it is time-efficient to obtain an effective smoke detection rule by using the EKF to train the smoke detection scheme; and 4) the proposed method is adaptive to the variations in weather conditions, time of the day, features of forest, etc.. It is worth-mentioning that it is also helpful to establish a database in advance based on the environmental variations, then choose the specific detection rule for the corresponding condition to accelerate the learning procedure.

5.1   Fundamental Information of Smoke Detection

Similar to the fire flame detection, smoke pixels can also be modelled. However, the smoke does not display chrominance characteristics as fire flame. At the start, the smoke is expected to show color from white-bluish to white when the temperature of smoke is relatively low; while the temperature of smoke increases and its color changes from black-grayish to black when it reaches the boundary of the start of fire flame [62].

Meanwhile, the burning with different combustible materials can produce different quantities and color of smoke. In general, most of the smoke display grayish colors, which can be classified into the following two grayish color regions: light gray and dark gray. Furthermore, based on the

features of smoke, it can imply that the three components R, G and B of smoke are almost equal or with a small difference. In order words, the R, G and B components of smoke are very close to each other. This phenomenon implies that the absolute difference of the maximum and minimum values among these three components should be constrained within a specific threshold. Thus, the first smoke detection rule can be established as follows:

$$Ts = \max(Ts_1, Ts_2, Ts_3) \leq T_{max}, \tag{57}$$

where

$$\begin{cases} |R(x,y) - G(x,y)| = Ts_1, \\ |G(x,y) - B(x,y)| = Ts_2, \\ |R(x,y) - B(x,y)| = Ts_3, \end{cases} \tag{58}$$

Ts_1, Ts_2, and Ts_3 are calculated as the difference between each two channels. Ts is the maximum absolute difference among the three components of the RGB model, $T_{max} \in [Ts_L, Ts_H]$ denotes a predetermined global threshold determining the intensity similarity of each RGB color channel, Ts_L and Ts_H are the lower and higher boundaries of thresholding values, respectively.

Since the primary color of smoke is grayish, in order to describe smoke in an effective manner, the HSI model is also employed, especially the intensity component of HSI model is used for describing the light and dark gray regions in $[I_{L1}, I_{L2}]$ and $[I_{D1}, I_{D2}]$, respectively. Therefore, the following second smoke detection rule can be formulated:

$$\begin{cases} I_{L1} \leq I \leq I_{L2}, & \text{For light grayish color,} \\ I_{D1} \leq I \leq I_{D2}, & \text{For dark grayish color,} \end{cases} \tag{59}$$

where I is the intensity value of each pixel in the current frame, the selection of I_{L1}, I_{L2}, I_{D1}, and I_{D2} depends on the statistical data of experiments.

Ultimately, the two conditions Eqs. (57) and (59) can be chosen in the design of decision

making functions for smoke recognition, in the case of considering chromatic analyses for smoke detection.
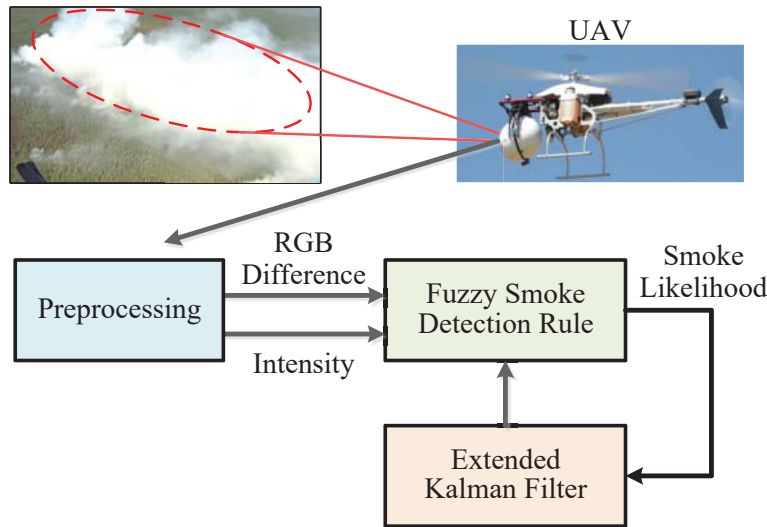
Figure 5.2: Illustration of the proposed learning-based smoke detection scheme.

5.2 Learning Based Smoke Detection Rule Design

As illustrated in Fig. 5.2, the main idea of the proposed method is to design a supervisory fuzzy logic based smoke detection method, which is capable of not only effectively segmenting smoke from background, but also adjusting the parameters of the fuzzy smoke detection rule adapting to environmental variations including different lighting conditions and background colors, so that the proposed learning-based fuzzy smoke detection approach is expected to successfully detect smoke with significant reduction of false fire alarm rate.

The learning-based fuzzy smoke detection methodology consists of an EKF and a fuzzy logic rule, which are synthesized as follows:

(1) First, the visual images are captured by the cameras installed on the bottom of UAV.

(2) Then, a fuzzy smoke detection rule is designed by selecting the RGB difference and intensity

94

as the inputs and smoke likelihood as the output.

(3) Next, an EKF is designed based on both the inputs and output of fuzzy smoke detection rule to provide it with additional regulating flexibility by reshaping its fuzzy membership functions and rules on-line.

(4) Eventually, the smoke can be effectively segmented from the background by the reconfigured smoke detection law regardless of the variation of environmental conditions.

What is worth mentioning is that the main concept of this scheme is to combine the advantages of the learning capability of EKF, and the ability of fuzzy logic method on dealing with automatic thresholding and segmentation with environmental uncertainties, to achieve a satisfactory performance of smoke detection without consuming much time of developer for tuning the fuzzy smoke detection rule in the absence of relative experienced technical personnels. The design details are introduced in the following subsections.
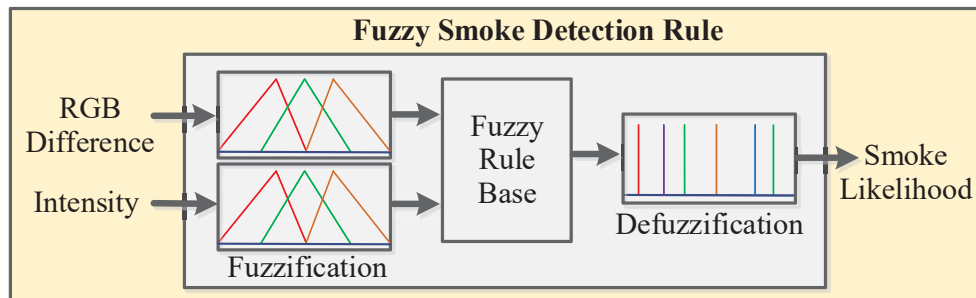
Figure 5.3: Illustration of the proposed fuzzy smoke detection scheme.

5.2.1 Fuzzy Smoke Detection Rule Design

Fuzzy logic method has been considered as an excellent choice for a variety of applications which come along with the requirements of real-time, high nonlinearity, and sophisticated computation [134].

In general, the triangle membership function is employed for each input, and it can be mathematically written into the following form:

$$
f_{ij}(z_j) = \begin{cases} 1 + (z_j - c_{ij})/b_{ij}^- & if \ -b_{ij}^- \leq (z_j - c_{ij}) \leq 0, \\ 1 - (z_j - c_{ij})/b_{ij}^+ & if \ 0 \leq (z_j - c_{ij}) \leq b_{ij}^+, \\ 0 & otherwise, \end{cases} \tag{60}
$$

where i and j denote the number of inputs and triangle membership functions, respectively. z_j is the jth input, c_{ij} is the ith centroid, while b_{ij}^- and b_{ij}^+ represent the lower and upper half-widths of the ith triangle membership function, respectively.

Moreover, as one of the most popularly applied defuzzification techniques, the max-min aggregation and centroid defuzzification method is employed in this thesis to compute the value of output. In this study, only one output is defined in the fuzzy smoke detection system. Similar to the inputs design, the defuzzification rule for output is constructed as follows:

$$
m_j(y) = \begin{cases} 1 + (y - \gamma_j)/\beta_j^- & if \ -\beta_j^- \leq (y - \gamma_j) \leq 0, \\ 1 - (y - \gamma_j)/\beta_j^+ & if \ 0 \leq (y - \gamma_j) \leq \beta_j^+, \\ 0 & otherwise, \end{cases} \tag{61}
$$

where $m_j(y)$, γ_j, and y denote the jth fuzzy output, modal point, and crisp number, respectively. β_j^- and β_j^+ are the lower and upper half-widths of the jth output rule, respectively.

Supposing that the jth rule is the result of $z_1 \in$ fuzzy set i and $z_2 \in$ fuzzy set k, the activation level of the consequence of the jth rule can be represented by w_j, this activation level can then be expressed as:

$$
w_j = min[f_{i1}(z_1), f_{k2}(z_2)]. \tag{62}
$$

Therefore, the corresponding fuzzy output can be obtained by the following representation:

$$\bar{m}_j(y) = w_j m_j(y), \tag{63}$$

where the fuzzy output $m(y)$ is calculated by:

$$m(y) = \sum_{j=1}^{M} \bar{m}_j(y). \tag{64}$$

Apply the selected centroid defuzzification scheme, it is possible to map the fuzzy output to a crisp number $\hat{y}$ as follows:

$$\hat{y} = \frac{\sum_{j=1}^{M} w_j C_j S_j}{\sum_{j=1}^{M} w_j S_j}, \tag{65}$$

where C_j and S_j are the centroid and region of the jth fuzzy membership function of output, respectively. In addition to that, the centroid C_j can be defined as follows:

$$C_j = \frac{\int y m_j(y) dy}{\int m_j(y) dy}. \tag{66}$$

5.2.2 Extended Kalman Filter

As a rather mature and well-known technique, EKF has been widely employed by engineers for a variety of engineering and industrial applications [135]. To take advantages of the online learning capabilities with relative low computational consumption and the massive number of existing application examples of using EKF, which is also employed in this study for training the proposed fuzzy smoke detection system in real time.

The system and measurement models [136] in discrete-time representation are first established as follows:

$$\begin{cases} x_i &= f(x_{i-1}) + \omega_{i-1}, \\ d_i &= h(x_i) + \nu_i, \end{cases} \tag{67}$$

where x_i is the stochastic variable when the system state is at time t_i. ω_{i-1} and ν_i denote the noises

from process and measurement, respectively. $f(\cdot)$ and $h(\cdot)$ represent the vector functions of the states which are nonlinear.

After that, the target of designing EKF is to find an estimate $\hat{x}_i$ of x_i considering $d_i(0, ..., j)$.

Considering the nonlinearities of system (67) are sufficiently smooth, and using Taylor series method, this system can then be expanded around the state estimate $\hat{x}_i$ in the following form:

$$\begin{cases} f(x_i) & = f(\hat{x}_i) + F_i \times (x_i - \hat{x}_i) + \text{higher order terms}, \\ h(x_i) & = h(\hat{x}_i) + H_i^T \times (x_i - \hat{x}_i) + \text{higher order terms}, \end{cases} \tag{68}$$

where

$F_i = \dfrac{\partial f(x)}{\partial x}\big|_{x=\hat{x}_i},$

$H_i^T = \dfrac{\partial h(x)}{\partial x}\big|_{x=\hat{x}_i}.$

After neglecting the higher order terms in Eq. (68), Eq. (67) can be approximated by the following equations:

$$\begin{cases} x_i & = F_{i-1}x_{i-1} + \omega_{i-1} + \phi_{i-1}, \\ d_i & = H_i^T x_i + \nu_i + \varphi_{i-1}, \end{cases} \tag{69}$$

where

$\phi_{i-1} = f(\hat{x}_{i-1}) - F_{i-1}\hat{x}_{i-1},$

$\varphi_{i-1} = h(\hat{x}_{i-1}) - H_{i-1}^T \hat{x}_{i-1}.$

Ultimately, the desired estimate $\hat{x}_i$ is achievable by employing the following general EKF recursive equations [136]:

$$\begin{cases} F_{i-1} & = \dfrac{\partial f(x)}{\partial x}\Big|_{x=\hat{x}_{i-1|i-1}}, \\ H_i & = \dfrac{\partial h(x)}{\partial x}\Big|_{x=\hat{x}_{i|i-1}}, \\ K_i & = P_{i|i-1}H_i^T(R_i + H_iP_{i|i-1}H_i^T)^{-1}, \\ \hat{x}_{i|i} & = f(\hat{x}_{i-1|i-1}) + K_i[d_i - h(\hat{x}_{i|i-1})], \\ P_{i|i} & = F_{i-1}(P_{i-1|i-1} - K_iH_iP_{i-1|i-1})F_{i-1}^T + Q_{i-1}, \end{cases} \tag{70}$$

where d_i, K_i, and P_i denote the Kalman gain, observation vector, and covariance matrix of state estimation error, respectively. The estimated state $\hat{x}_{i|i}$ represents the optimal solution that tends to approach the conditional mean value $E[x_i|(d_0, d_1, \ldots, d_i)]$.

5.2.3 Synthesis of Learning Based Fuzzy Smoke Detection Methodology

In this work, the two inputs are selected as the intensity I and the maximum absolute difference Ts among the three components of RGB model, respectively. Regarding the selection of I, as this study is intended to achieve an early forest fire detection, while the smoke normally shows light gray color in the early stage of forest fire. Meanwhile, due to the specific characteristic of trees, the smoke of trees, in general, also displays the light gray color. Thus, the intensity $I \in [I_{L1}, I_{L2}]$ is chosen as one of the inputs in this study. Regarding the maximum absolute difference among the three components of RGB model, Eq. (59) is first used to calculate the differences between each two components of the three components of RGB model; then the one with maximum value is chosen as the other input of the overall two inputs.

In order to synthesize the proposed learning-based fuzzy smoke detection methodology, the following critical design process is required: the optimization of fuzzy membership functions and rules adopting the recursive calculation capabilities of EKF.

Optimizing the membership functions of fuzzy system using EKF can be considered as a weighted least-squares minimization problem. Two inputs and one output are selected for the design of fuzzy system in this study. The intensity I and maximum absolute difference Ts among the three components of RGB model are selected as the two inputs, while the likelihood of forest fire are chosen as the output. In addition, n fuzzy sets are assigned to the first input, and m fuzzy sets are distributed to the second input, while the output is allocated with k fuzzy sets.

The synthesis procedure can be illustrated in the following steps:

- First, choose a state vector x which includes b_{ij}^-, b_{ij}^+, and c_{ij} of inputs in Eq. (60), and β_{ij}^-,

β_{ij}^{+}, and γ_i of output in Eq. (61) as the state of the nonlinear system Eq. (67):

$$x = [b_{11}^{-} \ b_{11}^{+} \ c_{11} \ \ldots \ b_{n1}^{-} \ b_{n1}^{+} \ c_{n1}$$

$$b_{12}^{-} \ b_{12}^{+} \ c_{12} \ \ldots \ b_{m2}^{-} \ b_{m2}^{+} \ c_{m2} \tag{71}$$

$$\beta_{1}^{-} \ \beta_{1}^{+} \ \gamma_1 \ \ldots \ \beta_{k}^{-} \ \beta_{k}^{+} \ \gamma_k]^{T}.$$

- Then, apply the Kalman recursion in Eq. (70), where d_i and $f(\cdot)$ are assigned as the target output of the fuzzy system and identity mapping, respectively. $h(\hat{x}_i)$ is chosen as the fuzzy system's actual output which provides the current membership function parameters, F_i is set as an identity matrix. H_i is selected as the partial derivative of the fuzzy output in regard to the membership function parameters.

- Next, after conducting the Kalman recursion, it is expected to obtain the estimate $\hat{x}_i$ that includes the new fuzzy membership function parameters for adjusting the fuzzy rules to segment the smoke candidate from background.

- Finally, the morphological operation is also employed to remove the imperfections and non-connected (nonconvex or concave) segments distorted by noises and textures after image processing.

5.3 Experimental Results

Table 5.1: The fuzzy rule base for the proposed smoke detection method.

		I				
		ZE	PS	PM	PB	PVB
	ZE	Z	Z	Z	M	B
	PS	Z	Z	S	M	B
Ts	PM	S	S	M	B	VB
	PB	M	M	M	B	VB
	PVB	M	M	M	B	VB

As displayed in Table 5.1, a fuzzy rule base with five membership functions for each of the two inputs and one output is designed, where "ZE" = "zero", "PS" = "positive small", "PM" = "positive medium", "PB" = "positive big", and "PVB" = "positive very big" are chosen to express the size of fuzzy values for the inputs; meanwhile, "Z" = "zero", "S" = "small", "M" = "medium", "B" = "big", and "VB" = "very big" are selected to express the size of fuzzy values for the output.

(a)   (b)

(c)
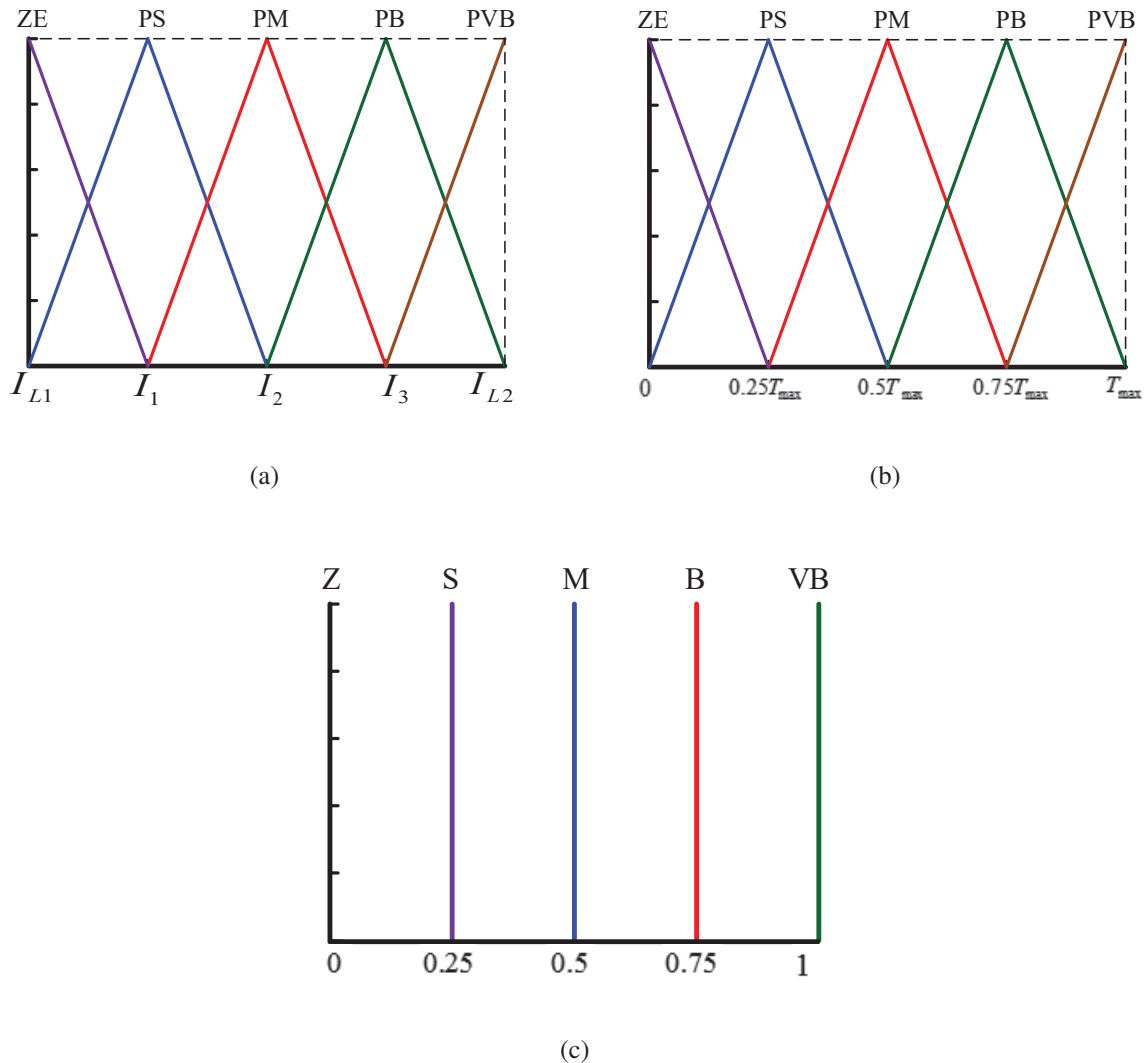
Figure 5.4: Initial membership functions of first input (a), second input (b), and output (c).

Fig. 5.4 illustrates the initial membership functions of intensity I and the maximum absolute difference Ts among the three components of RGB model for inputs, and the likelihood of forest fire for output, respectively. At the start of experiments, the first input, the intensity I is limited in

the range from $I_{L1} = 150$ to $I_{L2} = 255$, the second input, the maximum absolute difference Ts is constrained by $Ts \leq T_{max} = 30$, while the fuzzy sets width of each output is allocated in $[0, \ 1]$. $\Delta I = I_{L2} - I_{L1}$, $I_1 = I_{L1} + 0.25\Delta I$, $I_2 = I_{L1} + 0.5\Delta I$, and $I_3 = I_{L1} + 0.75\Delta I$.

It is worth-mentioning that the initial ranges selection for inputs and output are obtained from the experiences, while the optimal ranges will be achieved by the recursive regulation of EKF. Regarding the selection of membership functions for partitioning the ranges of inputs, generally, the more membership functions are chosen, the more complicated system will be, and the higher computational consumptions are required as well. Therefore, to balance the system performance and complication, five triangle membership functions are devised in this work. This selection strategy is designed based on the design experience obtained from the author's previous research works and the existing publications on fuzzy logic design for the consecutive and effective coverage of system states, while only acceptable computational efforts are demanded for the real-time applications with satisfactory performance.

5.3.1 Scenarios Description

The classic Otsu segmentation method is employed as the comparison to validate the proposed approach in a clearer manner. In addition to that, in order to demonstrate the effectiveness of the proposed smoke detection method with great robustness to environmental disturbances, three scenarios are selected, the corresponding descriptions are listed as follows:

(1) In the first scenario, the smoke with somewhat bright background in images are captured from a moving aircraft.

(2) In the second scenario, comparing with the first scenario, the smoke with relatively darker background in images are captured from a moving aircraft.

(3) The background in the above two scenarios is comparatively simple. In order to further testify the robustness of the proposed method, the third scenario covers a more complicated situation comparing with the previous two scenarios, a small size of light smoke with some

analogues similar in color from the background in images are captured from a moving aircraft.

5.3.2 Results of Scenario 1

As shown in Fig. 5.5, the left column lists the original images captured from a real moving aircraft, the middle column covers the images processed after Otsu segmentation approach, and the right column lists the images segmented after the proposed smoke detection method.

Although both of the compared two methods can successfully segment the smoke from background, less uninterested/non-smoke areas and noises are included by the proposed method comparing with the Otsu approach.

In addition, compared with Fig. 5.4, Fig. 5.6 clearly shows that both inputs and output functions are all adjusted by EKF. As observed in Figs. 5.6(a) and 5.6(b), either the first input function related to the intensity or second input function related to the absolute differences of RGB channels tends to the higher values of their corresponding segmentation levels. This phenomenon is due to the fact that the intensity and color contrast of images are higher than that of the initial setting. Fig. 5.6(c) displays that the membership functions of output moves towards the lower value than that of the initial state. This phenomenon indicates the likelihood of forest fire decreases with the initial setting.

5.3.3 Results of Scenario 2

From Fig. 5.7, same to Scenario 1, the left column includes the original images captured from a real moving aircraft, the middle column contains the images processed after Otsu segmentation approach, and the right column lists the images segmented after the proposed smoke detection method.

Similar to Scenario 1, more uninterested/non-smoke areas and noises are removed by the proposed method comparing with the Otsu approach, while the smoke regions are successfully segmented.
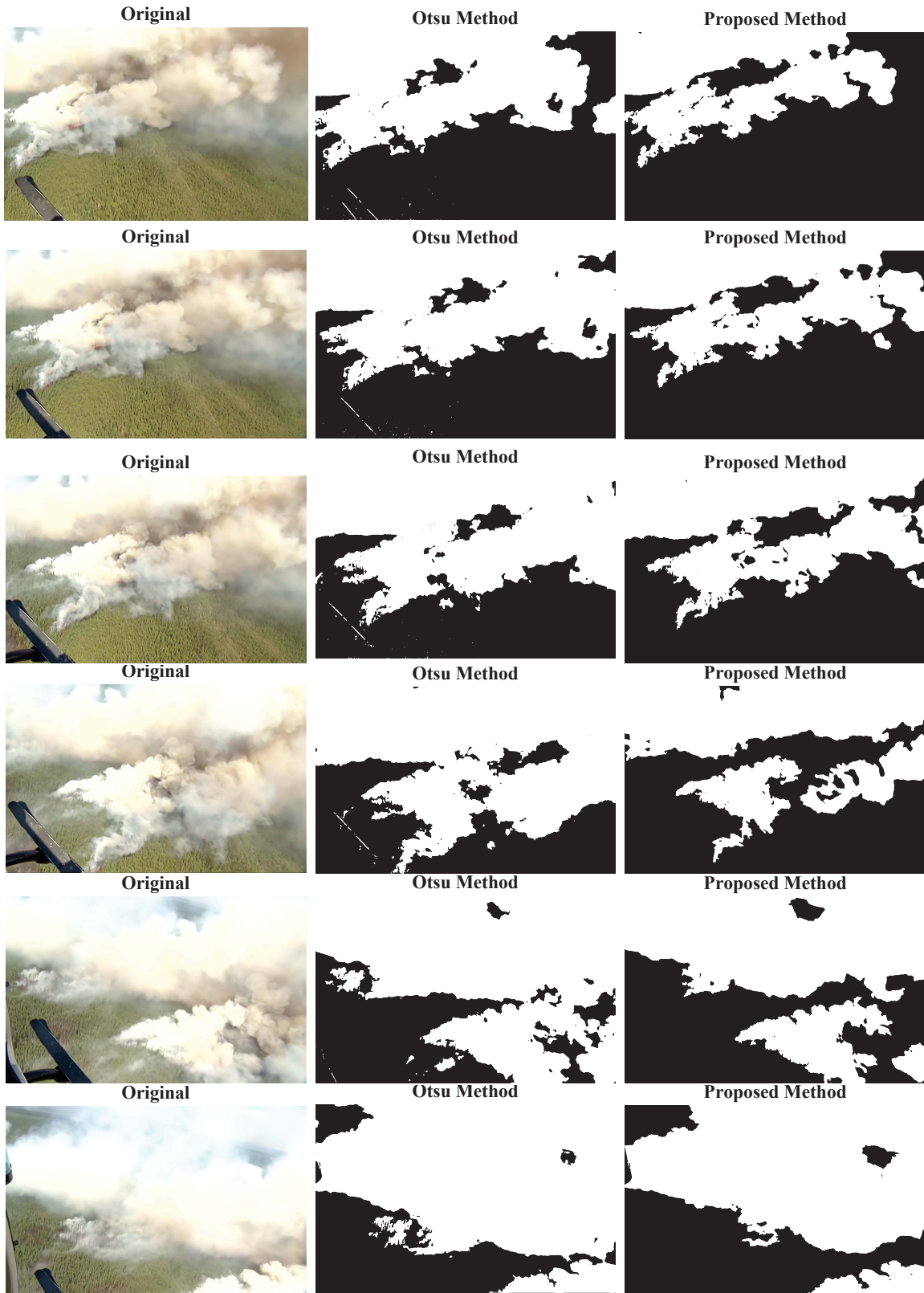
Figure 5.5: Performance of smoke segmentation: original images (left), results of Otsu method (middle), and results of proposed method (right).
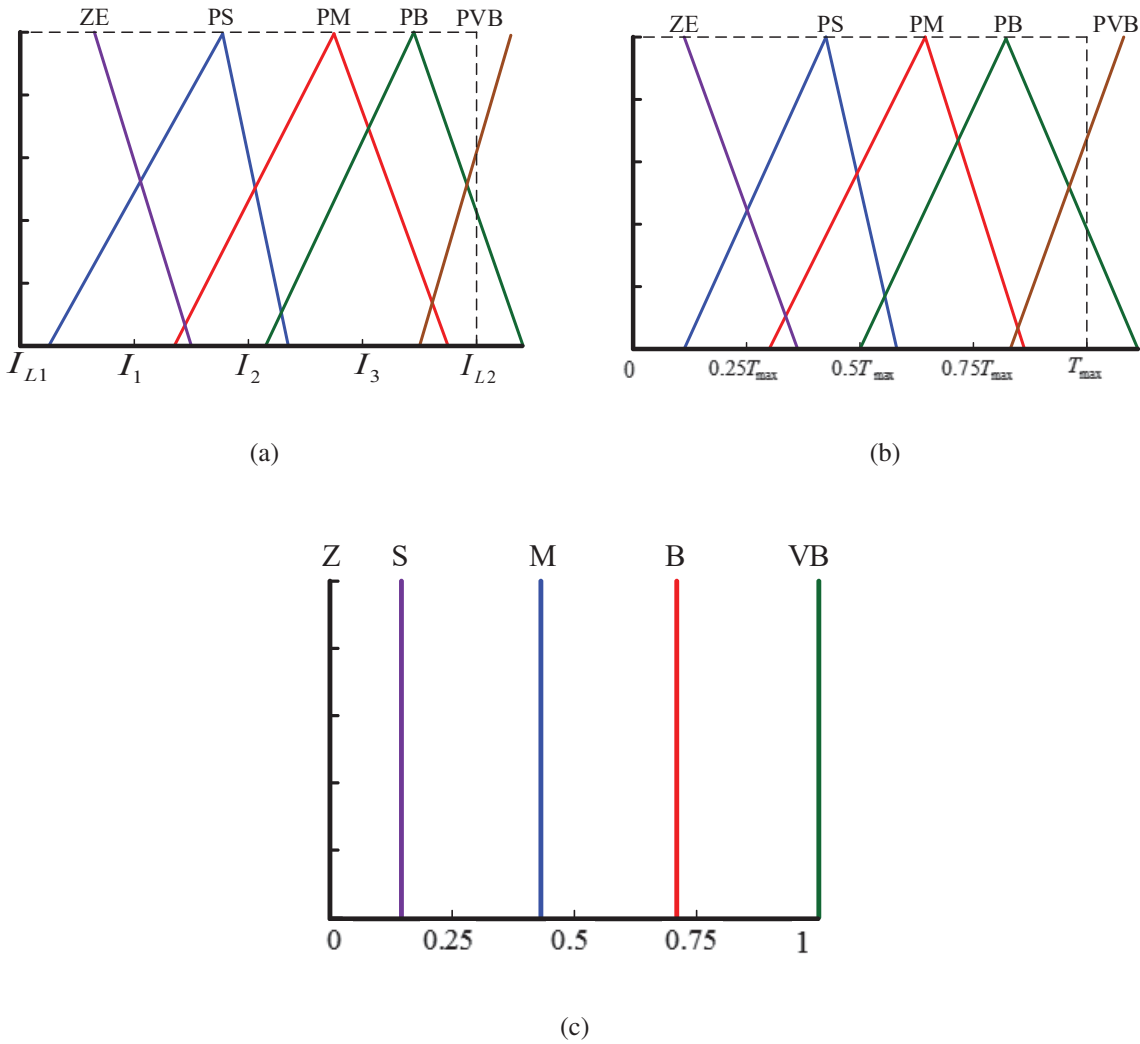
Figure 5.6: Reconfigured membership functions of first input (a), second input (b), and output (c).

Furthermore, compared with Fig. 5.4, both inputs and output functions are also adjusted by EKF as shown in Fig. 5.8. From Figs. 5.8(a) and 5.8(b), either the first input function related to the intensity or second input function related to the absolute differences of RGB channels tends to the higher values of their corresponding segmentation levels, but less value than that in the first scenario. This phenomenon is due to the fact that the intensity and color contrast of images are higher than that of the initial setting, but a little bit less value than that in the first scenario. Fig. 5.8(c) shows that the membership functions of output moves towards the higher value than that of the initial state. This phenomenon indicates the likelihood of forest fire increases with the
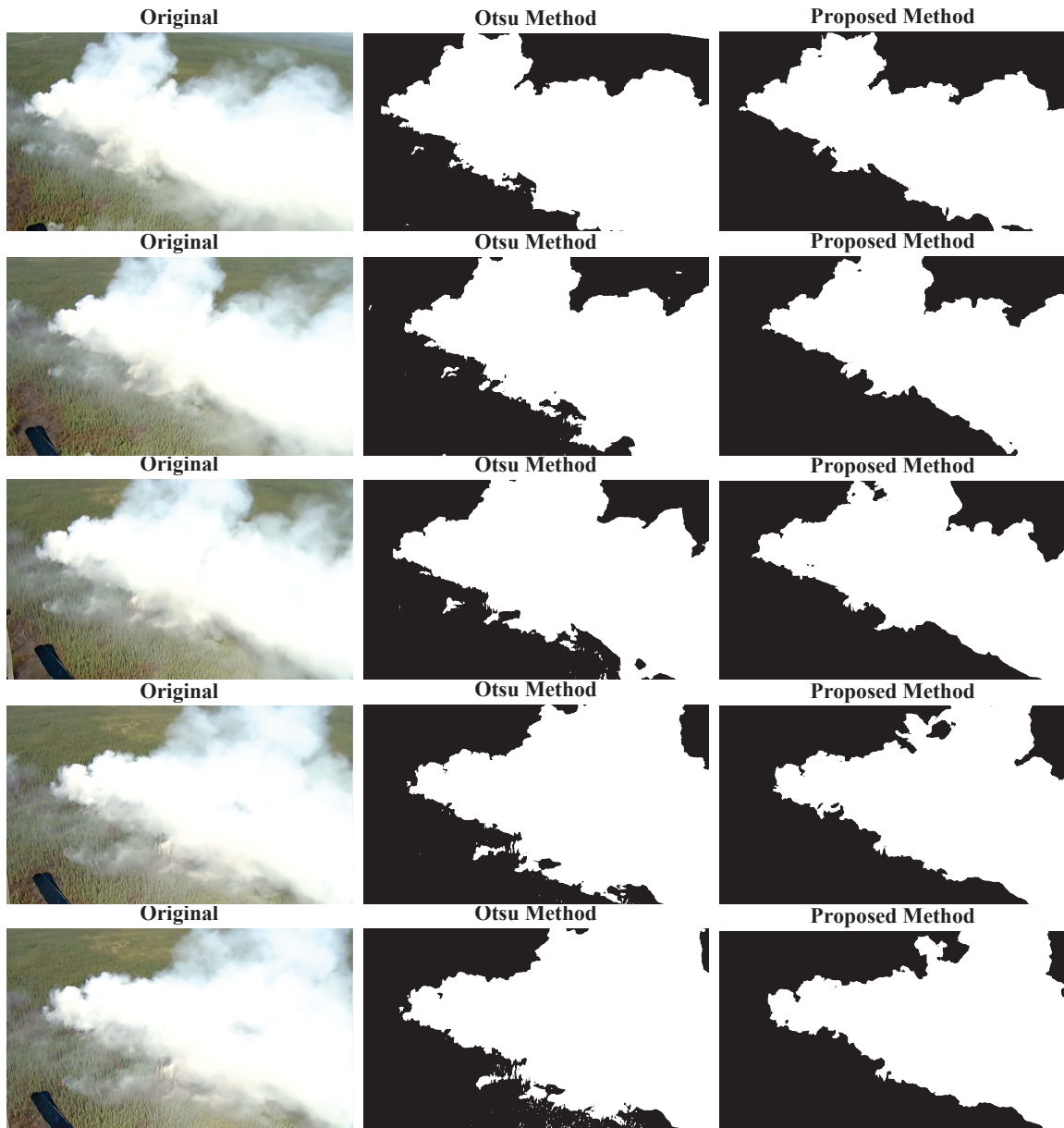
Figure 5.7: Performance of smoke segmentation: original images (left), results of Otsu method (middle), and results of proposed method (right).

initial setting.

(a)

(b)

(c)
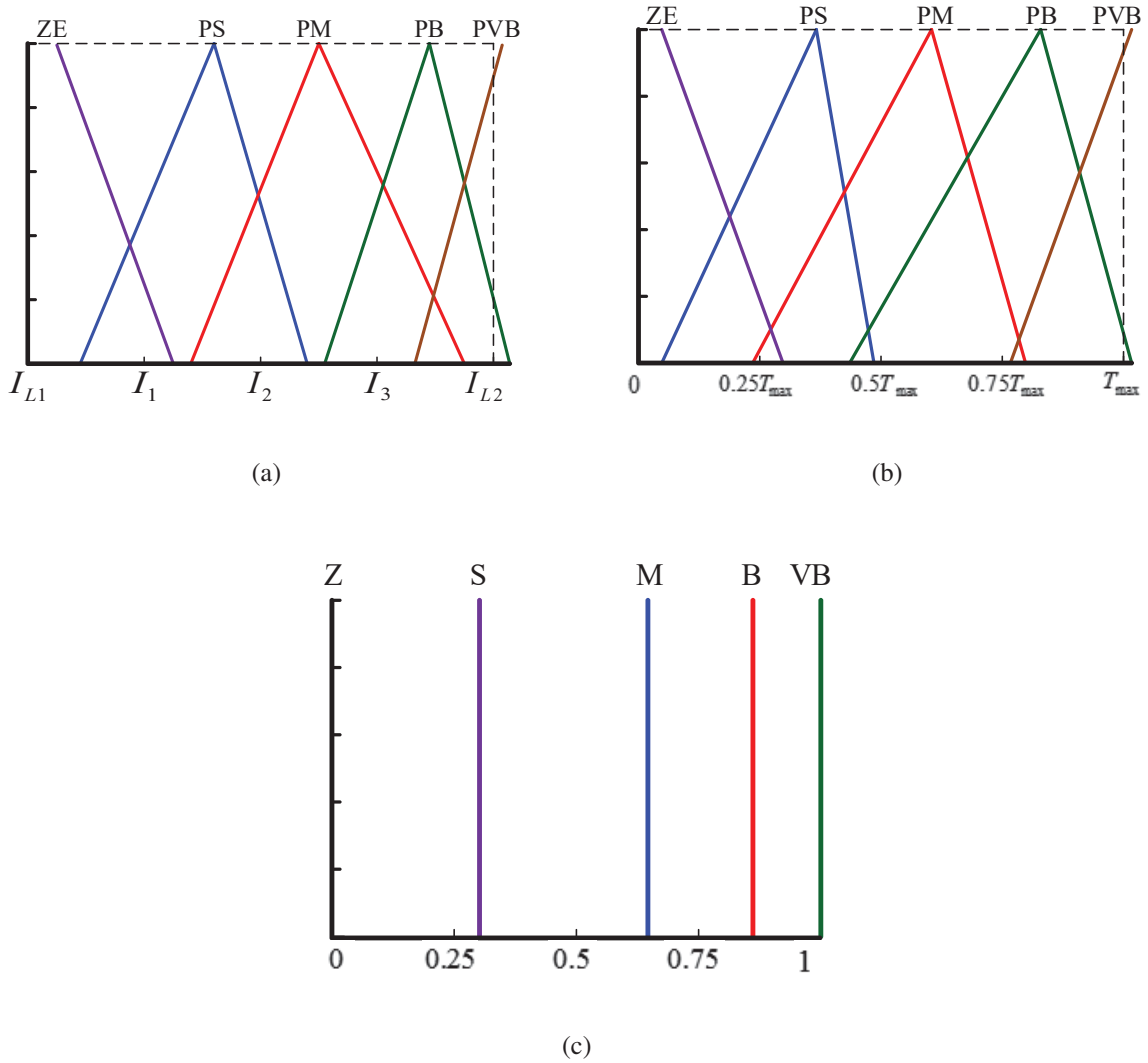
Figure 5.8: Reconfigured membership functions of first input (a), second input (b), and output (c).

5.3.4 Results of Scenario 3

As displayed in Fig. 5.9, the same as the previous two scenarios, the left column includes the original images captured from a real moving aircraft, the middle column contains the images processed after Otsu segmentation approach, and the right column lists the images segmented after the proposed smoke detection method.

In this more sophisticated scenario, there are some analogues including trees and ground in white or close-white color in the background. These analogues have caused a significant performance degradation in the compared method, numerous uninterested/non-smoke areas and noises are included, this phenomenon seriously affects the results of smoke detection. Thanks to the learning ability of EKF (which can automatically regulate the fuzzy scheme according to the lighting conditions of scenario), whereas, the proposed method can effectively distinguish the smoke from other analogues.

Similar to the previous two scenarios, both inputs and output functions are also adjusted by EKF as shown in Fig. 5.10 comparing with Fig. 5.4. From Figs. 5.10(a) and 5.10(b), either the first input function related to the intensity or second input function related to the absolute differences of RGB channels tends to the lower values of their corresponding segmentation levels. This phenomenon is induced by the fact that the intensity and color contrast of images are lower than that of the initial setting. As shown in Fig. 5.10(c), the membership functions of output moves towards the lower value than that of the initial state. This situation reveals the likelihood of forest fire decreases with the initial setting.
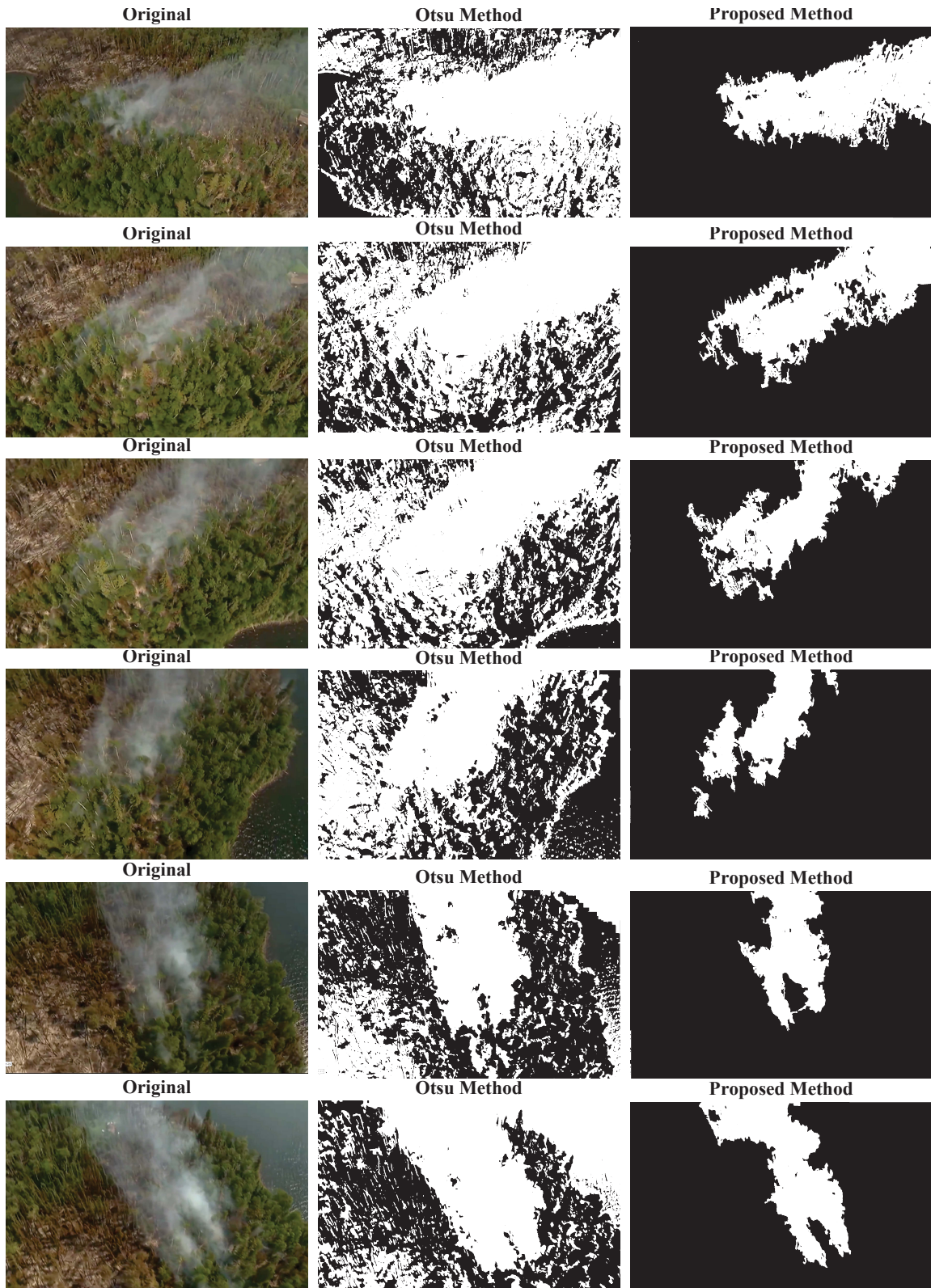
Figure 5.9: Performance of smoke segmentation: original images (left), results of Otsu method (middle), and results of proposed method (right).
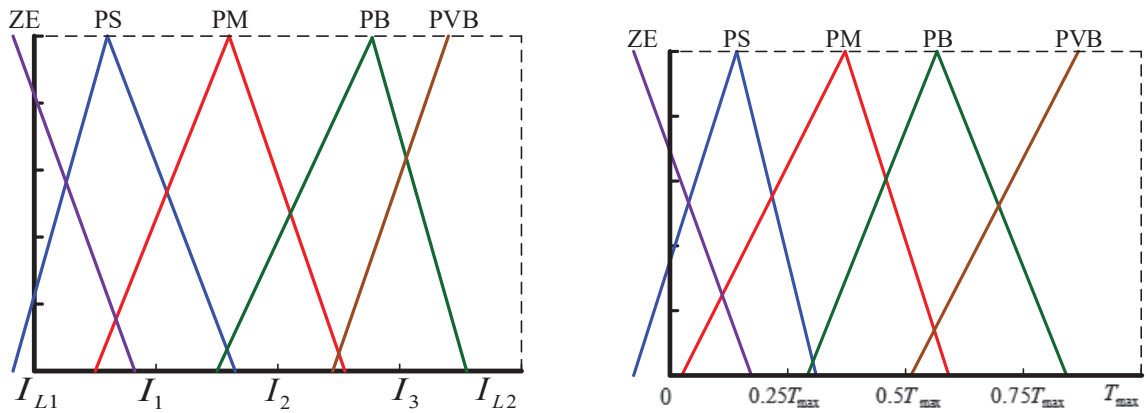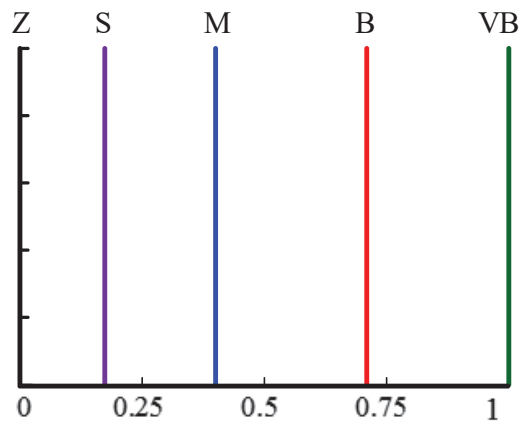
Figure 5.10: Reconfigured membership functions of first input (a), second input (b), and output (c).

Chapter 6

Conclusions and Future Works

6.1 Conclusions

In this thesis, current research progress related to forest fire detection are well investigated. Besides, several reliable and accurate UAV-based forest fire detection methodologies are also developed, these include:

- A comprehensive literature review on the existing UAV-based forest fire detection systems as well as vision-based forest fire detection techniques are provided.

- A method of vision-based forest fire detection in visible range images, which makes use of both color and motion analyses, is developed for the UAV-based surveillance application. The proposed method takes advantage of decision making rules established upon fire chroma and motion features to greatly reduce false alarm rates of fire detection. A color-based fire detection approach with light computation requirement is first designed to effectively extract the suspicious fire regions with high accuracy. Although there exists the motion of other objects and background in images caused by the movement of UAV, the proposed motion-based fire detection method can further identify and track fires effectively from background and other moving analogues of fire. Experimental verifications are conducted in two scenarios, one is a real forest fire video gathered by an aircraft and the other is a real-time video

111

collected by a UAV in an indoor environment. Experimental results have demonstrated that the designed forest fire detection approach is able to achieve satisfactory performance with greatly improved reliability and accuracy in forest fire detection applications.

- An IR images based forest fire detection method is also developed for the application of UAV-based forest fire surveillance. This approach employs both brightness and motion characteristics of fire in IR images to enhance the reliability and accuracy of fire detection. It can differentiate fires from background as well as non-fire hot moving objects by using histogram-based segmentation and optical flow analysis. Experimental validations are conducted in IR fire video sequences, good experimental results are obtained with greatly improved reliability.

- The fusion technique fusing information from both CCD camera and IR camera for the application of UAV-based forest fire detection is studied. Through image registration and data fusion, good performance has been achieved with low miss-detection rates.

- In order to achieve an effective early forest fire detection, a new learning-based fuzzy smoke detection algorithm considering color feature of smoke is developed. The visual images captured by the camera configured at the bottom of UAV are processed by a fuzzy smoke detection rule. The RGB difference and intensity are considered as the inputs while the smoke likelihood is treated as the output. Besides, an extended Kalman filter (EKF) is devised based upon the inputs and output of the fuzzy rule to offer it with additional regulating flexibility by training and reshaping its fuzzy membership functions and rules on-line. The effectiveness of the proposed methodology is verified and the experimental results indicate that smoke can be successfully segmented from the background regardless of the variation of environmental conditions.

6.2 Future Works

Based on the investigations of current research in this thesis, the following future directions are outlined:

- As vision-based detectors still suffer from a significant amount of missed detections and false alarms due to the variations of environmental conditions and the target characteristics, thus the combination of different fire features (flame and smoke) is worth further investigation.

- In order to improve the forest fire detection accuracy, how to correctly classify the different extracted features and effectively determine the probability of forest fire is an important future direction that needs further development.

- Although most of the developed schemes are verified in videos, more field tests are still needed.

- The rate of spread (ROS) is one of the most significant parameters for describing the forest fire behavior and predicting the moving direction of forest fire. It is necessary to develop a simple and practical method for computing the ROS of flame front from a sequence of images recorded by cameras.

- Because forests are highly complex and non-structured environments, the utilization of multiple sources of information at different locations is critical. The related research topic of using vision sensors and GPS systems to determine fire location is worth investigating.

Bibliography

[1] C. Yuan, Y. M. Zhang, and Z. X. Liu, "A survey on technologies for automatic forest fire monitoring, detection, and fighting using unmanned aerial vehicles and remote sensing techniques," *Canadian Journal of Forest Research*, vol. 45, no. 7, pp. 783–792, 2015.

[2] J. R. Martinez-de Dios, L. Merino, F. Caballero, A. Ollero, and D. X. Viegas, "Experimental results of automatic fire detection and monitoring with UAVs," *Forest Ecology and Management*, vol. 234, p. S232, 2006.

[3] R. C. Gonzalez and R. E. Woods, *Digital image processing*. Prentice-Hall, Inc., 2006.

[4] J. R. Martinez-de Dios, B. C. Arrue, A. Ollero, L. Merino, and F. Gomez-Rodriguez, "Computer vision techniques for forest fire perception," *Image and Vision Computing*, vol. 26, no. 4, pp. 550–562, 2008.

[5] D. Kolarić, K. Skala, and A. Dubravić, "Integrated system for forest fire early detection and management," *Periodicum Biologorum*, vol. 110, no. 2, pp. 205–211, 2008.

[6] "Fort McMurray wildfire costliest insured disaster in Canadian history," in *CBC News, July 7, 2016*, http://www.cbc.ca/news/canada/edmonton/fort-mcmurray-wildfire-costliest-insured-disaster-in-canadian-history-at-nearly-3-6b-1.3668602 (Accessed on 2017-03-19).

[7] H. Lin, Z. Liu, T. Zhao, and Y. Zhang, "Early warning system of forest fire detection based on video technology," in *Proceedings of the 9th International Symposium on Linear Drives for Industry Applications*, pp. 751–758, 2014.

[8] V. Vipin, "Image processing based forest fire detection," *Emerging Technology and Advanced Engineering*, vol. 2, no. 2, pp. 87–95, 2012.

[9] H. Olsson, M. Egberth, J. Engberg, J. E. S. Fransson, T. G. Pahlen, O. Hagner, J. Holmgren, S. Joyce, M. Magnusson, B. Nilsson, M. Nilsson, K. Olofsson, H. Reese, and J. Wallerman, "Current and emerging operational uses of remote sensing in swedish forestry," in *Proceedings of the 7th Annual Forest Inventory and Analysis Symposium*, 2005.

[10] R. W. Beard, T. W. Mclain, D. B. Nelson, D. Kingston, and D. Johanson, "Decentralized cooperative aerial surveillance using fixed-wing miniature UAVs," *Proceedings of the IEEE*, vol. 94, no. 7, pp. 1306–1324, 2006.

[11] J. Everaerts, "The use of unmanned aerial vehicles (UAVs) for remote sensing and mapping," *The International Archives of the Photogrammetry, Remote Sensing and Spatial Information Sciences*, vol. 37, pp. 1187–1192, 2008.

[12] J. A. J. Berni, P. J. Zarco-Tejada, L. Suarez, and E. Fereres, "Thermal and narrowband multispectral remote sensing for vegetation monitoring from an unmanned aerial vehicle," *IEEE Transactions on Geoscience and Remote Sensing*, vol. 47, no. 3, pp. 722–738, 2009.

[13] M. Li, W. Xu, K. Xu, J. Fan, and D. Hou, "Review of fire detection technologies based on video image," *Journal of Theoretical and Applied Information Technology*, vol. 49, no. 2, pp. 700–707, 2013.

[14] C. Yuan, Z. X. Liu, and Y. M. Zhang, "Aerial images-based forest fire detection for firefighting using optical remote sensing techniques and unmanned aerial vehicles," *Journal of Intelligent and Robotic Systems*, (First Online: 05 January 2017; DOI: 10.1007/s10846-016-0464-7).

[15] C. Yuan, Z. X. Liu, and Y. M. Zhang, "UAV-based forest fire detection and tracking using image processing techniques," in *International Conference on Unmanned Aircraft Systems*, pp. 639–643, 2015.

[16] C. Yuan, Z. X. Liu, and Y. M. Zhang, "Vision-based forest fire detection in aerial images for firefighting using UAVs," in *International Conference on Unmanned Aircraft Systems*, 2016.

[17] C. Yuan, K. A. Ghamry, Z. X. Liu, and Y. M. Zhang, "Unmanned aerial vehicle based forest fire monitoring and detection using image processing technique," in *The IEEE Chinese Guidance, Navigation and Control Conference*, 2016.

[18] F. Sharifi, Y. M. Zhang, and A. G. Aghdam, "A distributed deployment strategy for multi-agent systems subject to health degradation and communication delays," *Journal of Intelligent and Robotic Systems*, vol. 73, no. 1, pp. 623–633, 2014.

[19] L. Merino, F. Caballero, J. R. Martinez-de Dios, I. Maza, and A. Ollero, "An unmanned aircraft system for automatic forest fire monitoring and measurement," *Journal of Intelligent and Robotic Systems*, vol. 65, no. 1, pp. 533–548, 2012.

[20] Z. X. Liu, C. Yuan, Y. M. Zhang, and J. Luo, "A learning-based fault tolerant tracking control of an unmanned quadrotor helicopter," *Journal of Intelligent and Robotic Systems*, vol. 84, no. 1, pp. 145–162, 2015.

[21] Z. X. Liu, X. Yu, C. Yuan, and Y. M. Zhang, "Leader-follower formation control of unmanned aerial vehicles with fault tolerant and collision avoidance capabilities," in *International Conference on Unmanned Aircraft Systems*, 2015.

[22] A. Ollero, B. C. Arrue, J. R. Martinez-de Dios, and J. J. Murillo, "Techniques for reducing false alarms in infrared forest-fire automatic detection systems," *Control Engineering Practice*, vol. 7, no. 1, pp. 123–131, 1999.

[23] J. Ferruz and A. Ollero, "Real-time feature matching in image sequences for non-structured environments: applications to vehicle guidance," *Journal of Intelligent and Robotic Systems*, vol. 28, no. 1, pp. 85–123, 2000.

[24] L. Merino, F. Caballero, J. R. Martinez-de Dios, J. Ferruz, and A. Ollero, "A cooperative perception system for multiple UAVs: application to automatic detection of forest fires," *Journal of Field Robotics*, vol. 23, no. 3-4, pp. 165–184, 2006.

[25] I. Maza, F. Caballero, J. Capitan, J. R. Martinez-De-Dios, and A. Ollero, "Experimental results in multi-UAV coordination for disaster management and civil security applications," *Journal of Intelligent and Robotic Systems*, vol. 61, no. 1, pp. 563–585, 2011.

[26] V. G. Ambrosia, S. Wegener, T. Zajkowski, D. V. Sullivan, S. Buechel, F. Enomoto, B. Lobitz, S. Johan, J. Brass, and E. Hinkley, "The Ikhana unmanned airborne system (UAS) western states fire imaging missions: from concept to reality (2006–2010)," *Geocarto International*, vol. 26, no. 2, pp. 85–101, 2011.

[27] J. R. Martínez-de Dios, L. Merino, F. Caballero, and A. Ollero, "Automatic forest-fire measuring using ground stations and unmanned aerial systems," *Sensors*, vol. 11, no. 6, pp. 6328–6353, 2011.

[28] J. M. Bradley and C. N. Taylor, "Georeferenced mosaics for tracking fires using unmanned miniature air vehicles," *Journal of Aerospace Computing Information and Communication*, vol. 8, no. 10, pp. 295–309, 2011.

[29] V. G. Ambrosia and T. Zajkowski, "Selection of appropriate class UAS/sensors to support fire monitoring: experiences in the united states," in *Handbook of Unmanned Aerial Vehicles*, pp. 2723–2754, Springer Netherlands, 2015.

[30] I. Bosch, A. Serrano, and L. Vergara, "Multisensor network system for wildfire detection using infrared image processing," *Scientific World Journal*, 2013.

[31] L. Merino, J. R. Martinez-de Dios, and A. Ollero, "Cooperative unmanned aerial systems for fire detection, monitoring, and extinguishing," in *Handbook of Unmanned Aerial Vehicles*, pp. 2693–2722, Springer Netherlands, 2015.

[32] M. Shahbazi, J. Theau, and P. Menard, "Recent applications of unmanned aerial imagery in natural resource management," *GIScience and Remote Sensing*, vol. 51, no. 4, pp. 1–27, 2014.

[33] M. Kontitsis, K. P. Valavanis, and N. Tsourveloudis, "Automatic forest fire monitoring and measurement using unmanned aerial vehicles," in *Proceedings of the 6th International Congress on Forest Fire Research*, 2010.

[34] F. Sharifi, Y. M. Zhang, and A. G. Aghdam, "Forest fire detection and monitoring using a network of autonomous vehicles," in *The 10th International Conference on Intelligent Unmanned Systems*, 2014.

[35] F. Sharifi, M. Mirzaei, Y. M. Zhang, and B. W. Gordon, "Cooperative multi-vehicle search and coverage problem in an uncertain environment," *Unmanned Systems*, vol. 3, no. 1, pp. 35–47, 2015.

[36] C. Wilson and J. B. Davis, "Forest fire laboratory at riverside and fire research in California: past present, and future," in *General Technical Report PSW-105 (Pacific Southwest Forest and Range Experiment Station, Forest Service, U.S. Department of Agriculture*, 1988.

[37] M. Tranchitella, S. Fujikawa, T. L. Ng, D. Yoel, D. Tatum, P. Roy, C. Mazel, S. Herwitz, and E. Hinkley, "Using tactical unmanned aerial systems to monitor and map wildfires," in *Proceedings of AIAA Infotech@Aerospace Conference*, 2007.

[38] R. Charvat, R. Ozburn, J. Bushong, and K. Cohen, "SIERRA team flight of Zephyr UAS at west Virginia wild land fire burn," in *AIAA Infotech@Aerospace Conference*, pp. 19–21, 2012.

[39] V. Ambrosia, "Remotely piloted vehicles as fire imaging platforms: the future is here," *Available from http://geo.arc.nasa.gov/sge/UAVFiRE/completeddemos.html*, 2002.

[40] A. Ollero, S. Lacroix, L. Merino, and J. Gancet, "Multiple eyes in the skies: architecture and perception issues in the COMETS unmanned air vehicles project," *IEEE Robotics and Automation Magazine*, vol. 12, no. 2, pp. 46–57, 2005.

[41] J. R. Martinez-de Dios, L. Merino, A. Ollero, L. M. Ribeiro, and X. Viegas, "Multi-UAV experiments: application to forest fires," *Springer Tracts in Advanced Robotics*, vol. 37, pp. 207–228, 2007.

[42] A. Restas, "Wildfire management supported by UAV based air reconnaissance: experiments and results at the Szendro fire department, Hungary," *First International Workshop on Fire Management*, 2006.

[43] E. Pastor, C. Barrado, P. Royo, E. Santamaria, J. Lopez, and E. Salami, "Architecture for a helicopter-based unmanned aerial systems wildfire surveillance system," *Geocarto International*, vol. 26, no. 2, pp. 113–131, 2011.

[44] M. Van Persie, A. Oostdijk, J. Fix, M. C. Van Sijl, and L. Edgardh, "Real-time UAV based geospatial video integrated into the fire brigades crisis management GIS system," *ISPRS - International Archives of the Photogrammetry, Remote Sensing and Spatial Information Sciences*, vol. 38, pp. 173–175, 2012.

[45] D. W. Casbeer, R. W. Beard, T. W. McLain, S. M. Li, and R. Mehra, "Forest fire monitoring with multiple small UAVs," in *Proceedings of American Control Conference*, pp. 3530–3535, 2005.

[46] D. W. Casbeer, R. W. Beard, T. W. McLain, S. M. Li, and R. Mehra, "Cooperative forest fire surveillance using a team of small unmanned air vehicles," *International Journal of Systems Science*, vol. 37, no. 6, pp. 351–360, 2006.

[47] V. G. Ambrosia, S. S. Wegener, D. V. Sullivan, S. W. Buechel, S. E. Dunagan, J. A. Brass, J. Stoneburner, and S. M. Schoenung, "Demonstrating UAV-acquired real-time thermal data

119

over fires," *Photogrammetric Engineering and Remote Sensing*, vol. 69, no. 4, pp. 391–402, 2003.

[48] J. R. Martinez-de Dios, L. Merino, and A. Ollero, "Fire detection using autonomous aerial vehicles with infrared and visual cameras," in *Proceedings of the 16th IFAC World Congress*, 2005.

[49] F. Esposito, G. Rufino, A. Moccia, P. Donnarumma, M. Esposito, and V. Magliulo, "An integrated electro-optical payload system for forest fires monitoring from airborne platform," in *Proceedings of IEEE Aerospace Conference*, pp. 1–13, 2007.

[50] G. P. Jones IV, L. G. Pearlstine, and H. F. Percival, "An assessment of small unmanned aerial vehicles for wildlife research," *Wildlife Society Bulletin*, vol. 34, no. 3, pp. 750–758, 2006.

[51] G. P. Jones IV, *The feasibility of using small unmanned aerial vehicles for wildlife research*. University of Florida, 2003.

[52] J. R. Martinez-De Dios and A. Ollero, "A new training-based approach for robust thresholding," in *Proceedings of the World Automation Congress*, pp. 121–126, 2004.

[53] L. Merino, F. Caballero, J. R. Martinez-De Dios, and A. Ollero, "Cooperative fire detection using unmanned aerial vehicles," in *IEEE International Conference on Robotics and Automation*, pp. 1884–1889, 2005.

[54] L. Merino, F. Caballero, J. R. MartinezDe Dios, J. Ferruz, and A. Ollero, "A cooperative perception system for multiple UAVs: application to automatic detection of forest fires," *Journal of Field Robotics*, vol. 23, no. 3-4, pp. 165–184, 2006.

[55] M. Kontitsis, K. P. Valavanis, and N. Tsourveloudis, "A UAV vision system for airborne surveillance," *IEEE International Conference on Robotics and Automation*, 2004.

[56] J. R. Martinez-de Dios, J. Andre, J. C. Gonalves, B. C. Arrue, A. Ollero, and D. X. Viegas, "Laboratory fire spread analysis using visual and infrared images," *International Journal of Wildland Fire*, vol. 15, no. 2, pp. 179–186, 2006.

[57] A. Ollero, J. R. Martinez-De Dios, and L. Merino, "Unmanned aerial vehicles as tools for forest-fire fighting," *Forest Ecology and Management*, vol. 234, no. 1, pp. 263–274, 2006.

[58] A. E. Cetin, K. Dimitropoulos, B. Gouverneur, N. Grammalidis, O. Gunay, Y. H. Habiboglu, B. U. Toreyin, and S. Verstockt, "Video fire detection–review," *Digital Signal Processing*, vol. 23, no. 6, pp. 1827–1843, 2013.

[59] T. Celik, H. Ozkaramanlt, and H. Demirel, "Fire pixel classification using fuzzy logic and statistical color model," in *IEEE International Conference on Acoustics*, pp. 1205–1208, 2007.

[60] E. Mahdipour and C. Dadkhah, "Automatic fire detection based on soft computing techniques: review from 2000 to 2010," *Artificial Intelligence Review*, vol. 42, no. 4, pp. 1–40, 2012.

[61] S. Rudz, K. Chetehouna, A. Hafiane, O. Sero-Guillaume, and H. Laurent, "On the evaluation of segmentation methods for wildland fire," in *International Conference on Advanced Concepts for Intelligent Vision Systems*, pp. 12–23, 2009.

[62] T. Chen, P. Wu, and Y. Chiou, "An early fire-detection method based on image processing," in *Proceedings of the International Conference on Image Processing*, pp. 1707–1710, 2004.

[63] B. U. Toreyin, Y. Dedeoglu, and A. E. Cetin, "Flame detection in video using hidden Markov models," in *IEEE International Conference on Image Processing*, pp. 1230–1233, 2005.

[64] B. U. Toreyin, Y. Dedeoglu, U. Gudukbay, and A. E. cetin, "Computer vision based method for real-time fire and flame detection," *Pattern Recognition Letters*, vol. 27, no. 1, pp. 49–58, 2006.

[65] B. U. Toreyin, Y. Dedeoglu, and A. E. Cetin, "Contour based smoke detection in video using wavelets," in *Proceedings of the IEEE European Signal Processing Conference*, pp. 123–128, 2006.

[66] T. Celik and H. Demirel, "Fire detection in video sequences using a generic color model," *Fire Safety Journal*, vol. 44, no. 2, pp. 147–158, 2009.

[67] O. Gunay, K. Tademir, B. U. Toreyin, and A. E. Cetin, "Video based wildfire detection at night," *Fire Safety Journal*, vol. 44, no. 6, pp. 860–868, 2009.

[68] O. Gunay, B. U. Toreyin, K. Kose, and A. E. Cetin, "Entropy-functional-based online adaptive decision fusion framework with application to wildfire detection in video.," *IEEE Transactions on Image Processing*, vol. 21, no. 5, pp. 2853–2865, 2012.

[69] T. Celik, H. Demirel, H. Ozkaramanli, and M. Uyguroglu, "Fire detection using statistical color model in video sequences," *Journal of Visual Communication and Image Representation*, vol. 18, no. 2, pp. 176–185, 2007.

[70] W. Phillips, M. Shah, and N. V. Lobo, "Flame recognition in video," in *IEEE Workshop on Applications of Computer Vision*, pp. 224–229, 2000.

[71] B. C. Ko, K. H. Cheong, and J. Y. Nam, "Fire detection based on vision sensor and support vector machines," *Fire Safety Journal*, vol. 44, no. 3, pp. 322–329, 2009.

[72] T. Toulouse, L. Rossi, M. Akhloufi, T. Celik, and X. Maldague, "Benchmarking of wildland fire colour segmentation algorithms," *IET Image Processing*, vol. 9, no. 12, pp. 1064–1072, 2015.

[73] T. Toulouse, L. Rossi, T. Celik, and M. Akhloufi, "Automatic fire pixel detection using image processing: a comparative analysis of rule-based and machine learning-based methods," *Signal, Image and Video Processing*, vol. 10, no. 4, pp. 647–654, 2016.

[74] T. H. Chen, Y. H. Yin, S. F. Huang, and Y. T. Ye, "The smoke detection for early fire-alarming system based on video processing," in *International Conference on Intelligent Information Hiding and Multimedia*, pp. 427–430, 2006.

[75] C. Yu, Y. Zhang, J. Fang, and J. Wang, "Texture analysis of smoke for real-time fire detection," in *International Workshop on Computer Science and Engineering*, pp. 511–515, 2009.

[76] F. Yuan, "A fast accumulative motion orientation model based on integral image for video smoke detection," *Pattern Recognition Letters*, vol. 29, no. 7, pp. 925–932, 2008.

[77] C. C. Ho and T. H. Kuo, "Real-time video-based fire smoke detection system," in *Proceedings of the IEEE/ASME International Conference on Advanced Intelligent Mechatronics*, pp. 1845–1850, 2009.

[78] S. Surit and W. Chatwiriya, "Forest fire smoke detection in video based on digital image processing approach with static and dynamic characteristic analysis," in *Proceedings of the 1st ACIS/JNU International Conference on Computers, Networks, Systems, and Industrial Engineering*, pp. 35–39, 2011.

[79] D. Zhang, A. Hu, Y. Rao, J. Zhao, and J. Zhao, "Forest fire and smoke detection based on video image segmentation," in *Proceedings of the International Symposium on Multispectral Image Processing and Pattern Recognition*, 2007.

[80] C. Yu, J. Fang, J. Wang, and Y. Zhang, "Video fire smoke detection using motion and color features," *Fire Technology*, vol. 46, no. 3, pp. 651–663, 2010.

[81] S. J. Ham, B. C. Ko, and J. Y. Nam, "Fire-flame detection based on fuzzy finite automation," in *Proceedings of the 20th International Conference on Pattern Recognition (ICPR)*, pp. 3919–3922, 2010.

[82] E. Pastor, A. Agueda, J. Andrade-Cetto, M. Munoz, Y. Perez, and E. Planas, "Computing the rate of spread of linear flame fronts by thermal image processing," *Fire Safety Journal*, vol. 41, no. 8, pp. 569–579, 2006.

[83] A. E. Ononye, A. Vodacek, and E. Saber, "Automated extraction of fire line parameters from multispectral infrared images," *Remote Sensing of Environment*, vol. 108, no. 2, pp. 179–188, 2007.

[84] J. J. Huseynov, S. Baliga, A. Widmer, and Z. Boger, "Infrared flame detection system using multiple neural networks," in *Proceedings of the International Joint Conference on Neural Networks*, vol. 11, pp. 608–612, 2007.

[85] B. C. Arrue, A. Ollero, and J. R. M. de Dios, "An intelligent system for false alarm reduction in infrared forest-fire detection," *IEEE Intelligent Systems*, vol. 15, no. 3, pp. 64–73, 2000.

[86] B. H. Cho, J. W. Bae, and S. H. Jung, "Image processing-based fire detection system using statistic color model," in *International Conference on Advanced Language Processing and Web Information Technology*, pp. 245–250, 2008.

[87] J. Zhao, Z. Zhang, S. Han, C. Qu, Z. Yuan, and D. Zhang, "SVM based forest fire detection using static and dynamic features," *Computer Science and Information Systems*, vol. 8, no. 3, pp. 821–841, 2011.

[88] X. Qi and J. Ebert, "A computer vision based method for fire detection in color videos," *International Journal of Imaging*, vol. 2, no. S09, pp. 22–34, 2009.

[89] H. Jin and R. B. Zhang, "A fire and flame detecting method based on video," in *Proceedings of the International Conference on Machine Learning and Cybernetics*, pp. 2347–2352, 2009.

[90] H. D. Duong and N. A. Tuan, "Using Bayes method and fuzzy C-mean algorithm for fire detection in video," in *Proceedings of the International Conference on Advanced Technologies for Communications*, pp. 141–144, 2009.

[91] J. Hou, J. Qian, W. Zhang, Z. Zhao, and P. Pan, "Fire detection algorithms for video images of large space structures," *Multimedia Tools and Applications*, vol. 52, no. 1, pp. 45–63, 2010.

[92] W. Philips, M. Shah, and N. da Vitoria Lobo, "Flame recognition in video," *Pattern Recognition Letters*, vol. 23, no. 1-3, pp. 319–327, 2002.

[93] J. Hou, J. Qian, Z. Zhao, and P. Pan, "Fire detection algorithms in video images for high and large-span space structures," in *International Congress on Image and Signal Processing*, pp. 1–5, 2009.

[94] J. Chen, Y. He, and J. Wang, "Multi-feature fusion based fast video flame detection," *Building and Environment*, vol. 45, no. 5, pp. 1113–1122, 2010.

[95] M. Wirth and R. Zaremba, "Flame region detection based on histogram back projection," in *Proceedings of the Canadian Conference Computer and Robot Vision*, pp. 167–174, 2010.

[96] S. Verstockt, *Multi-modal video analysis for early fire detection.* PhD thesis, Ghent University, 2011.

[97] R. T. Collins, A. J. Lipton, T. Kanade, H. Fujiyoshi, D. Duggins, Y. Tsin, D. Tolliver, N. Enomoto, O. Hasegawa, and P. Burt, "A system for video surveillance and monitoring," *CMU-RI-TR-00-12, Technical Report,Carnegie Mellon University*, 2000.

[98] B. K. P. Horn and B. G. Schunck, "Determining optical flow," *Artificial Intelligence*, vol. 17, pp. 185–203, 1981.

[99] B. D. Lucas and T. Kanade, "An iterative image registration technique with an application to stereo vision," in *Proceedings of Imaging Understanding Workshop*, pp. 121–130, 1981.

[100] B. C. Ko, K. H. Cheong, and J. Y. Nam, "Early fire detection algorithm based on irregular patterns of flames and hierarchical Bayesian networks," *Fire Safety Journal*, vol. 45, no. 4, pp. 262–270, 2010.

[101] P. V. K. Borges and E. Izquierdo, "A probabilistic approach for vision-based fire detection in videos," *IEEE Transactions on Circuits and Systems for Video Technology*, vol. 20, no. 5, pp. 721–731, 2010.

[102] O. Gunay, K. Tademir, B. U. Toreyin, and A. E. Cetin, "Fire detection in video using LMS based active learning," *Fire Technology*, vol. 46, no. 3, pp. 551–577, 2010.

[103] D. V. Hamme, P. Veelaert, W. Philips, and K. Teelen, "Fire detection in color images using Markov random fields," in *Proceedings of Advanced Concepts for Intelligent Vision Systems*, pp. 88–97, 2010.

[104] L. Jiao, Y. Wu, G. Wu, E. Y. Chang, and Y. F. Wang, "Anatomy of a multicamera video surveillance system," *Multimedia Systems*, vol. 10, no. 2, pp. 144–163, 2004.

[105] D. M. Hansen, P. T. Duizer, S. Park, T. B. Moeslund, and M. M. Trivedi, *Multi-view video analysis of humans and vehicles in an unconstrained environment*. Springer Berlin Heidelberg, 2008.

[106] G. R. Rodriguez-Canosa, S. Thomas, J. del Cerro, A. Barrientos, and B. MacDonald, "A real-time method to detect and track moving objects (DATMO) from unmanned aerial vehicles (UAVs) using a single camera," *Remote Sensing*, vol. 4, no. 4, pp. 1090–1111, 2012.

[107] A. Miller, P. Babenko, M. Hu, and M. Shah, *Person tracking in UAV video*. Springer Berlin Heidelberg, 2008.

[108] C. H. Huang, Y. T. Wu, J. H. Kao, M. Y. Shih, and C. C. Chou, "A hybrid moving object detection method for aerial images," in *Pacific-Rim Conference on Multimedia*, pp. 357–368, 2010.

[109] N. Suganuma and T. Kubo, "Fast dynamic object extraction using stereo vision based on oc- cupancy grid maps and optical flow," in *IEEE/ASME International Conference on Advanced Intelligent Mechatronics (AIM)*, pp. 978–983, 2011.

[110] M. Mueller, P. Karasev, I. Kolesov, and A. Tannenbaum, "Optical flow estimation for flame detection in videos," *IEEE Transactions on Image Processing*, vol. 22, no. 7, pp. 2786–2797, 2013.

[111] J. G. Quintiere, *Principles of fire behavior*. CRC Press, 2016.

[112] T. H. Chen, C. L. Kao, and S. M. Chang, "An intelligent real-time fire-detection method based on video processing," in *Proceedings of IEEE 37th Annual International Carnahan Conference on Security Technology*, pp. 104–111, 2003.

[113] Y. Amit, *2D object detection and recognition: models, algorithms, and networks*. MIT Press, 2002.

[114] V. I. Utkin, *Sliding modes in control and optimization*. Springer Science & Business Media, 2013.

[115] B. L. Stevens and F. L. Lewis, *Aircraft control and simulation*. John Wiley, 2004.

[116] N. Otsu, "A threshold selection method from gray-level histograms," *IEEE Transactions on Systems, Man and Cybernetics*, vol. 9, no. 1, pp. 62–66, 1979.

[117] M. Shah and R. Kumar, *Video registration*. Kluwer Academic Publishers, 2004.

[118] B. Zitova and J. Flusser, "Image registration methods: a survey," *Image and Vision Comput- ing*, vol. 21, no. 11, pp. 977–1000, 2003.

[119] O. Faugeras and Q. T. Luong, *Video registration*. The MIT Press, 2001.

[120] Y. Caspi and M. Irani, "Alignment of nonoverlapping sequences," in *International Confer- ence on Computer Vision*, vol. 2, pp. 76–83, 2001.

[121] M. Irani and P. Anandan, "Robust multi-sensor image alignment," in *IEEE International Conference on Computer Vision*, pp. 959–966, 1998.

[122] C. Lee, C. Lin, C. Hong, M. T. Su, *et al.*, "Smoke detection using spatial and temporal analyses," *International Journal of Innovative Computing, Information and Control*, vol. 8, no. 7, pp. 4749–4770, 2012.

[123] C. C. Ho, "Machine vision-based real-time early flame and smoke detection," *Measurement Science and Technology*, vol. 20, no. 4, 2009.

[124] T. X. Tung and J. M. Kim, "An effective four-stage smoke-detection algorithm using video images for early fire-alarm systems," *Fire Safety Journal*, vol. 46, no. 5, pp. 276–282, 2011.

[125] T. H. Chen, Y. H. Yin, S. F. Huang, and Y. T. Ye, "The smoke detection for early fire-alarming system base on video processing," in *IEEE International Conference on Intelligent Information Hiding and Multimedia Signal Processing*, pp. 427–430, 2006.

[126] Z. Wei, X. Wang, W. An, and J. Che, "Target-tracking based early fire smoke detection in video," in *IEEE International Conference on Image and Graphics*, pp. 172–176, 2009.

[127] J. Yang, F. Chen, and W. Zhang, "Visual-based smoke detection using support vector machine," in *IEEE International Conference on Natural Computation*, vol. 4, pp. 301–305, 2008.

[128] J. Gubbi, S. Marusic, and M. Palaniswami, "Smoke detection in video using wavelets and support vector machines," *Fire Safety Journal*, vol. 44, no. 8, pp. 1110–1115, 2009.

[129] B. U. Töreyin, Y. Dedeoğlu, and A. E. Cetin, "Wavelet based real-time smoke detection in video," in *IEEE European Signal Processing Conference*, pp. 1–4, 2005.

[130] Z. Xu and J. Xu, "Automatic fire smoke detection based on image visual features," in *IEEE International Conference on Computational Intelligence and Security Workshops*, pp. 316–319, 2007.

[131] J. Vicente and P. Guillemant, "An image processing technique for automatically detecting forest fire," *International Journal of Thermal Sciences*, vol. 41, no. 12, pp. 1113–1120, 2002.

[132] Z. Xiong, R. Caballero, H. Wang, A. M. Finn, M. A. Lelic, and P. Y. Peng, "Video-based smoke detection: possibilities, techniques, and challenges," *Journal of Hubei Radio & Televison University*, 2007.

[133] Y. Cui, H. Dong, and E. Z. Zhou, "An early fire detection method based on smoke texture analysis and discrimination," in *Congress on Image and Signal Processing*, vol. 3, pp. 95–99, 2008.

[134] M. Sugeno and T. Yasukawa, "A fuzzy-logic-based approach to qualitative modeling," *IEEE Transactions on Fuzzy Systems*, vol. 1, no. 1, pp. 7–31, 1993.

[135] K. K. Ahn and D. Q. Truong, "Online tuning fuzzy PID controller using robust extended Kalman filter," *Journal of Process Control*, vol. 19, no. 6, pp. 1011–1023, 2009.

[136] M. S. Grewal, *Kalman filtering*. Springer, 2011.